.

Dissertation

# Mutations in FHL1 impair expression and functionality of potassium voltage-gated channel $K_{v1.5}$ in myopathy patients

Submitted by

Ivana POPARIC, M.Sc.

For the Academic Degree of

Doctor of Philosophy (PhD)

At the

Medical University of Graz

Institute of Human Genetics

Under supervision of

Prof. Dr. Klaus Wagner

2011

# ACKNOWLEDGEMENTS

First and foremost, I would like to thank to my supervisor Professor Klaus Wagner for giving me an opportunity to enroll into the PhD program and work under his supervision. In addition, I would like to show my gratitude to Ass. Prof. Christian Windpassinger for daily guidance, many advices and heartily discussions over the last four years. I am much obliged to head of the Institute, Professor Michael Speicher, who has helped me and advised me on many occasions.

I am indebted and thankful to Professor Wolfgang Schreibmayer and to Astrid Gorischek, best teachers in the lab a student could have, for all the knowledge and many hours we have spent together. This dissertation would also not have been possible without Professor Ernst Malle and his devoted and meticulous work on publication manuscript for which I am very grateful.

I am much obliged to Professor Gernot Desoye and his group, especially Heidi Miedl, for all the hard work and wonderful moments spent in their lab. Many thanks must also go to Professor Stefan Quasthoff, Dr. Sonja Hochmeister, Dr. Josepha Binder and Dr. Benedict Schoser for clinical work and for providing materials and technical advices.

It is a great pleasure to thank to all of my colleagues at the Institute of Human Genetics for all help and support over the years. I would especially like to mention Ingrid Janisch and Peter Ulz whose technical knowledge helped me on many occasions. Many thanks go to Ida Tieber for all the help with paper work and for encouragement during learning Styrian. I would like to thank girls in the office: Karin, Anna, Eva, Martina, Kristina and Christine for being great friends as well as colleagues.

I am obliged to many of my colleagues from the PhD program, especially Lada, Senka, Luciana and Valerie, who were always great friends and made life in Graz even more fun. It is a pleasure to thank to all of my friends at home who have encouraged me and

patiently waited for me to come back. I am very grateful to my boyfriend Ivan for all the love, support and patience over the last four years.

At the end, I would like to thank my family, especially my parents, who have provided much moral and material support during the long years of my education.

# DECLARATION

I hereby declare that this thesis is my own original work and that I have full acknowledged by name all those individuals and affiliated organizations that have contributed to the presented work. Due acknowledgements have been made in the text in all the respective sections of the thesis.

Throughout the thesis the guidelines of Good Scientific Practice were followed.

Date, Signature,

**INDEX**

**SUMMARY**

Four-and-a-half LIM domain protein 1 (FHL1) is expressed predominantly in skeletal but also in cardiac muscle. It is suggested to play a role in sarcomere synthesis and assembly. Three alternatively-spliced isoforms of FHL1 exist (FHL1A, FHL1B and FHL1C), which differ in amino acid sequence, localization, expression patterns and protein interactions. Mutations in FHL1 were identified as causative in four different myopathies including X-linked myopathy with postural muscle atrophy, termed XMPMA. Mutations in patients with XMPMA affect variants A and B, isoform C remaining intact. Recently FHL1A was identified as a possible regulator of the human atrial potassium voltage-gated channel $K_{v1.5}$. Here we describe the physical and functional interaction between $K_{v1.5}$ and FHL1 proteins. Quantitative PCR experiments showed altered mRNA expression for $K_{v1.5}$ and FHL1 variants in myoblasts of XMPMA patients compared to controls. Western blot analysis further confirmed absence of FHL1A protein and reduction/absence of $K_{v1.5}$ in these cells. Patient myoblasts showed a decreased proliferation rate compared to controls and a higher number of cells in the $G_0/G_1$ phase. Colocalization of FHL1 and $K_{v1.5}$ in the cell cytoplasm and plasma membrane was confirmed in HL-1 cells. Two-electrode voltage clamp experiments demonstrated that Xenopus oocytes expressing $K_{v1.5}$ and FHL1 variants exerted markedly reduced currents when compared to oocytes expressing $K_{v1.5}$ only, FHL1C variant having the most prominent effect. Potential physical interaction between FHL1C and $K_{v1.5}$ was proven *in vitro* by a pull down assay.

In conclusion, we have described the functional interaction of FHL1 and $K_{v1.5}$.. Since $K_{v1.5}$ expression and functionality are altered in XMPMA patients we propose FHL1 might regulate this channel in both cardiac and skeletal muscle. Absence of FHL1 could result in lack of regulation of the channel and explain the pathophysiology found in our patients.

**ZUSAMMENFASSUNG**

Das viereinhalb LIM Domäne Protein 1 (FHL1) ist vorwiegend im Skelett-, aber auch im Herzmuskel exprimiert. Wahrscheinlich spielt das Protein eine Rolle in der Synthese und beim Aufbau des Sarkomers. Drei alternativ-gespleißte Isoformen von FHL1 wurden beschrieben (FHL1A, FHL1B und FHL1C), welche sich durch ihre Aminosäuresequenz, die Lokalisierung, den Proteininteraktionen und ihr Expressionsmuster unterscheiden. Mutationen von FHL1 wurden im Zusammenhang mit vier verschiedenen Myopathien beschrieben, darunter der X-chromosomalen Myopathie mit Atrophie der posturalen Muskeln, XMPMA. Mutationen in Patienten mit XMPMA betreffen die Varianten A und B, die Isoform C bleibt unverändert. Kürzlich wurde FHL1A mit der Regulierung des humanen herzspezifischen spannungsabhängigen Kaliumkanals $K_{v1.5}$ in Verbindung gebracht. Hier beschreiben wir die physikalischen und funktionellen Interaktionen zwischen $K_{v1.5}$ und FHL1.Quantitative PCR Experimente zeigten eine veränderte mRNA Expression für $K_{v1.5}$ und FHL1 Varianten in Myoblasten von XMPMA Patienten im Vergleich zu einer Kontrolle. Anschließende Western Blot Experimente bestätigten ein Fehlen des FHL1A Proteins und eine Reduktion/Fehlen von $K_{v1.5}$ in diesen Zellen. Myoblasten von Patienten zeigten im Vergleich zu einer Kontrolle eine verminderte Proliferationsrate, und eine höhere Anzahl von Zellen in der $G_0/G_1$ Phase. In HL-1 Zellen wurde eine Kolokalisierung von FHL1 und $K_{v1.5}$ im Zytoplasma und der Plasmamembran bestätigt. Zwei-Elektroden-Voltage-Clamp Experimente bestätigten in Xenopus Oozyten, welche $K_{v1.5}$ und FHL1 Varianten exprimierten, eine deutliche Reduktion des Ionenkanalstroms im Vergleich zu Oozyten, die nur $K_{v1.5}$ besitzen, wobei FHL1C den stärksten Effekt zeigte. Eine potenzielle physikalische Wechselwirkung zwischen FHL1C und $K_{v1.5}$ wurde *in vitro* mittels eines Pulldown Assays nacgewiesen. Zusammenfassend beschrieben wir die funktionelle Interaktion von FHL1 und $K_{v1.5}$.. Da eine veränderte Expression und Funktion von $K_{v1.5}$ in XMPMA Patienten vorliegt, vermuten wir eine Rolle von FHL1 in der Regulierung der Kaliumkanäle im Skelett- und Herzmuskel. Der Verlust

eines funktionellen FHL1 könnte eine Fehlregulierung dieser Kanäle auslösen und die Pathophysiologie unserer Patienten erklären.

**ABBREVIATIONS**

| | |
|---|---|
| AF | atrial fibrillation |
| BMD | Becker muscular dystrophy |
| CSNK1D | casein kinase 1, delta |
| Cβ | β catalytic subunit of type 2A protein phosphatase |
| DMD | Duchenne muscular dystrophy |
| DM1 | myotonic dystrophy type 1 |
| EDMD | Emery-Dreifuss muscular dystrophy |
| ER (ESR) | estrogen receptor |
| ERK | extracellular-signal-regulated kinase |
| FHL | four-and-a-half LIM domain protein |
| FISH | fluorescent in situ hybridization |
| GIRK | G protein-activated inward rectifier potassium channel |
| GpI | glycosylphosphatidylinositol |
| Gq | galphaq |
| GST | Glutathione S-Transferase |
| hERG | human ether-a-go-go-related gene |
| IK | K+ current |
| $I_{Kr}$ | delayed rectifier K+ current, rapid component |
| $I_{Kur}$ | delayed rectifier K+ current, ultra rapid component |
| $I_{Ks}$ | delayed rectifier K+ current, slow component |
| KCNA5 | voltage-gated potassium channel subunit $K_{v1.5}$ |
| KCNE | potassium voltage-gated channel subfamily E |
| $K_{v1.5}$ | potassium voltage gated potassium channel 1.5 |
| LGMD | Limb-girdle muscular dystrophy |

| | |
|---|---|
| MAPK (MEK) | mitogen-activated protein kinase |
| MyoD | myogenin D |
| $Na_{v1.5}$ | sodium channel protein alpha subunit type 5 |
| NCAM | neural cell adhesion molecule |
| NFATC1 | nuclear factor of activated T-cells, cytoplasmic 1 |
| PASMC | pulmonary artery smooth muscle cells |
| PH | pulmonary hypertension |
| PP2A | protein phosphatase type 2A |
| RAF1 | RAF proto-oncogene serine/threonine-protein kinase 1 |
| RBM | reducing body myopathy |
| RIP140 | receptor-interacting protein of 140 kDa |
| RSS | rigid spine syndrome |
| Sdpr | serum deprivation response factor |
| SMAD | mothers against decapentaplegic homolog |
| SPM | scapuloperoneal myopathy |
| $SR^{ß}$ | ß-subunit of the signal recognition particle receptor |
| SRF | serum response factor |
| SIFT | Sorting Intolerant From Tolerant |
| TAD | thoracic aortic dissection |
| TFN | tumor necrosis factor |
| TIN | human cardiac titin |
| TLN | talin |
| TNF | tumor necrosis factor receptor |
| XMPMA | X-linked myopathy with postural muscle atrophy |

# 1 INTRODUCTION

Myopathies (myo- μυο "muscle", pathos -pathy "suffering") are neuromuscular disorders characterized by dysfunction of muscle fiber. Muscle weakness, occurring mainly in the muscles of the shoulders, upper arms, thighs and pelvis, is a main symptom in the most myopathies. In exceptions, such as myotonia and paramyotonia congenital, instead of weakness, disease is characterized by muscles enlargement resulting in inability to relax after contraction. Other symptoms of myopathies usually include muscle cramps, stiffness, and spasms. This is a heterogeneous group of conditions with a diverse etiology; myopathies can be classified as primary and secondary. In primary, disease arises primarily to the cause in the muscle fiber. Most of the primary myopathies are hereditary dystrophies, less common are the hereditary congenital myopathies, familial periodic paralysis and other metabolic disorders. Causes for the secondary myopathies originate from outside the muscle fibers and can be divided into inflammatory, endocrine and metabolic disorders.

Inflammatory myopathies are characterized by weakness, endomysial inflammation and elevated muscle enzymes and include dermatomyositis, polymyositis and myositis ossificans. Myositis ossificans is known to be an inherited disorder while causes for dermatomyositis and polymyositis, although speculated to have an autoimmune origin, still remain unknown.

Endocrine-related myopathies are caused by malfunction of endocrine glands resulting change in production of hormones. For example, hyperthyroid myopathy and hypothyroid myopathy are caused by abnormal activity of the thyroid gland. Hyperthyroid myopathy, caused by upregulation of thyroxin, leads to muscle weakness, muscle wasting in hips and shoulders, and less commonly problems in ocular muscles. The hypothyroid myopathy results in stiffness, cramps, and weakness of arm and leg muscles.

Metabolic myopathies are caused by enzymatic defects, usually affecting the ATP supply pathways, and are relatively rare. The condition can be also hereditary and includes glycogen storage diseases, lipid storage diseases, disorders of purine nucleotide metabolism and mitochondrial disorders.

Inherited myopathies are caused by genetic defects leading to the absence or malformation of proteins relevant for contractile properties of the muscle. They include muscular dystrophies, congenital myopathies and periodic paralysis. Although technically myopathies muscular dystrophies are regarded by many authors separately and are defined as diseases of muscle membrane or supporting proteins characterized by on-going muscle degeneration and regeneration leading to far more severe phenotype than common myopathies. For example, defects in dystrophin, protein maintaining the muscle membrane during contraction, lead to Duchenne muscular dystrophy (DMD) or Becker muscular dystrophy (BMD), two most common inherited dystrophies.

Congenital myopathies cause hypotonia and weakness at birth or during the neonatal period and delayed motor development later in childhood. Hypotonia is the clinical hallmark of congenital myopathies. Condition includes nemaline myopathy, myotubular myopathy, central core myopathy, congenital fiber type disproportion and multicore myopathy.

Periodic paralysis is a group of disorders that are part of a broader class of disorders, ion channelopathies, in which a genetic defect in a muscle ion channel lead to episodic stiffness or weakness in response to certain triggers. Common triggers include cold, heat, stress, physical activity and certain foods.

Most inherited myopathies are caused by an autosomal dominant or sometimes autosomal recessive mode of inheritance. However, some myopathies are caused by mutations in X-linked genes. Interestingly, same condition can have different modes of inheritance depending on the gene affected (e.g., Limb-girdle muscular dystrophy (LGMD) can be caused

by defect of a recessive gene either on an autosomal or on the X chromosome. Mitochondrial myopathies have a separate mode of inheritance as they are inherited only through the mother.

X-linked myopathies include conditions such as Duchenne muscular dystrophy, Becker muscular dystrophy, scapuloperoneal myopathy (SPM), reducing body myopathy (RBM), rigid spine syndrome (RSS) and Emery-Dreifuss muscular dystrophy (EDMD).

DMD is the most common muscular dystrophy in children with an incidence of one in 3500 live male births presenting in early childhood. As mentioned previously, DMD, as well as BMD, is caused by mutations in dystrophin gene. It is characterized by proximal muscle weakness and calf hypertrophy. Disease progresses very fast as patients usually become wheelchair-bound by 12 years of age and die in late teens to early twenties. Milder presentation of disease is termed BMD and has an incidence of one in 14 000 live male births. The clinical severity varies but the majority of patients remains ambulant for life (Beggs *et al*., 1991).

Recently our group has described a phenotypically distinct, X-linked myopathy with postural muscle atrophy, termed XMPMA (MIM ID #300696), and linked it to mutations in the human four-and-a-half LIM domain protein 1 (*FHL1*) gene (Windpassinger *et al.*, 2008). XMPMA patients exhibit an adult-onset scapulo-axio-peroneal myopathy. Condition is affecting both skeletal and cardiac muscle; it is characterized by atrophy of postural muscles with rigid spine syndrome, which is also occurring in other FHL1opathies. However, initial muscle hypertrophy is characteristic exclusively for XMPMA (Schoser *et al.*, 2009). Other common features includes pseudoathleticism and hypertrophic cardiomyopathy sometimes accompanied by other cardiac features such as rhythm abnormalities, aneurysm of the sinus of valsalva, increased myocardial mass and increased wall thickness (Windpassinger *et al.*, 2008; Schoser *et al.*, 2009; Binder *et al.*, 2011). Muscle biopsies in younger patients show degenerative myopathy with myofiber hypertrophy in both fiber types and cytoplasmic bodies are found in the majority of the samples. Interestingly, before discovery of FHL1 mutations

many of the XMPMA were diagnosed as to have a Becker dystrophy although no dystrophin mutations or dystrophin expression reduction was found in their muscle samples. Age of onset and age at death are both very variable in affected patients and cause of death is typically respiratory and cardiac failure.

FHL1 is part of the FHL family of proteins that consists of five members: FHL1, FHL2, FHL3, FHL4 and ACT (FHL5); all sharing particular secondary structure consisting of four and a half highly conserved LIM domains. As they lack other functional or structural domains, they belong to the LIM-only protein family. Eight amino residues separate each LIM domain. Conservation of LIM domains is evident in cysteine and histidine residues allowing formation of the finger as well as other amino acids residues suggesting FHL family members might origin from the same ancestor gene-by-gene duplication (Fimia *et al.*, 2000). Through the interactions via LIM domains, FHL proteins are involved in number of cellular functions, including transcription, signal transduction and regulation of cell survival.

LIM-domain is highly conserved protein interaction domain characterized by consensus amino acid sequence Cys-$X_2$-Cys-$X_{16-23}$-His-$X_2$-Cys-$X_2$-Cys-$X_2$-Cys-$X_{16-23}$-Cys-$X_2$-Cys/His/Asp (X representing any amino acid) where cysteine and histidine residues coordinate binding of the two $Zn^{2+}$ in each LIM domain (Michelsen *et al.*, 1993; Kosa *et al.*, 1994). The acronym LIM was first is derived from three homeobox genes encoding structurally similar *Lin 11*, *Isl-1* and *Mec-3* proteins that, besides a homeodomain, contain two copies of a conserved LIM domain (Freyd *et al.,* 1990; Karlsson *et al.,* 1990; Way *et al.*, 1988). Lin-11 is the founding member of the LIM family (Ferguson and Horvitz, 1985; Ferguson *et al.*, 1987; Freyd *et al.,* 1990] and has a role in morphogenesis and asymmetric cell division in *C.elegans* during vulval development (Newman *et al.*, 1999; Gupta *et al.*, 2003). Expression of the transcription factor Islet-1 (Isl-1) is the first molecular indicator of murine motor neuron generation and development (Ericson *et al.,* 1992; Tsuchida *et al.,* 1994;

Pfaff *et al.,* 1996). Mec-3 is the regulator of mechanosensory neuron differentiation in *C.elegans* (Way *et al.*, 1988).

Interestingly, LIM proteins were found in all so far investigated eukaryotes, in human genome alone 135 different LIM domains within more than 50 genes, but none in some of the prokaryote species (Kadrmas *et al.*, 2004). They are involved in various cellular functions as adaptor molecules or as part of scaffolding proteins including linking proteins with both the actin cytoskeleton and transcriptional machinery (Kadrmas *et al.*, 2004; Bach, 2000; Kleiber *et al.*, 2007). By providing protein-protein interacting surfaces LIM proteins modulate assembly of multimeric protein complexes (Kadrmas *et al.*, 2004). They can interact with other LIM proteins, PDZ domains, tyrosine-containing motifs, ankyrin repeats and helix-loop-helix domains (Brown *et al.*, 1999). Possibility of interactions with DNA is still only speculated on (Kadrmas *et al.*, 2004; Morgan *et al.*, 1996).

All FHL proteins are expressed in a tissue-specific manner. FHL1 is predominantly expressed in skeletal and cardiac muscle where it plays a role in sarcomere synthesis and assembly (McGarth *et al*., 2006). It also can be also found in other tissues e.g. brain, placenta, lung, liver and kidney, although at a lower abundance. FHL2 and FHL3 are predominantly expressed in the heart and skeletal muscle, lower levels can be found in the ovary, testis, adrenal and pituitary glands (for FHL2) and in ovary, spleen, and adrenal glands (FHL3) [Fimia, 2000]. FHL4 and ACT are exclusively expressed in the testis (Fimia *et al.*, 2000; Morgan and Madgwick, 1999).

FHL2 participates in cellular processes such as regulation of gene expression, cyto architecture, cell adhesion, cell survival, cell mobility and signal transduction. FHL2 plays a significant role in cancer both as oncoprotein and as a tumor suppressor in a tissue-dependent fashion (Johannessen *et al.*, 2006). On the other hand, depending on the cell-type, FHL2 can repress or activate transcriptional activity (Johannessen *et al.*, 2006). It has been previously reported that FHL2 interacts with more than 50 binding partners from different functional

classes: receptors, structural proteins, signal transducers, transcription factors, splicing factors, DNA replication and repair enzymes, and metabolic enzymes (Johannessen *et al.*, 2006). One of the binding partners is MinK, single transmembrane domain peptide encoded by potassium voltage-gated channel subfamily E (KCNE, see Kupershmidt *et al*., 2002). By interacting with MinK FHL2 allows generation the slowly activating delayed rectifier K+ current (IKs) in a heterologous system (Kupershmidt *et al*., 2002). In addition, recent report by Lin et al showed FHL2 binds human ether-a-go-go-related gene (HERG) (Lin *et al*., 2008). HERG is encoding the a-subunit of the potassium channel underlying the rapid component of the cardiac delayed rectifier current. Mutations in *HERG* gene are one of the common causes of long-QT syndrome (Curran *et al*., 1995). Patch-clamp experiments showed FHL2 interacts with and regulates the HERG channel (Lin *et al*., 2008). Since FHL1 and FHL2 share similar protein structure and localization, it could be speculated FHL1 might also interact with HERG channel.

FHL3 acts as co-activators for transcription factors and is regulated by activation of the Rho signaling pathway (Muller *et al*., 2002). In skeletal muscle, FHL3 interacts with actin and regulates the formation of actin cytoskeleton (Coghill *et al*., 2003). Also by interacting with myogenin D (MyoD) FHL3 negatively regulates MyoD-dependent transcription of muscle genes and thereby myogenesis (Cottle *et al*., 2007). FHL3 was also shown to participate in regulation of myogenic progenitor cell population and skeletal muscle regeneration (Meeson *et al*., 2007). Another research has shown that FHL2 and FHL3 both interact with muscle α7β1 integrin receptor suggesting a role in mechanical stabilization of muscle cells (Samson *et al*., 2004). Since FHL3 has almost the same expression profile as FHL1 and numerous roles in skeletal and cardiac muscle, as a part of our project, we have decided to perform the screening of undiagnosed myopathy patients to look for mutations in FHL3 gene.

FHL4 is exclusively expressed in the testis where it is suggested to be involved in spermatogenesis (Fimia *et al*., 2000; Morgan and Madgwick, 1999).

Similar to FHL4, ACT is expressed in the testis, but also at even higher levels in a variety of tumor cell lines derived from squamous cell carcinomas, melanomas, and leukemia (Morgan *et al*., 2000). High levels of FHL1, FHL2, and FHL3 (but not FHL4) mRNA expression were found in same cell lines (Morgan *et al*., 2000). These findings suggest that FHL proteins play a role in the regulation of transcription in tumor cell lines. In testis, ACT activates cAMP-responsive element modulator (Morgan *et al*., 2000).

FHL1 is the least characterized member of the FHL1 family. Gene was first localized by Lee and collaborators to the human chromosome at Xq27.2 by somatic cell hybrid mapping, fluorescent in situ hybridization (FISH) and radiation hybrid mapping and termed it *SLIM1* (Lee *et al*., 1998). Same group has first detected high expression of FHL1 in skeletal muscle, a moderate one in the heart and low expression in the placenta, ovary, prostate, testis, small intestine, colon and spleen (Lee *et al.*, 1998). Only a year later Brown and collaborators have reported there are at least two isoforms of FHL1 and second one was termed SLIMMER (Brown *et al*., 1999). First three LIM domains are identical in both proteins but SLIMMER contains a novel C-terminal domain containing three nuclear localization signals, a putative nuclear export sequence, and sequence identical to the RBP-J binding region of KyoT2, a murine isoform of SLIM1 (Brown *et al*., 1999). Different structural organization and cellular localization suggested distinct roles for these two proteins. Thanks to the discovery of role of FHL1 in muscular myopathies and as a tumor suppressor FHL1 is currently researched by numerous groups from various backgrounds and more data on proteins role and interactions becomes available each month.

It is today known that FHL1 is expressed in at least three alternatively spliced isoforms (A, B and C, Scheme 1) which differ in their amino acid sequence, expression pattern, binding partners and subcellular localization (Windpassinger *et al*., 2008). Most of

available data today is on the prevalently expressed FHL1A and most of the papers naming FHL1 (especially those from 1990') actually refer to this isoform.

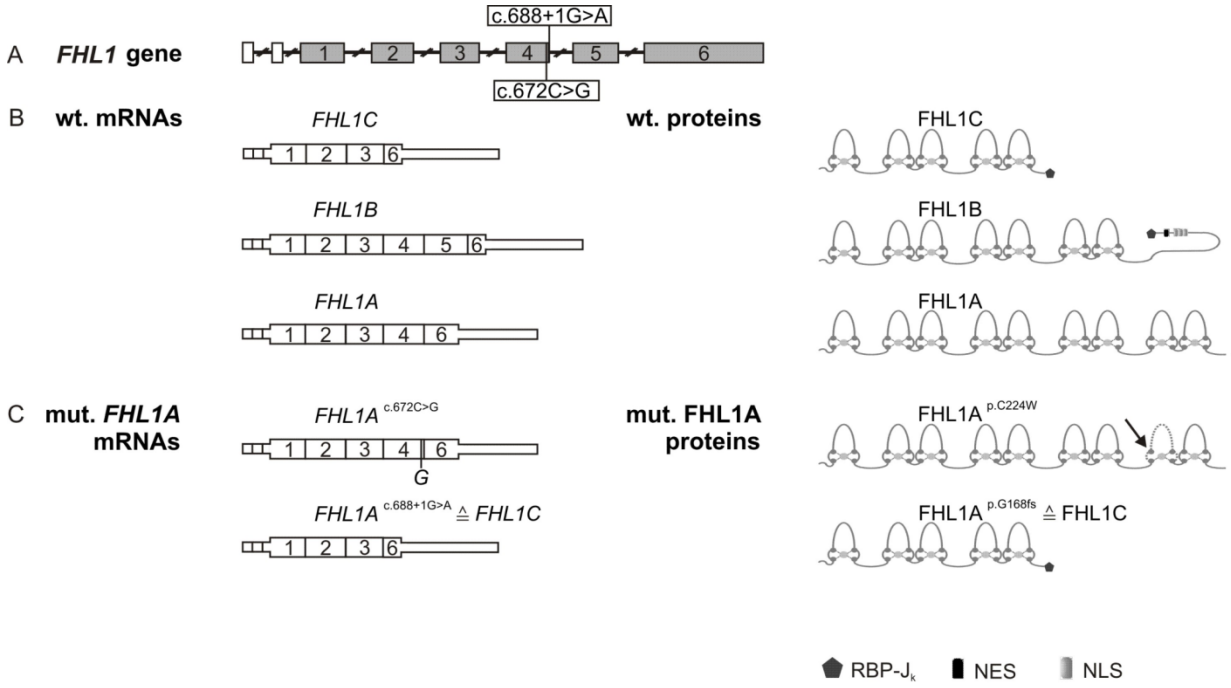


**Scheme 1** (**A**) **Genomic organization of the FHL1 gene** Numbering of exons (1 to 6) in human *FHL1* gene begins with the first coding exon (coding exons are highlighted in grey). The noncoding exons are shown as white rectangles. Positions for the mutations c.672C>G and c.688+1G>A found in XMPMA patients corresponding to the first nucleotide of the start codon of the mRNA (NM_001449) are indicated. (**B**) **Molecular organizations of wild-type FHL1 mRNA and protein variants** *Left*: Wild type (wt) mRNAs of *FHL1A*, *FHL1B* and *FHL1C* are shown. Coding areas of mRNAs are indicated as broad segments, untranslated areas are indicated as narrow segments. *Right*: Wild type (wt) FHL1A, FHL1B and FHL1C protein structures including the LIM domain architecture and functional domains (*RBP-Jκ*, recombination signal-binding protein 1 for J-kappa; *NLS*, nuclear localization signals; *NES*, nuclear export sequence) of the corresponding FHL1 isoforms is shown. (**C**) **Molecular consequences of FHL1A mutations** Molecular consequences of the mutations c.672C>G and c.688+1G>A on mRNA and the corresponding mutated FHL1A proteins at position 224 (FHL1A$^{p.C224W}$) and 168 (FHL1A$^{p.\ G168fs}$) are shown. *Left*: Mutated (mut.) mRNAs of *FHL1A* are shown. Coding areas of mRNAs are indicated as broad segments, untranslated areas are indicated as narrow segments. Note: mutated *FHL1A*$^{c.688+1G>A}$ is identical to wild-type *FHL1C* mRNA. The position of the missense mutation c.672C>G within the mutated *FHL1A* mRNA is indicated. *Right*: Mutated (mut.) FHL1A protein structures including the LIM domain architecture and the functional RBP-Jκ domain are shown. Note: mutated FHL1A at position 224 (termed FHL1A$^{p.C224W}$) is identical to wild-type FHL1C protein. An arrow in the fourth LIM domain indicates the position of the amino acid exchange within the mutated FHL1A protein and the dotted line suggests alterations in the LIM-like architecture. Note: mutated FHL1A$^{p.G168fs}$ is identical to wild-type FHL1C protein (G=glycine, fs = frame shift).

FHL1A (280 amino acids, originally referred as SLIM1) is the full-length isoform predominantly expressed in striated muscles (Lee *et al.*, 1998) and it is localized to the sarcolemma, sarcomere, and nucleus of muscle cells (Brown *et al*., 1999). Intermediate levels of the FHL1A can be found in heart and low level expression in prostate, colon, testis, ovary, small intestine, and placenta (Brown *et al*., 1999). Through the interaction with muscle relevant proteins FHL1A is involved in several functions in the striated muscles. Underlying mechanism for most of the interactions remains unknown. However, in 2006 McGarth and collaborators have described in detail interaction between N' terminal part of FHL1A and myosin binding protein-C (McGarth *et al*., 2006). This interaction was shown to result in regulation of sarcomere assembly (McGarth *et al*., 2006). FHL1A is also known to be involved in the mechanism of pathological hypertrophy by sensing biomechanical stress responses via activation of the extracellular-signal-regulated kinase (ERK) pathway (Sheikh *et al*., 2008). In addition to the prevalently expressed FHL1A, two minor splice variants, originally identified from murine studies, exist. Alternative splicing is resulting in novel domains in the C-terminal part of FHL1B and FHL1C (Lee *et al.*, 1999; Ng *et al.*, 2001). FHL1B (323 amino acids, the homolog of murine KyoT3) is specifically expressed in brain (Lee *et al.*, 1999). It comprises the N-terminal three and a half LIM domains and a novel C-terminus containing three nuclear localization signals, a nuclear export sequence, and a C-terminal binding site for RBP-Jκ (Lee *et al.*, 1999). Due to the first nuclear localization signal domain, this isoform, originally referred as SLIMMER, is predominantly expressed in the cell nucleus of the C2C12 myoblasts (Brown *et al*., 1999). However, in differentiated myotubes localization of the protein shifts to the cytosol suggesting a role in cytoskeleton and nuclear-cytoplasmic communication (Brown *et al*., 1999). It has been recently reported that FHL1B shuttles between nucleus and cytoplasm at different phases of the cell cycle and that C-terminus domain of FHL1B interacts with the β catalytic subunit (Cβ) of a type 2A protein phosphatase (PP2A) (Wong *et al*., 2010). It is speculated that, through the interaction with

Cβ, FHL1B might regulate cell cycle. FHL1B also has a function in delaying skeletal muscle apoptosis via an interaction with the proapoptotic factor Siva-1 (Cottle *et al*., 2009). Siva-1 is a zinc containing protein involved apoptosis by interaction with CD27 antigen, a member of the tumor necrosis factor receptor (TFNR) superfamily (Prasad *et al.*, 1997). In C2C12 myoblasts, FHL1B delays Siva-1-dependent apoptosis (Cottle *et al*., 2009). Two proteins were found to colocalize in the nucleus of apoptotic myofibers of skeletal muscle sections from the mdx mouse model of Duchenne muscular dystrophy (Cottle *et al*., 2009). These findings suggest FHL1B may protect skeletal muscle from apoptosis.

FHL1C (194 amino acids, the homolog of murine KyoT2) is the least characterized variant of FHL1. It contains the N-terminal two and a half LIM domains and the C-terminal binding site for RBP-Jκ. Interaction between FHL1C and RBP-Jκ leads to repression of transcription activity of RBP-Jκ and could results in lack of regulation of RBP-Jκ activity (Ng *et al.*, 2001). FHL1C is localized both to the cell nucleus and to cytoplasm. Since FHL1C, unlike B isoform, has no nuclear localization signal domains, shuttling to the cell nucleus might be mediated by interaction with another protein (Ng *et al.*, 2001). FHL1C is specifically expressed in testis, skeletal muscle and heart, however at a relatively low level compared to FHL1A (Ng *et al.*, 2001). In the human heart, FHL1C expression was more precisely localized in the left and right ventricles, with lower expression in the aorta and the left atrium (Ng *et al.*, 2001).

Presence of RBP-Jκ binding domain in the protein structure allows both FHL1B and C isoforms involvement in Notch signaling pathway (Taniguchi *et al*., 1998; High *et al*., 2008; Liang *et al*., 2008). Notch signaling is a pathway involved in control of numerous developmental processes including cell fate determination, differentiation, proliferation and apoptosis (High *et al*., 2008). RBP-J is a DNA binding protein that suppresses the transcription of Notch target genes. FHL1B and FHL1C compete with transcriptional

activators for interaction with RBP-Jκ and repress RBP-J-mediated transactivation pathway (Scheme 2). (Taniguchi *et al*., 1998; Liang *et al*., 2008; Qin *et al*., 2004, Qin *et al*., 2005).

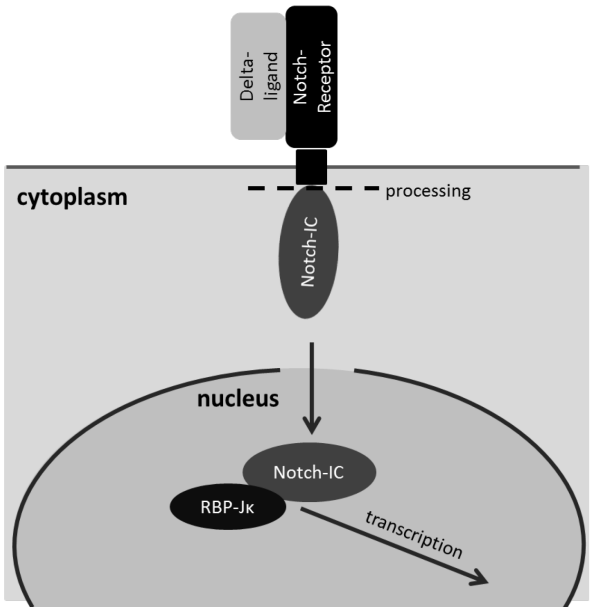


**Scheme 2**: **Notch-1/RBP-Jk signaling pathway in mammalian cells**. Delta binding to Notch invokes regulated intramembrane proteolysis and nuclear translocation of the Notch intracellular domain. The cleaved intracellular domain enters the nucleus and heterodimerizes with RBP-Jk to activate specifically target gene transcription. Scheme adapted from Schraets *et al.,* 2003.

As previously mentioned FHL family members are implicated to play a role in the regulation of transcription in tumor cell lines. FHL1 solely is reported to be downregulated in number of different cancer types including lung, breast, ovarian, prostate, colon, brain, renal, liver, gastric, thyroid, melanoma, hepatocellular carcinoma and skin cancers (Bhattacharje *et al*., 2001; Jiang *et al*., 2004; Fryknäs *et al*., 2006; Shen *et al*., 2006; Li *et al*., 2008; Sakashita *et al*., 2008; Aldred *et al*., 2004; Finley *et al*., 2004; LaTulippe *et al*., 2002; Dhanasekaran *et al*., 2001; Perou *et al*., 2000; Ding *et al*., 2009). Besides being downregulated in various cancers FHL1 was shown to act as a tumor suppressor in breast, kidney, and prostate cancer by inducing expression of serum deprivation response factor (Sdpr) in Src-transformed cells (Shen *et al*., 2006; Li *et al*., 2008). It was previously reported by the same group that Src tyrosine kinase suppresses FHL1 activity resulting in non-anchored tumor-cell growth and

migration (Shen *et al*., 2006). Less than a year later, in 2009, Ding and collaborators have demonstrated that FHL family members FHL1, FHL2, and FHL3 physically and functionally interact with Smad2, Smad3, and Smad4, regulators of cancer development and progression through a TGF-beta-like signaling pathway (Ding *et al*., 2009).

Interestingly, two of the XMPMA patients, both smokers, have died of lung cancer. FHL1A is reported to be moderately expressed in human lung tissue while isoforms B and C were not detected (Lee *et al*., 1999; Ng *et al*., 2001). Recent report shows FHL1 is downregulated in lung cancer patients and inhibits growth of human lung cancer cell lines (Niu *et al*., 2011). On the other hand, FHL1A protein was found to be significantly upregulated in rat model of pulmonary hypertension and in lungs from patients with idiopathic pulmonary arterial hypertension (Kwapiszewska *et al*., 2008). Much like cancer, pulmonary hypertension is caused by the uncontrolled proliferation of cells. Silencing of FHL1 in primary human pulmonary artery smooth muscle cells (PASMC) also inhibits cell migration and proliferation, whereas overexpression has the opposite effect (Kwapiszewska *et al*., 2008). Taken in consideration FHL1 expression is also altered in human lung carcinoma, one could speculate similar mechanism could lead to both conditions (Bhattacharjee *et al*., 2001; Jiang *et al*., 2004).

Besides differences in the primary structure and expression patterns, different subcellular localization between FHL1 and corresponding isoforms suggests a specific interaction with various binding partners. To date, at least six putative FHL1 protein interactions exist while up to 19 FHL1 full-length interacting protein partners have been identified. Identified binding partner display variety of different functions and represent another prove for multifunctional roles of FHL1 in skeletal muscle as well as cancer. Muscle relevant proteins that interact with FHL1 (Table 1) include proteins such as Myosin-binding protein C (MyBPC), ERK2, SRF, FHL2 (McGarth *et al*., 2006; Sheikh *et al*., 2008; Foster *et al*., 2006; Cottle *et al*., 2009).

**Table 1: FHL1A binding partners.** Muscle relevant (white) and other (gray) proteins. Table adapted from Shathasivam et al, 2011.

| Gene | Protein | Function | Interaction with FHL1A |
|---|---|---|---|
| *MYBPC1* | Myosin binding protein C, slow type | Contributes to the stability and maintenance of sarcomeres by regulating myosin, actin, and titin | C10 domain of MyBP-C 1 interacts with N-terminal domain of FHL1 |
| *MYBPC3* | Myosin binding protein C, cardiac | Involved in cardiac contraction, regulated by phosphorylation by cAMP-dependent protein kinase (PKA) upon adrenergic stimulation | C10 domain of MyBP-C 3 interacts with N-terminal domain of FHL1 |
| *ERK2* | Extracellular signal-regulated kinase 2 | Part of the protein kinase cascade regulating cell growth and differentiation | Interacts with FHL1 LIM 1 and 2 domains |
| *ERK2 (TYDD)* | Constitutively phosphorylated ERK2 mutant | Impaired functionality of ERK2 leading to lack of regulation of cell growth and differentiation | Interacts with FHL1 LIM 1 and 2 domains |
| *SRF* | Serum response factor | Cell proliferation and differentiation: transcriptional regulation of growth-factor-inducible genes | Interacts with FHL1 LIM domains |
| *FHL2* | Four and a half LIM domains protein 2 | Regulation of gene expression, cyto architecture, cell adhesion, cell survival, cell mobility and signal transduction | Unknown |
| *KCNA5* | Voltage-gated potassium channel subunit $K_{v1.5}$ | Myocardial repolarization, in skeletal muscle: cell proliferation | C-terminal part of $K_{v1.5}$ interacts with FHL1 N-terminal domain |
| *NFATC1* | Nuclear factor of activated T-cells, cytoplasmic 1 | Regulation of T-cell development and function, control of gene expression in embryonic cardiac cells | Unknown |
| *TLN1* | Talin 1 | Actin filaments assembly, spreading and migration of various cell types | Unknown |
| *TTN* | Human cardiac titin | Contraction of striated muscle: responsible for | N2B domain of titin |

| | | | |
|---|---|---|---|
| | | the passive elasticity of muscle | |
| *RAF1* | RAF proto-oncogene serine/threonine-protein kinase | Involved in the MAPK/ERK signal transduction pathway as part of a protein kinase cascade | Interacts with FHL1 LIM 1 and 2 domains |
| *MAPK2 (MEK2)* | Mitogen-activated protein kinase kinase 2 | Part of a RAS/MAPK signaling pathway responsible for proliferation, differentiation, migration and apoptosis | Interacts with FHL1 LIM 1 and 2 domains |
| *RIP140* | Receptor-interacting protein of 140 kDa | Regulation of lipid and glucose metabolism, regulation of gene expression in metabolic tissues including heart, skeletal muscle, and liver | All FHL1 domains are required for interaction |
| *SMAD2* | Mothers against decapentaplegic homolog 2 | Regulates cell proliferation, apoptosis, and differentiation by mediating transcriptional effects of TGF-β signaling | Unknown |
| *SMAD3* | Mothers against decapentaplegic homolog 3 | Regulates cell signaling by modulating signaling of activin and TGFβ | Unknown |
| *SMAD4* | Mothers against decapentaplegic homolog 4 | Regulates cell signaling by modulating signaling of TGFβ | Unknown |
| *CSNK1D* | Casein kinase 1, delta | control of cytoplasmic and nuclear processes, including DNA replication and repair by phosphorylation of various proteins | Unknown |
| *ERα (ESR1)* | Estrogen receptor α (NR3A1) | Nuclear receptor transcription factor | N-terminal (1-185) *ERα* estrogen independent activation function domain interacts with FHL1 LIM 1, 2, and 3 domains |
| *ERβ (ESR2)* | Estrogen receptor β (NR3A2) | Nuclear receptor transcription factor | N-terminal (1-145) *ERβ* estrogen independent activation function domain interacts with FHL1 LIM 1, 2, and 3 domains |

FHL1 has several important functions in skeletal muscle most of which are mediated through these interactions. For example, interaction between second LIM domain of FHL1 and C-terminus MyBP-C allows FHL1 to sarcomere formation during myogenesis (McGarth *et al*., 2006). MyBPC is the one of the major myosin-associated proteins in striated muscle that upregulates the lateral association and stabilization of myosin thick filaments and regulates actomyosin interactions (McGarth *et al*., 2006). Interestingly, mutations in the same C-terminus part result in truncation of MyBP-C leading to loss of the myosin, titin and FHL1 binding sites (McGarth *et al*., 2006; Flashman *et al*., 2004). MyBP-C are also reported to be are one of the leading causes of familial hypertrophic cardiomyopathy (Watkins *et al*., 1995; Bonne *et al*., 1995).

Through the interaction with Raf1, MEK2 and ERK2, FHL1 interacts with the Gq signaling pathway and by acting as an endogenous positive regulator of Raf-1/MEK/ERK–mediated signaling; FHL1 plays a role in the development of cardiac hypertrophy (Skeikh *et al*., 2008).

Regarding the role in skeletal muscle, FHL1 also promotes myoblast fusion and postnatal muscle growth by activation of the calcineurin/NFAT pathway; overexpression of FHL1 in mouse skeletal muscle promotes myocardial fusion and hypertrophy (Crowling *et al*., 2008). In murine model FHL1-induced hypertrophy is mediated via coactivation of NFATc1-dependent transcription, a downstream target of the calcineurin signaling pathway (Crowling *et al*., 2008). This interaction is particularly important for hereditary myopathies as NFATc1 stimulates production of utrophin, a homolog of dystrophin. As mentioned above, mutations in dystrophin gene lead to reduced expression of dystrophin at the sarcolemma causing DMD or BMD. An increase in levels of utrophin is currently believed to be a possible approach in treatment of DMD and there are several clinical trials offering promising results. Another report by Sheikh et al describes hypertrophic response and a beneficial functional response to pressure overload induced by transverse aortic constriction in FHL1 knockout

mice (Sheikh *et al*., 2008). It has been also shown that FHL1 interferes with Galphaq (Gq) signaling pathway as FHL1 deficiency prevents the cardiomyopathy in Gq transgenic mice (Sheikh *et al*., 2008). These observations have potential implications for human myopathy. Indeed, several mutations in the FHL1 gene are associated with hereditary (cardio) myopathy and four distinct types of muscular dystrophies and myopathies (Windpassinger *et al*., 2007; Schoser *et al*., 2009; Gueneau *et al*., 2009; Schessl *et al*., 2009).

This will be addressed in more detail later in the text.

Yang et al (Yang *et al*., 2008) have recently identified $K_{v1.5}$ as another binding partner of FHL1 and described the interaction between FHL1A and C terminal part of the $K_{v1.5}$ channel. $K_{v1.5}$ (KCNA5) is a potassium channel abundantly expressed in skeletal muscle (Lesage *et al*., 1992). $K_{v1.5}$ plays a role in myocardial repolarization where $K_{v1.5}$ -subunit forms the major basis of an atrial-specific, ultra-rapid delayed rectifier K+ current ($I_{Kur}$) vital for atrial repolarization (Wang *et al*., 1993). In the human heart, K+ current ($I_K$) consists of three different components: the ultra rapid ($I_{Kur}$), rapid ($I_{Kr}$) and slow ($I_{Ks}$) current (Tamargo *et al*., 2003). $K_{v1.5}$ and Kvβ1.2 subunit together form the $I_{Kur}$ in human atrium (Martens *et al.,* 1999).

$K_{v1.5}$ mutations are reported to trigger atrial fibrillation (AF) (Van Wagoner *et al*., 1997; Olson *et al*., 2006; Yang *et al*., 2010). AF is a common cardiac arrhythmia characterized by rapid, erratic electrical activation of the atrial myocardium, resulting in loss of effective contractility, an increased likelihood of clot formation and an increased risk of stroke (Yang *et al*., 2010). $K_{v1.5}$ mutations usually lead to truncation of the protein resulting in inability to generate the ultra rapid delayed rectifier current $I_{Kur}$ (Olson *et al*., 2006; Yang *et al*., 2010). For that reason $K_{v1.5}$ is presently a major focus of research efforts seeking new therapeutic strategies for treatment of AF (Ehrlich *et al*., 2008). Interestingly AF was also reported in two heterozygous women caring FHL1 mutations (Binder *et al*., 2011).

In 2002, Chittajallu and collaborators have described how $K_{v1.5}$ together with $K_{v1.3}$ plays a role in glial proliferation (Chittajallu *et al*., 2002). It has been recently reported that $K_{v1.5}$ also plays a role in skeletal muscle proliferation by controlling G1-phase progression through by negatively regulating cyclins A and D1 and accumulating p21cip-1 and p27kip1 (Villalonga *et al*., 2008).

Both, FHL1 and $K_{v1.5}$ are expressed in skeletal muscle (Brown *et al*., 1999; Lesage *et al*., 1992; Feng *et al*., 1997) and FHL1 modulates $K_{v1.5}$ channel currents. FHL1 is a key molecular component in the *I*Kur complex (Yang *et al*., 2008). As dysfunction in FHL1 would have serious clinical consequences, and may cause genetically determined arrhythmia and/or cardiomyopathy, the present study aimed at investigating the role of two FHL1A mutations/isoforms (associated with XMPMA), to modulate $K_{v1.5}$ channel currents. Our first aim was to investigate whether the skeletal muscle cells in patients with FHL1 mutations exhibit change in proliferation compared to the wild type muscle. Also taken in consideration that XMPMA patients show different cardiac involvement and cause of death is heart failure we have characterized functional interaction of $K_{v1.5}$ and FHL1 by performing electrophysiological experiments.

A recent study has indicated there might be another potential candidate for binding FHL1 among the potassium channels. Lin et al have described human ether-a-go-go-related gene (HERG) interaction FHL2, another member of FHL family very similar to FHL1 (Lin *et al*., 2008). HERG encodes the pore-forming K+ channel subunit that underlies the $I_{Kur}$ and plays an important role in control of cardiac excitability (Trudeau *et al*., 1995; Sanguinetti *et al*., 1995). Mutations in HERG can result in blockage of the channel leading to reduction in $I_{Kur}$; consequently cardiac action potential is prolonged and long-QT syndrome occurs (Sanguinetti *et al*., 2006). Long QT syndrome is a disorder of myocellular repolarization that can lead to ventricular tachyarrhythmia and sudden cardiac death. Interaction of FHL2 with

the HERG channel has a regulatory effect on channel function by upregulating the maximum current amplitude (Lin *et al*., 2008).

In our experimental work, we have focused on two mutations found in XMPMA patients. Most prominent FHL1 mutation in XMPMA patients, an amino acid substitution, termed p.C224W, was found in a large Austrian family and later confirmed in several other families (Windpassinger *et al*., 2007; Schoser *et al*., 2009). It is a missense mutation that replaces a highly conserved cysteine within the fourth LIM domain of FHL1 leaving the LIM domain disrupted (Scheme 1). As a result, almost complete absence of FHL1A protein is recorded in skeletal muscle biopsies of affected individuals. Mutations in conserved cysteines coordinating the zinc finger can disrupt the stability of the LIM tertiary structure and cause the collapse of the entire domain. It has been previously reported that such mutations can lead to hypertrophic cardiomyopathy, feature that is also present in XMPMA patients (Schoser *et al*., 2009). For example, in another LIM protein MLP (also termed CSRP3) mutations of a $Zn^{2+}$-coordinating cysteine residue disrupt the $Zn^{2+}$ binding within the LIM domain, destabilizing the protein and reducing its ability to interact with other proteins directly leading to hereditary hypertrophic cardiomyopathy (Geier *et al*., 2003; Geier *et al*., 2008). Therefore, we can speculate that mutations such as p.C224W could also be responsible for hypertrophy in XMPMA patients. Much like other FHL1 mutations in XMPMA patients' p.C224W is not affecting FHL1C isoform.

The second mutation addressed in our functional studies is the splice site mutation pA168GfsX195, termed p.G168fs, it is located after the second LIM domain, and is affecting FHL1A and FHL1B isoforms only (Schoser *et al*., 2009). As a new splice donor site occurs after exon 4 FHL1A transcript is lacking exon 4, and the resulting messenger RNA is translated into a truncated FHL1A protein identical to FHL1C (Scheme 3).

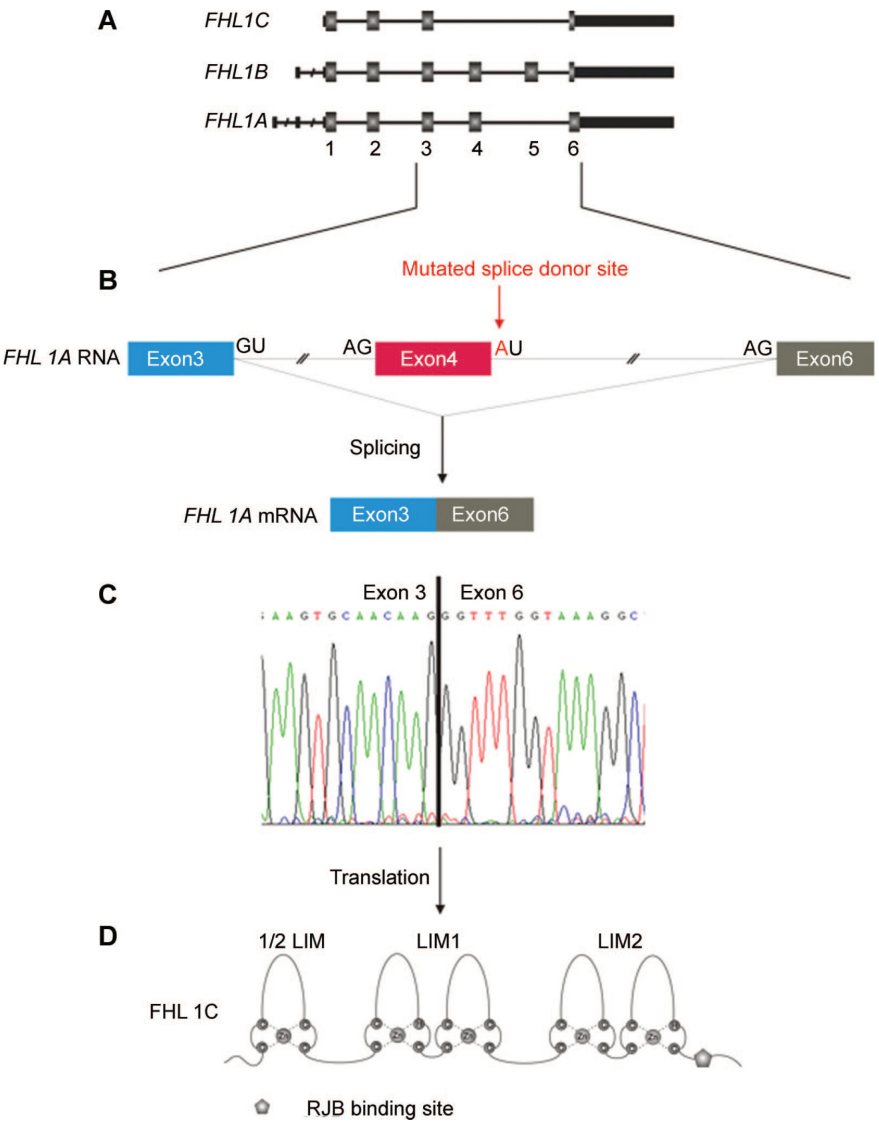


**Scheme 3: p.G168fs mutation** (A) the genomic organization of *FHL1,* (B) overview of the p.G168fs mutation site and the consequences of the donor splice-site mutation in intron 4 of *FHL1A* on messenger RNA (mRNA) level, (C) electropherogram showing the sequence of the reverse transcriptase PCR from myoblasts with skipped exon 4, (D) the resulting protein (FHL1C). Figure from Schoser *et al*, Neurology, 2010.

Other mutations reported in XMPMA patients include p.H246Y and p.V280M (Schoser *et al*., 2009). p.H246Y is a hemizygous missense mutation in exon 6 of FHL1A leading to exchange of a highly conserved histidine coordinating a Zn finger with a tyrosine. Because of amino acid change, much like p.C224W, p.H246Y leads to destabilization of the fourth LIM domain. For FHL1B this is mutation a synonymous mutation on protein level. Isoform C is also not affected. On the other hand the amino acid substitution V280M only affects FHL1B; mutation is located between the nuclear export signal and the RBP-J binding

domain of this isoform and although not affecting any of the functional domains it is predicted as “not tolerated” by the SIFT (Sorting Intolerant From Tolerant) prediction program (Schoser *et al*., 2009).

Our aim in this study was to describe physical and functional interaction between $K_{v1.5}$ and FHL1 proteins in XMPMA patients. We were particularly interested to investigate whether there is a difference in skeletal muscle cells protein expression patterns and proliferation in patients with FHL1 mutations compared to the wild type muscle. Also taken in consideration that XMPMA patients show different cardiac involvement and cause of death is heart failure we have characterized functional interaction of $K_{v1.5}$ and FHL1 by performing electrophysiological experiments. Also, as an additional project we have attempted to identify novel mutations in FHL3 gene of undiagnosed myopathy patients. Since FHL3 shares similar localization and functionality in human skeletal muscle, it could be a good candidate gene in cases where cause of hereditary myopathy remains unknown.

# 2 MATERIALS AND METHODS

## 2.1 Materials

Fetal Calf Serum (FCS), Glutamax, Gentamycin, 0.25% trypsin, Hank's Balanced Salt Solution (HBSS) buffer, Phosphate Buffered Saline (PBS), TRIzol®, SuperScript III Reverse Transcriptase (RT), sodium pyruvate, Lipofectamine, NuPage® 4-12% Bis-Tris Gel, NuPage® MES SDS running buffer, NuPage® LDS sample buffer, NuPage® sample reducing agent and 4',6-diamidino-2-phenylindole were from Gibco Invitrogen (Lofer, Austria). Skeletal muscle cell growth medium was from PromoCell GmbH (Heidelberg, Germany). DC Protein Assay Kit and Bradford reagent were from Bio-Rad (Vienna, Austria). TRI Reagent was from MRC Inc. (Vienna, Austria). Pepsin, Claycomb medium and protease inhibitors P8340 were from Fluka Sigma Aldrich (Munich, Germany). CyStain DNA/protein staining solution was from Partec GmbH (Muenster, Germany). Lysate containing [$^{35}$S] Met-labeled and glutathione-Sepharose beads and pGEX-MXT-4T vector were from Amersham GE Healthcare (Vienna, Austria). Rabbit reticulocyte Lysate System Promega Cat. No. M6101 and RQ1 RNase-Free DNAse Cat. No. M6101 were from Promega (Mannheim, Germany). Nitrocellulose membranes (0.45 μm pore size) were from Schleicher and Schuell (Dassel, Germany). Restore™ Western Blot Stripping buffer was from Pierce Fisher Scientific GmbH (Vienna, Austria). Films for Autoradiography were from Agfa (Vienna, Austria). Immobilon Western Chemiluminescent Horseradish Peroxidase (HRP) substrate and IHC Select® Fast Red Chromogen A were from Millipore (Billerica, MA, USA). HotStart Taq Master Mix was from Qiagen (Hilden, Germany). BigDye Terminator 3.1 Cycle Sequencing Kit and SYBER Green PCR master mix were from Applied Biosystems (Vienna, Austria). Dako-Pen was from Dako (Dako UK Ltd, Cambridgeshire, UK). Vector pEYFP-N1 was from Clontech Laboratories, Inc. (Mountain View, CA, USA).

Mouse anti-human neural cell adhesion molecule (Clone 123C3) was from Monosan (Uden, Netherlands). Mouse Anti-Myogenin (1:20) and Mouse Anti-MyoD (1:40) antibody were from BD Pharmingen$^{TM}$ (San Diego, CA, USA). Polyclonal rabbit anti-human FHL1 antibody cross-reacting with the fourth LIM domain (coded for by exon 4-6) of FHL1A was from AVIVA Systems Biology (San Diego, CA, USA). Polyclonal goat anti-human $K_{v1.5}$, monoclonal mouse anti-human β-actin and HRP-conjugated donkey anti-goat IgG antibodies were from Santa Cruz Biotechnology, Inc. (Santa Cruz, CA, USA). Anti-mouse IgG biotinylated (RPN1001V) and Anti-sheep/goat Ig, biotinylated (RPN1025V) were from GE Healthcare (Vienna, Austria). Cyanine 3 (Cy3)-conjugated AffiniPure goat anti-mouse IgG was from Jackson ImmunoResearch (West Grove, PA, USA). HRP-conjugated swine anti-rabbit IgG were from Dako (Vienna, Austria) and HRP-conjugated goat anti-mouse IgG was from Rockland (Gilbertsville, PA, USA).

## 2.2 Methods

### 2.2.1 Cell culture and tissue acquisition

(i) Human myoblast cultures were established from muscle biopsies of two male unaffected individuals (controls, termed WT1 and WT2) and two male XMPMA patients (termed p.C224W and p.G168fs). The ethic board of the Ludwig-Maximilians University, Munich, Germany, gave ethical approval. Tissue sources for myoblast isolation were Tibialis anterior muscle biopsy (WT1 and p.C224W) and Anterior biceps brachii muscle biopsy (WT2 and p.G168fs). Myoblasts were grown in skeletal muscle cell growth medium including supplement mix containing 10% (v/v) FCS, 1.5% (v/v) 100 x Glutamax**,** 50 µl/ml gentamycin. Protocol including growing myoblasts without adding FCS in the medium prior to measuring proliferation was also tested but the cells were not surviving in the given conditions.

Therefore, FCS was present in the medium at all times. Purity of isolated cells was investigated by staining with suitable antibodies as described below (see 2.2.2).

(ii) The cardiac muscle cell line HL-1 established from the AT-1 mouse atrial cardiomyocyte cell lines was used (Claycomb *et al.*, 1998). Cells were grown in Claycomb medium including 10% [v/v] FCS at 37°C on atmosphere of 5% $CO_2$ and 95% air at the relative humidity of 95%.

(iii) Tissue samples from human heart ears (sample size around 1 $cm^3$) were obtained from non-XMPMA patients (patients with no signs of cardiac hypertrophy) and served as controls. Samples were taken during undergoing cardiac surgery. After cutting into smaller sections (around 0.2 $cm^3$) samples were immediately frozen in liquid $N_2$.and stored on -70°C.

(iv) Tissue samples from human cardiac compartments (sample size around 1 $cm^3$) were obtained from autopsies from healthy controls, frozen in liquid $N_2$ and stored on -70°C.

### 2.2.2 Immunocytochemistry

Myoblasts ($2x10^5$ cells) were seeded in four-well Lab-Tek®II Chamber slides™ (Nunc) and cultured for 48 h. Cells were fixed with fixation buffer (100 ml PBS [pH 7.0] containing 650 mg $Na_2HPO_4$, 400 mg $NaHPO_4$, 1.5 ml MetOH, 10 ml 37% [v/v] formaldehyde) and then washed with PBS only. Then, the cells were incubated with the primary antibody (1:20 for NCAM, 1:40 for Myogenin and 1:40 for MyoD) overnight at 4°C in the humidity chamber. After washing with PBS the cells were incubated with Cy3-conjugated goat anti-mouse IgG (1:400) in the dark for 30 min at 25°C. All antibodies were diluted in Antibody Diluents from Dako (Vienna, Austria). Nuclei were stained with 4', 6-diamidino-2-phenylindole (Kennett *et al.*, 2010). Fluorescent signals were detected using Axiovert 200M microscope (Zeiss) and Axiovision Rel4.6 Software. Filter settings were for Cy3 excitation (band pass: 546/12) and emission (band pass: 575-640) and for DAPI excitation (365 nm) and emission (band pass: 445/50).

### 2.2.3 DNA constructs

For protein expression in *Xenopus* oocytes, FHL1A, FHL1A$^{p.C224W}$, FHL1C and $K_{v1.5}$ inserts were synthesized by the PCR using suitable PCR primers **(**Table 2, white rows**)** and cloned into the pBSmxt oocyte expression vector (Supplements, Scheme I). cDNA templates from a full-length human cDNA library (human fetal brain marathon cDNA), clone $K_{v1.5}$-pcDNA3.1 (obtained from J. Ehrlich), clone Herg-pSP64 (obtained from M. Sanguinetti) and patients' cDNA (for FHL1A$^{p.C224W}$) were used as PCR templates. The resulting pBSmxt constructs were linearized, cRNA was synthesized as described (Wagner *et al.*, 2010), aliquots were shock frozen in liquid nitrogen and stored at -70$^{o}$C until use.

Integrity of all DNA constructs was verified by DNA-sequencing as described below (see 2.2.4). DNA was prepared by Qiagen midiprep kit and concentration and purity was tested with Nanodrop (Thermo Scientific, Waltham, MA, USA).

**Table 2: Description of primers for DNA constructs, the expected amplified fragment size, and the annealing temperature.** White: primers for pBSmxt constructs used in Two-electrode voltage clamp experiments; light grey: primers for pGEX-4T construct used in pull-down assay; dark grey: primers for fluorescently labeled construct used in colocalization experiments.

| Gene - vector **Accession Nr**. | **Primers** | **Fragment size (bp)** | **Annealing temp. (°C)** |
|---|---|---|---|
| $K_{v1.5}$ - pBSmxt **NM_002234** | F 5' TATGAATTCATGGAGATCGCCCTGGTGCC 3'<br>R 5' TATGCGGCCGCTCACAAATCTGTTTCCCGGCTGG 3' | 1850 | 58 |
| *Herg* - pBSmxt **NM_000238** | F 5' TATGAATTCATGCCGGTGCGGAGGGGC 3'<br>R 5' TATGCGGCCGCCTAACTGCCCGGGTCCGAGC 3' | 3480 | 57 |
| *FHL1A* – pBSmxt **NM_001449** | F 5' TATGAATTCATGGCGGAGAAGTTTGACTGCCA 3'<br>R 5' TATGCGGCCGCTTACAGCTTTTTGGCACAGTCGGG 3' | 851 | 57 |
| *FHL1A*$^{p.C224W}$ - pBSmxt **NM_001449** | F 5' TATGAATTCATGGCGGAGAAGTTTGACTGCCA 3'<br>R 5' TATGCGGCCGCTTACAGCTTTTTGGCACAGTCGGG 3' | 851 | 57 |
| *FHL1C* - pBSmxt **NM_001159703** | F 5' TATGAATTCATGGCGGAGAAGTTTGACTGCCA 3'<br>R 5'TATGCGGCCGCTCACGGAGCATTTTTTGCAGTGGAAG 3' | 777 | 57 |
| $K_{v1.5}$ *C' terminus* - GST **NM_002234** | F 5' TATGAATTCAACTACTTCTACCACCGGGAAACG 3'<br>R 5' TATGCGGCCGCTCACAAATCTGTTTCCCGGCTGG 3' | 296 | 57 |
| *FHL1A* - pEYFP-N1**NM_001449** | F 5' TATGAATTCATGGCGGAGAAGTTTGACTGCCA 3'<br>R 5' TATGTCGACCAGCTTTTTGGCACAGTCGGGA 3' | 849 | 57 |
| *FHL1A*$^{p.C224W}$ - pEYFP-N1**NM_001449** | F 5' TATGAATTCATGGCGGAGAAGTTTGACTGCCA 3'<br>R 5' TATGTCGACCAGCTTTTTGGCACAGTCGGGA 3' | 849 | 57 |
| *FHL1C* - pEYFP-N1 **NM_001159703** | F 5' TATGAATTCATGGCGGAGAAGTTTGACTGCCA 3'<br>R 5' TATGTCGACCGGAGCATTTTTTTGCAGTGGAAGC 3' | 778 | 57 |

### 2.2.4 Sequencing analysis

Reaction mix consisting of 75 ng genomic DNA, 0.1 mmol of each primer, and HotStart Taq (Qiagen) in a total volume of 10 µL was amplified by PCR. Denaturation was performed at 95°C for 15 min and then followed by 30 cycles of 95°C for 45 s, 57°C for 45 s, and 72°C for 45 s and a final extension step of 72°C for 10 min. PCR products were sequenced with the BigDye Terminator 3.1 Cycle Sequencing Kit (Applied Biosystems). Primers listed in Table 3 were designed with the Primer3 program and used to amplify and sequence all exons of the PCR product. Sequencing reactions were size-separated on the 3130xl DNA Analyzer (Applied Biosystems, Vienna, Austria), and sequence was analyzed with the Chromas Lite version 2.1 software (Technelysium Pty Ltd, Eden Prairie, Minnesota, USA). Same procedure was applied for FHL3 sequencing analysis using the primers listed in Table 3.

**Table 3: Description of primers for FHL3 sequencing, the expected amplified fragment size, and the annealing temperature.**

| Primer name | Primer | Sequenced exons | Annealing temperature (°C) |
|---|---|---|---|
| FHL3E1+2F | 5' CTTTGCCAGGAGCCAAGC 3' | 1,2 | 62 |
| FHL3E1+2R | 5' ACACATGCAAAGACCCTACG 3' | 1,2 | 59 |
| FHL3E3+4F | 5' GCTCACGCTGAGAGAGGAGT 3' | 3, 4, 5 | 60 |
| FHL3E3+4R | 5' CTGAGTCCCAGAGGTGGTTT 3' | 3, 4, 5 | 59 |
| FHL3-c740-F | 5' TCCTTTGAAGACCGACACTG 3' | 5 | 59 |
| FHL3-c740-R | 5' CAGAGCACTTGGTCTCCATC 3' | 5 | 58 |

### 2.2.5 p.G168fs and p.R227H mutations analysis

Genomic DNA from the patient was previously extracted from blood samples as described (Schoser *et al.*, 2009). Concentration and purity of the isolated DNA was checked with Nanodrop (Thermo Scientific). PCR and sequencing was performed as described above (2.2.4) using primers listed in Table 4.

**Table 4: Sequencing primers for sequence verification of produced clones and for mutation analysis of XMPMA patients DNA samples.** Primers already used in Table 1 used for both production of clones and for sequencing are indicated in grey.

| Gene | Primer name | Primer | Exons |
|---|---|---|---|
| $K_{v1.5}$ | Kv1.5-R1 | 5‘ CCGTGCCCAGGCCGGGAT 3‘ | 1 |
| | Kv1.5-R2 | 5‘ AGCGCCTGCGCTACTTCGAC 3‘ | 1 |
| | Kv1.5-R3 | 5‘ CCAACGGCAGCGGGGTCAT 3‘ | 1 |
| | Kv1.5-R4 | 5‘ CTCTAGCATCCCTGACGCCTTC 3‘ | 1 |
| | Kv1.5clon-F | 5’ TATGAATTCATGGAGATCGCCCTGGTGCC 3’ | 1 |
| | Kv1.5clon-R | 5’ TATGCGGCCGCTCACAAATCTGTTTCCCGGCTGG 3’ | 1 |
| Herg | HERGseq-R1 | 5‘ CATCTTTCCGGTAGAAGGCGATTTC 3‘ | 1, 2 |
| | HERGseq-F2 | 5‘ GAGGTGGTGATGGAGAAGGACAT 3‘ | 3, 4 |
| | HERGseq-F3 | 5‘ ACGCGCTCCCGAGAAAGCTG 3‘ | 4- 6 |
| | HERGseq-F4 | 5‘ TGTCTTCACACCCTACTCGGCT 3‘ | 6, 7 |
| | HERGseq-F5 | 5‘ CAACATGGAGCAGCCACACATG 3‘ | 7-9 |
| | HERGseq-F6 | 5‘ GCCTGCAGGCTGACATCTGC 3‘ | 9-11 |
| | HERGseq-F7 | 5‘ CGGCAGTACGGAGTTAGAGGG 3‘ | 11-13 |
| | HERGseq-F8 | 5‘ CTCAACATCCCCCTCTCCAGC 3‘ | 13-15 |
| | HERGclon-F | 5’ TATGAATTCATGCCGGTGCGGAGGGGC 3’ | 1, 2 |
| | HERGclon-R | 5’ TATGCGGCCGCCTAACTGCCCGGGTCCGAGC 3’ | 14, 15 |
| FHL1 | fhl1-f-mutation | 5‘ GAAGTG TGCTGGATGC AAGAACC 3’ | 5, 6 |
| | fhl1-r-mutation | 5’ TTGGCCACAAAGTTCTTGTAGCAATACA 3’ | 3, 4 |
| | FHL1-PCR | 5’ CACCTCCTTGGAGTCCGCAC 3’ | 1 |
| | FHL1clon-F | 5’ TATGAATTCATGGCGGAGAAGTTTGACTGCCA 3’ | 1-3 |
| | FHL1clon-R-isoformA | 5’ TATGCGGCCGCTTACAGCTTTTTGGCACAGTCGGG 3’ | 4,6 |
| | FHL1clon-R-isoformC | 5’ TATGCGGCCGCTCACGGAGCATTTTTTGCAGTGGAAG 3’ | 4-6 |

### 2.2.6 RNA isolation and reverse transcription PCR

Myoblasts ($2x10^5$ cells) were seeded out in six-well plates, cultured for 48 h and harvested by treatment with 0.25% (v/v) trypsin. TRI Reagent was used for total RNA isolation according to the manufacturer's suggestions. Frozen sections of human heart ears were thawed on ice and total RNA was isolated using TRIzol® reagent.

Final RNA concentration for all samples was measured by Nanodrop (Thermo Scientific). Genomic DNA degradation was performed with Promega RQ1 RNase-Free DNAse according to the manufacturer's instructions. Reverse transcription was performed from 2 µg of total RNA with random hexamer primers and SuperScript III Reverse Transcriptase (RT) (Invitrogen) (Kovacevic *et al.*, 2006). PCR primers (Table 5) were used to amplify the corresponding PCR products for FHL1 and $K_{v1.5}$. To ensure equal RNA loading, RT-PCR for human hypoxanthine phosphoribosyltransferase was performed for each experiment. Two control reactions in the absence of cDNA were included for each sample; RNA template (without primers) and water template were used.

**Table 5: Description of primers for the RT-PCR assay, expected amplified fragment size, and annealing temperature**

| *Gene* **Accession Nr.** | **Primers** | **Fragment size (bp)** | **Annealing temperature (°C)** |
|---|---|---|---|
| *FHL1 N' terminus* **NM_001449** | F 5' GCTGCCTGAAATGCTTTGAC 3'<br>R 5'GCCAGAAGCGGTTCTTATAGTG 3' | 105 | 58 |
| *FHL1A* **NM_001449** | F 5' CTGGATGCAAGAACCCCATC 3'<br>R 5' AAAGCGCTTGTTGGCCAG 3' | 128 | 58 |
| *FHL1B* NM_001159702 | F 5' CTGTTTCCCAGCGCCAA 3'<br>R 5' CACACTGGAGCCTTTACCAAAC 3' | 137 | 59 |
| *FHL1C* **NM_001159703** | F 5' GACTGGAAGCTTCTTCCCTAAAG 3'<br>R 5' GCCTTTACCAAACCCTTGTTG 3' | 105 | 57 |
| $K_{v1.5}$ **NM_002234** | F 5' CCGGGAAACGGATCACGAGG 3'<br>R 5' GCTGACCTTCCGCTGGACTC 3' | 100 | 60 |
| *hHPRT1* **NM_000194** | F 5' CCTGGCGTCGTGATTAGTGAT 3'<br>R 5' AGACGTTCAGTCCTGTCCATAA 3' | 131 | 58 |

### 2.2.7 Real time RT-PCR

Using the same primers as in for reverse transcription PCR (Table III) together with several other designed primers, we have attempted to perform Real time RT-PCR analysis. Real-time RT–PCR analysis for $K_{v1.5}$, *FHL1A, FHL1B, FHL1C and hHPRT* (house keeping gene) was performed using an ABI PRISM 7500 (Applied Biosystems) and SYBR® Green PCR Master Mix (Applied Biosystems) assay reagents. PCR was performed according to the manufacturer's protocol. Briefly, 1.5 µl (50 ng) of complementary DNA was used as a template in a total reaction volume of 20 µl containing 10 µl of SYBR® Green PCR Master Mix, 1 µl primer mix and nuclease-free water. Normalization of the target genes ($K_{v1.5}$ and *FHL1* variants) with an endogenous control (*hHPRT*) was performed. All experiments were done in triplicates.

### 2.2.8 Protein isolation and Western blotting

For Western-blot experiments, protein extracts from myoblast cell culture and human heart ears were used. Briefly, human myoblasts ($2x10^5$ cells) were seeded in six-well plates, cultured for 48 h and harvested by treatment with 0.25% (v/v) trypsin. The cells were washed with HBSS buffer, mixed with lysis buffer (0.1 M Tris pH 7.4, 10% [v/v] SDS, 0.1 M $Na_3VO_4$, 0.5 M NaF, 0.1 M sodium pyrophosphate buffer) and heated at 95°C for 10 min. Total cell lysate was frozen and stored at -20°C until use. Proteins from the human heart ears were isolated by homogenization of cardiac tissue with TissueRuptor® (Qiagen) in RIPA buffer (50 mM Tris/HCl, 1% [v/v] NP-40, 150 mM NaCl, 1 mM EDTA, 1 mM $Na_3VO_4$, 1 mM NaF plus protease inhibitors [1 µl/ml], pH 7.4) followed by 20 min centrifugation at 13000*g*. Protein concentrations of the supernatants were measured with the Bradford Protein Assay Kit (Bio-Rad). Aliquots of proteins were supplemented with NuPage® LDS sample buffer and NuPage® sample reducing agent (5%, v/v). After boiling for 5 min at 95°C, protein samples were subjected to electrophoresis at 4-12% NuPage® gradient SDS-PAGE

gels (Rauh *et al.*, 2008). Proteins were then transferred to nitrocellulose membranes (90 min, 200 mA). The membranes were blocked (30 min) with TBST (10 mM Tris-HCl [pH 7.4], 140 mM NaCl, 0.1% [v/v] Tween-20) containing 3% (w/v) non-fat dry milk followed by incubation overnight at 4°C with anti-FHL1 (1:1000) or anti-$K_{v1.5}$ (1: 200) as a primary antibody (diluted in 3% (w/v) BSA). After washing, the membranes were incubated (2 h, 25°C) with swine anti-rabbit IgG (1:750) or donkey anti-goat IgG (1:2000) as secondary antibodies (diluted in TBST containing 3% [w/v] non-fat dry milk). For normalization, membranes were stripped with Restore$^{TM}$ Western Blot Stripping buffer (Pierce) and reprobed with anti-β-human actin antibody (1:1000, in 3% [w/v] BSA) overnight at 4°C. Following incubation with goat anti-mouse IgG (1:2500, 1 h, 25°C) immunoreactive bands were visualized with Immobilon Western Chemiluminescent HRP substrate (Millipore, Billerica, MA, USA).

### 2.2.9 Immunohistochemistry

Frozen tissue samples were thawed on ice, and incubated for 4 min in 50% [v/v] methanol in acetone followed by 30 min incubation in 20% [v/v] acetone in $H_2O_2$. Samples were than 10 min air- dried and defined with Dako-Pen (Dako). Slides were incubated for 20 minutes in 10% [v/v] FCS (in Dako antibody diluents) followed by incubation overnight at 4°C with anti-FHL1 (1:50) or anti-$K_{v1.5}$ (1: 200) as a primary antibody (diluted in 10% [v/v] FCS). Next day tissue sections were washed three times in PBS buffer (pH 7.4) and incubated (1 h, 25°C) with biotinylated anti-mouse IgG or biotinylated Anti-sheep/goat Ig as secondary antibodies (diluted in 10% [v/v] FCS). After washing three times in PBS buffer (pH 7.4) avidin (1:100 in 10% [v/v] FCS) was applied and incubated (1h, 25°C). Sections were then developed using IHC Select® Fast Red Chromogen A (Millipore) and DAB-Nickel solution (0.05% 3.3'-diaminobenzidine (DAB), 0.05% Nickel Ammonium Sulfate and 0.015% $H_2O_2$ in PBS, pH 7.2) and counterstained with hematoxylin for 5 min and dehydrated in n-butyl

acetate before the cover glass was mounted. FHL1 and $K_{v1.5}$ localization was detected using Axioplan 2 microscope (Zeiss) and with AxioCam MRc5 camera (Zeiss).

### 2.2.10 Myoblast Proliferation assay

Myoblasts ($2x10^5$ cells, 40% confluence) were seeded in six-well plates at a density of $2.7x10^4/cm^2$, cultured up to 96 h in skeletal muscle cell growth medium including supplement mix containing 10% (v/v) FCS, 1.5% (v/v) 100 x Glutamax, 50 µl/ml gentamycin. Cells were harvested after 24, 48, 72 and 96 h using 0.25% (v/v) trypsin. Cell proliferation was determined by measuring the number of viable cells at the indicated times using a cell counter and analyzer system CASY®Model TT (Roche Innovatis AG, Bielefeld, Germany) as described (Weiss *et al.*, 2001).

### 2.2.11 Cell cycle analysis by flow cytometry

Myoblasts ($2x10^5$ cells, 40% confluence) were seeded in six-well plates at a density of $2.7x10^4/cm^2$ and cultured for 48 h, collected in PBS and centrifuged 5 min at 200*g*. Cells were then resuspended in 0.5 ml PBS and fixed in ice-cold 70% ethanol overnight. Thereafter, 0.25% (w/v) pepsin was added followed by CyStain DNA/protein staining solution. Samples were kept for 30 min at 4°C in the dark. Initially we have attempted to use propidium iodide (PI) staining but there were lots of aggregates and debris and we could not establish correct gates and distinguish between the cell cycle phases.

Flow cytometric measurements were carried out using CyFlow® flow cytometer (Partec) according to the manufacturer's suggestions. For data analysis, MultiCycleAV DNA cell cycle analysis software (Phoenix, San Diego, CA, USA) was used.

### 2.2.12 Xenopus oocytes expression and electrophysiology

*Xenopus* oocytes, prepared as described (Hofer *et al.*, 2006), were injected with 50 nl

of the following RNAs (alone or in combination): $K_{v1.5}$ (2 ng RNA/nl), FHL1 (500 ng RNA/nl), $FHL1^{p.C224W}$ (500 ng RNA/nl), FHL1C (500 ng RNA/nl), G protein-activated inward rectifier potassium channel 1 (GIRK1, 0.35 ng RNA/nl), G protein-activated inward rectifier potassium channel 4 (GIRK4, 0.7 ng RNA/nl), sodium channel protein alpha subunit type 5 ($Na_{v1.5}$, 1 ng RNA/nl ) and muscarinic acetylcholine receptor (30 ng RNA/nl). Oocytes were incubated in ND-96 solution (96 mM NaCl, 2 mM KCl, 1 mM $CaCl_2$, 1 mM $MgCl_2$, 5 mM HEPES/NaOH [pH 7.6]) supplemented with gentamycin (50 μg/ml) and sodium pyruvate (2.5 mM) at 19°C.

Protocol was adjusted to provide optimal $K_{v1.5}$ channel expression and conductivity; different doses of channel and FHL1 mRNA were injected to the oocytes: 1 to 10 ng RNA/nl for $K_{v1.5}$ and for FHL1 5 to 500 ng RNA/nl. In addition, currents were measured on different days of expression starting from one up to seven days after injection.

Three to seven days after injection of oocytes, whole cell currents were recorded using agarose cushion electrodes (Schreibmayer *et al.,* 1994). $K_{v1.5}$ channels were characterized by the following voltage jump protocols: voltage-dependent activation was assessed by keeping the oocytes at a resting potential of -80 mV. $K^+$ currents were elicited by consecutive voltage jumps repeated every 7 sec (from -35 mV to +45 mV in 5 mV increments). Inactivation of the $K_{v1.5}$ channel was quantified by the ratio of the magnitude of K+ current 1.8 sec after a suprathreshold pulse to +15 mV divided by the peak current at this potential. Current traces were sampled at 300 μs sampling rate and low pass filtered at 500 kHz using a 4-pole Bessel filter. $Na_{v1.5}$ and G-protein activated currents were elicited as described (Hofer *et al.,* 2006; Wagner *et al.,* 2010). Parameters were normalized to the control oocytes for a given experimental day and batch of oocytes. Data acquisition and analysis was done using the digidata 1322A interface and the pClamp 9.2 software (both Molecular Devices, Sunnyvale, CA, USA).

Preliminary experiments were also performed to examine conductivity of the hERG

channel when coexpressed with FHL1 variants. Oocytes were injected with 50 nl of the following RNAs (alone or in combination): hERG (250 ng RNA/nl), FHL1 (500 ng RNA/nl), $FHL1^{p.C224W}$ (500 ng RNA/nl), FHL1C (500 ng RNA/nl). Whole cell currents were recorded three to seven days after injection of oocytes. Following protocol was used for the hERG channel characterization: voltage-dependent activation was assessed by keeping the oocytes at a resting potential of -80 mV. $K^+$ currents were elicited by consecutive voltage jumps repeated every 9 sec (from -65 mV to +45 mV in 5 mV increments). Inactivation of the $K_{v1.5}$ channel was quantified by the ratio of the magnitude of K+ current 1.8 sec after a suprathreshold pulse to +15 mV divided by the peak current at this potential. Current traces were sampled at 500 μs sampling rate and low pass filtered at 500 kHz using a 4-pole Bessel filter.

### 2.2.13 Pull-Down assay

The Glutathione S-Transferase (GST)-$K_{v1.5}$ C-terminal fusion construct for the pull-down assay was produced by the PCR. The DNA fragment for the specific primary structure (C-terminal Kv1.5 sequence including amino acid residues 518 to 613) was transcribed from cDNA clone (obtained from J. Ehrlich) and cloned into the vector pGEX-4T-1 (Supplements, Scheme II) using suitable primers (Table 1, light grey row). Border of Kv1.5 C-terminal region was determined using CBS and DAS prediction programs (Scheme 4).

The recombinant protein was heterologously expressed in *E.coli* and purified as described (Ivanina *et al.*, 2003). Four hundred fifty ng cRNAs encoding FHL1C (or $G\beta_1$ and $G\beta_2$, respectively) were translated and radiolabeled in-*vitro* using 9.4 μL rabbit reticulocyte lysate (Promega) and 0.95 μL $^{35}$S-methionine (Amersham GE Healthcare) by incubation at 37°C for 2 h. Purified GST-$K_{v1.5}$ fusion protein (10–20 μg) was used as bait and incubated with 10 μL of lysate containing $^{35}$S-labeled FHL1C in 300 μL buffer (25 mM HEPES-Na, 5 mM $MgCl_2$, 5 mM EGTA, 0.05% Tween-20 [v/v, pH 7.0]), for 2 h at 25°C, with gentle rocking. GST protein was used as a negative control (i.e. no binding to FHL1C was expected).

GIRK1 C-terminus (G1-CT) was used both as a positive control (in combination with $^{35}$S-labeled βγ subunits (Gβγ)) and as a negative control (in combination with $^{35}$S-labeled FHL1C lysate). Control proteins were prepared as described (Ivanina *et al.*, 2003). Then, 30 µl of previously washed Glutathione Sepharose beads were added, the mixture was incubated (30 min, 25°C) and then washed three times in 1 mL of the same buffer. After washing, GST-fusion proteins were eluted with 30 µL of 15 mmol/L reduced glutathione in elution buffer (120 mM NaCl, 100 mM Tris, 0.05% Tween-20 [v/v, pH 8]) and subjected to 12% linear SDS-PAGE.

A

Kv1.5:NP_002225length=613
MEIALVPLENGGAMTVRGGDEARAGCGQATGGELQCPPTAGLSDGPKEPAPKGRGAQRDADSGVRPLPPLPDPGVRPLPPLPEELPRPRRRPPPEDEEEEGD
PGLGTVEDQALGTASLHHQRVHINISGLRFETQLGTLAQFPNTLLGDPAKRLRYFDPLRNEYFFDRNRPSFDGILYYYQSGGRLRRPVNVSLDVFADEIRFYQLGD
EAMERFREDEGFIKEEEKPLPRNEFQRQVWLIFEYPESSGSARAIAIVSVLVILISIITFCLETLPEFRDERELLRHPPAPHQPPAPAPGANGSGVMAPPSGPTVAPL
LPRTLADPFFIVETTCVIWFTFELLVRFFACPSKAGFSRNIMNIIDVVAIFPYFITLGTELAEQQPGGGGGGQNGQQAMSLAILRVIRLVRVFRIFKLSRHSKGLQILGK
TLQASMRELGLLIFFLFIGVILFSSAVYFAEADNQGTHFSSIPDAFWWAVVTMTTVGYGDMRPITVGGKIVGSLCAIAGVLTIALPVPVIVSNFNYFYHRETDHEEPAVL
KEEQGTQSQGPGLDRGVQRKVSGSRGSFCKAGGTLENADSARRGSCPLEKCNVKAKSNVDLRRSLYALCLDTSRETDL

B

CBS prediction program:
# Sequence Length: 613
# Sequence Number of predicted TMHs: 3
# Sequence Exp number of AAs in TMHs: 100.91749
# Sequence Exp number, first 60 AAs: 0
# Sequence Total prob of N-in: 0.30538

| | | | | |
|---|---|---|---|---|
| Sequence | TMHMM2.0 | outside | 1 | 246 |
| Sequence | TMHMM2.0 | TMhelix | 247 | 269 |
| Sequence | TMHMM2.0 | inside | 270 | 433 |
| Sequence | TMHMM2.0 | Tmhelix | 434 | 456 |
| Sequence | TMHMM2.0 | outside | 457 | 494 |
| Sequence | TMHMM2.0 | TMhelix | 495 | 517 |
| Sequence | TMHMM2.0 | inside | 518 | 613 |

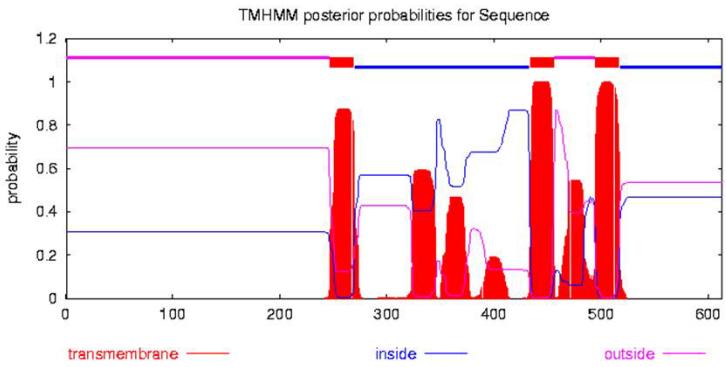


C

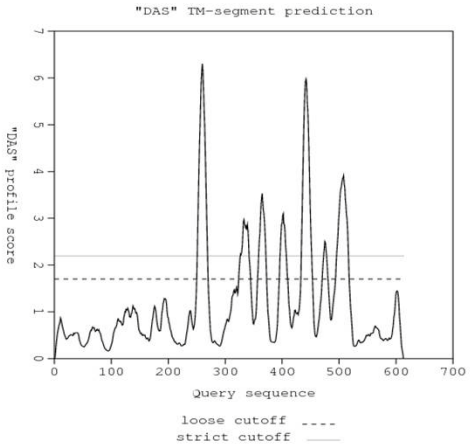


Potential transmembrane segments

| Start | Stop | Length | ~ | Cutoff |
|---|---|---|---|---|
| 251 | 269 | 19 | ~ | 1.7 |
| 251 | 269 | 19 | ~ | 2.2 |
| 324 | 344 | 21 | ~ | 1.7 |
| 327 | 341 | 15 | ~ | 2.2 |
| 357 | 372 | 16 | ~ | 1.7 |
| 359 | 371 | 13 | ~ | 2.2 |
| 395 | 409 | 15 | ~ | 1.7 |
| 397 | 407 | 11 | ~ | 2.2 |
| 433 | 453 | 21 | ~ | 1.7 |
| 434 | 451 | 18 | ~ | 2.2 |
| 471 | 480 | 10 | ~ | 1.7 |
| 473 | 478 | 6 | ~ | 2.2 |
| 494 | 517 | 24 | ~ | 1.7 |
| 496 | 516 | 21 | ~ | 2.2 |

**Scheme 4: Determination of border for the Kv1.5 C-terminal region by using CBS and DAS prediction programs** (A) Kv1.5 protein sequence. Underlined amino acids represent C-terminal region of the channel. (B) CBS prediction program: program predicted three transmembrane helixes; region after from amino acid 517 to the end of the sequence is located inside the cell. (C) "DAS" TM-segment prediction: program marks amino acid 516 as the last one in the transmembrane domains. Both predictions correspond to calculations found in literature.

Radioactivity was quantified by autoradiography of the dried gels, using a PhosphorImager Storm™ (GE Healthcare, Vienna, Austria). The amount of radioactivity was normalized to the amount of protein of a given band, as measured by staining of bands with Coomassie Brilliant Blue (= relative specific radioactivity).

We have also attempted to produce FHL1A and FHL1A$^{C224W}$ reticulocyte lysate to test binding with C-terminal $K_{v1.5}$. Several adjustments to the protocol were introduced. Firstly, as suggested by manufacturer, lysate/radioactivity and RNA/lysate ratio were changed in several steps (both lowering and increasing amounts in total volume). Following the troubleshooting protocol, we have tried adding different salt to the lysate master mix (0.5 to 4 mM $MgCl_2$ and 1 to 200 mM KCl). Additionally we have tested different washing solutions by adding various amounts of glycine. However, none of the attempts resulted in strong radioactive signal.

### 2.2.14 HL-1 cells transfection

FHL1A-, FHL1A$^{p.C224W}$- and FHL1C-pEYFP-N1 clones were raised using a PCR and suitable primers (Table 1) and constructs mentioned above (see 2.2.3). PECFP-C1+H $K_{v1.5}$ clone was kindly (provided by A. Felipe). GpI$^{eCFP}$ and Srβ$^{eCFP}$ clones were prepared as described [27, 28].

Transfection of HL-1 cells with pECFP-C1 and pEYFP-N1 clones (mentioned above, see 2.2.10) were performed with Lipofectamine according to the manufacturer's suggestions. Cells were screened for signal after 24 to 48 h using confocal imaging. In order to label lipid raft domains within the plasma membrane *in vivo*, a glycosylphosphatidylinositol (GpI) anchor domain was added to the short wavelength shifted version of the green fluorescence protein (eCFP; GpI$^{eCFP}$; Glebov *et al.*, 2004).The endoplasmic reticulum was labeled by expression of the ß-subunit of the signal recognition particle receptor fused to eCFP (Srβ$^{eCFP}$ (Ward *et al.*, 2004). Detection of signals was achieved as described below (see 2.2.11).

### 2.2.15 Confocal microscopy

HL-1 cells were scanned using a Leica inverted microscope with a laser-scanning module attached (DMIRE2 and TCS SL2; Leica Microsystems, Heidelberg, Germany). Using the 63× (NA: 1:20) water immersion objective, confocal sections were obtained at a 12-bit resolution (1024×1024 pixels). Filter settings were: *eYFP*: excitation (514 nm); excitation beam splitter: DD 458/514; emission (540–570 nm). *eCFP*: excitation (458 nm); excitation beam splitter: DD 458/514; emission (477–500 nm). Interference between eCFP and eYFP channels was negligible. Analysis of confocal images was done using the ImageJ software (ImageJ 1.42h by Wayne Rasband, NIH, and Bethesda, MD) supported with deconvolution plug-in (Bob Dougherty; http://www.optinav.com/imagej.html).

### 2.2.16 Statistics

Each experiment was performed at least three times. Data of representative experiments are expressed as mean ±SD or ±SEM. Experimental parameters were analyzed between groups using Student's *t*-test (Sigma plot for Windows, v11, Systat Software). Means were considered as significantly different (* $p<0.05$, ** $p<0.01$, and *** $p<0.001$). Sequence analysis and alignments were performed using Chromas Lite (v2.01, Technelysium Pty Ltd).

# 3 RESULTS

## 3.1 FHL3 sequence analysis

DNA from 150 undiagnosed myopathy patients and 200 control chromosomes were screened for FHL3 mutations. Sequence analysis of *FHL3* in patients with undiagnosed myopathy revealed a heterozygous missense mutation c.G676A (p.R227H) in one patient resulting in change of one amino acid in the fourth LIM domain (Figure 1). This mutation is not detected in the control samples. Unfortunately, family member data was not available for further studies of inheritance within the pedigree.


**Figure 1: p.R227H mutation sequencing analysis and protein prediction**. Mutation site is marked red, start codon is underlined, and stop codon is marked purple. DNA sequencing analysis: exons 1-5 (dark blue), exon boundaries (light blue), analysis performed by SWIFT protein sequence prediction.

### 3.2 Splice site mutation sequence analysis

DNA was isolated from the blood of an XMPMA patient as described previously (Schoser *et al.*, 2009). Direct sequencing of the complete coding sequence of *FHL1* identified a previously described splice donor site mutation in intron 4 (IVS4 _1, c.688_1G3A, Schoser *et al.*, 2009). The splicing of *FHL1A* from exon 3 to exon 6 would lead to a premature stop codon at amino acid position 195 (pA168GfsX195, termed p.G168fs) resulting in a truncated protein identical to FHL1C isoform.

In addition, another splicing option was revealed. In this case exon 4 is still transcribed and followed by additional 49 base pairs belonging to intron DNA ending mRNA sequence with exon 6 (Figure 2). Novel FHL1 protein amino acid sequence was predicted using SWIFT protein structure predictor (http://www.bioinfo.org.cn/SWIFT/). Due to a frame shift a new stop codon is introduced in the additional sequence and only seven amino acids is translated after exon 4 forming a new truncated protein with three and a half LIM domains (Figure 2 B and C).

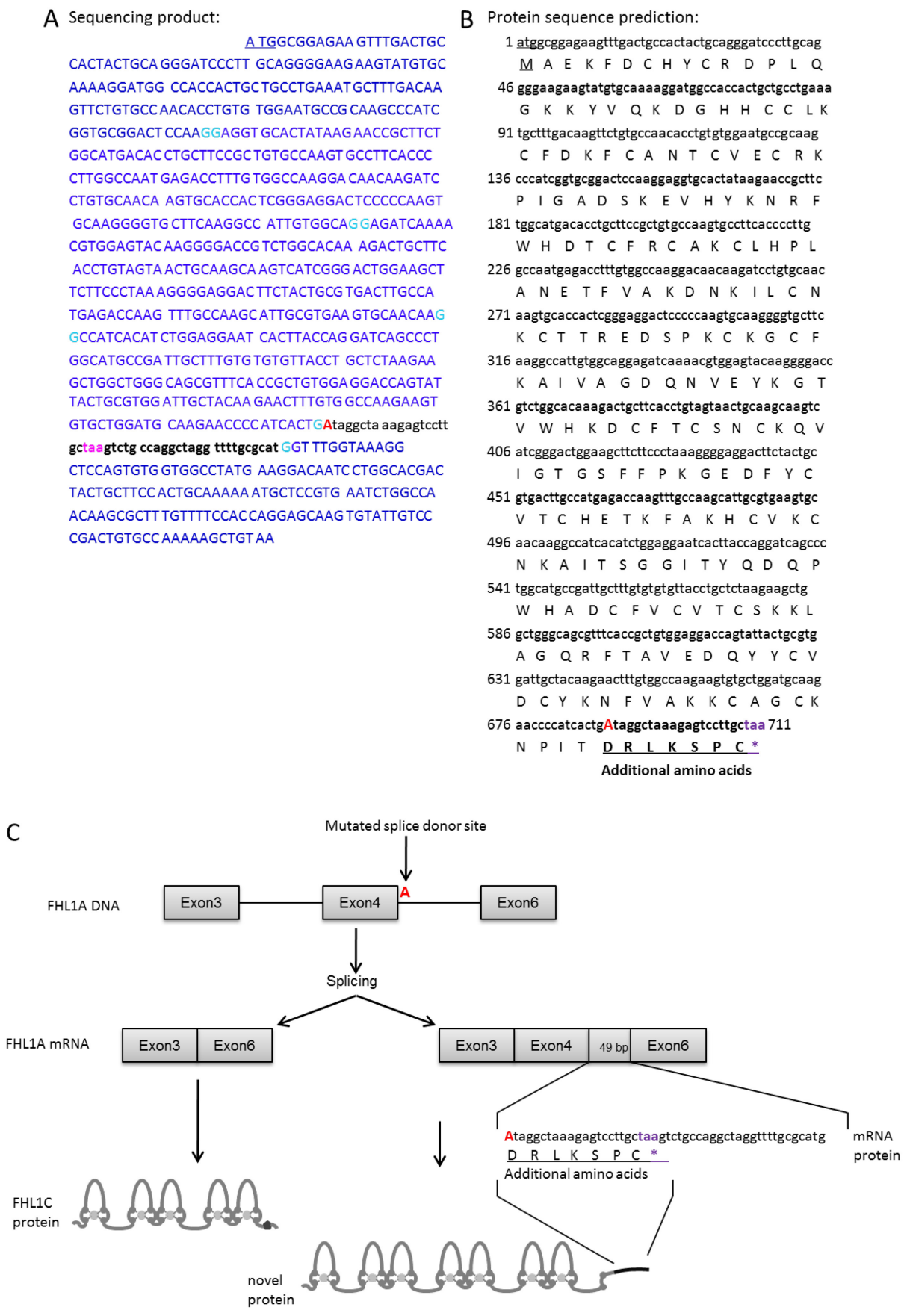


**Figure 2: p.G168fs mutation sequencing analysis and protein prediction.** Mutation site is marked red, start codon is underlined, and stop codon is marked purple. (A) DNA sequencing

analysis, exons 1-6 (dark blue), exon boundaries (light blue), sequenced intron DNA black. (B) SWIFT protein sequence prediction. (C) Alternative splicing because of the p.G168fs mutation Note: G=glycine, fs = frame shift. Upper panel: part of the FHL1A mRNA sequence, arrow marks the mutation site. Middle panel: two splicing possibilities for p.G168fs mutation; left: previously described skipping of the exon 4 and 5, exon 3 is followed by exon 6; right: second splicing option, after exon 3 and 4 additional 49 base pair are transcribed. (Bottom panel) truncated FHL1 proteins left: previously described truncated FHL1Ap.G168fs protein identical to FHL1C right: mutated FHL1Ap.G168fs protein with 3 and a half LIM domains and truncated fourth LIM domain.

### 3.3 FHL1 and Kv1.5 expression in myoblasts of XMPMA patients and controls

To follow expression of FHL1 transcripts in myoblasts from controls and XMPMA patients, RT-PCR using specific forward and reverse primer pairs (Table III) was performed.

In controls, abundant expression of all FHL1 transcripts could be verified (Figure 3). Expression of all FHL1 transcripts in p.C224W myoblasts was similar as observed in WT1; in p.G168fs myoblasts expression of FHL1A and FHL1B transcript is impaired while FHL1C is increased when compared to WT2 and WT1.

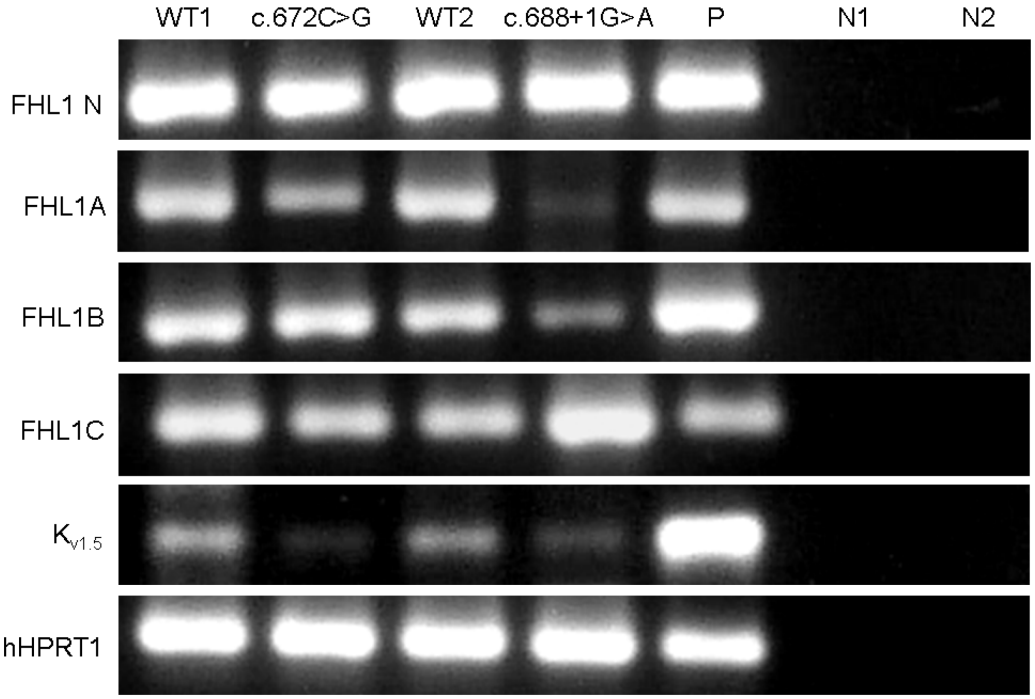


**Figure 3: RT-PCR for FHL1 and Kv1.5 in human myoblasts.** RNA was isolated from myoblasts from controls (WT1, WT2) and XMPMA patients (p.C224W, p.G168fs) and the corresponding FHL1 and Kv1.5 regions were amplified by RT-PCR using specific forward and reverse oligonucleotide primer pairs (Table III): Primers, spanning from exon 1 to 2 (termed N, see Scheme), amplify the mRNA stretch coding for the N-terminus of FHL1 in all three FHL1 isoforms, FHL1A, FHL1B and FHL1C. P (positive control: human fetal brain

marathon cDNA), N1 (negative control: RNA template without primers), N2 (negative control: water template). To ensure equal gel loading, RT-PCR for human HPRT1 (Table III) was performed. One representative experiment out of three is shown.

As $K_{v1.5}$ has been identified as a likely binding partner for FHL1 (Yang *et al.*, 2008) expression of this channel was checked by RT-PCR technique. In contrast to control myoblasts, $K_{v1.5}$ mRNA expression is decreased in myoblast preparations from both XMPMA patients (Figure 3). While only trace amounts of $K_{v1.5}$ transcripts were found in p.C224W myoblasts, $K_{v1.5}$ mRNA expression in p.G168fs was reduced by approximately 50% when compared to both controls.

Using the same primers as in for reverse transcription PCR (Table III) together with several other designed primers, we have attempted to perform Real time RT-PCR analysis. Since FHL1C isoform has no unique part of sequence characteristic for only this variant several primer pair were designed on the exon-exon boundaries. Unfortunately, we were not able to obtain a primer pair that would amplify FHL1C PCR product alone with no contamination from other isoforms.

Another problem occurred with measuring $K_{v1.5}$ mRNA expression levels; as $K_{v1.5}$ contains only one exon there is no possibility to design exon-exon spanning primers. To eliminate any remaining cDNA from mRNA isolations we have used DNA degradation kit (RQ1 RNase-Free DNAse from Promega). However, none of the kits available is 100% effective. Probably for these two reasons, we were not able to obtain any conclusive results by Real time RT-PCR experiments.

Next, we tried to quantify expression of FHL1 and $K_{v1.5}$ at the protein levels. As no isoform specific FHL1 primer pairs could be designed for quantitative-PCR experiments, and due to the lack of commercially available anti FHL1B/FHL1C antibodies, only FHL1A protein expression was followed. Western blotting experiments demonstrated the presence of FHL1A in myoblasts from controls while only trace amounts were present in XMPMA patient

myoblasts (Figure 4).

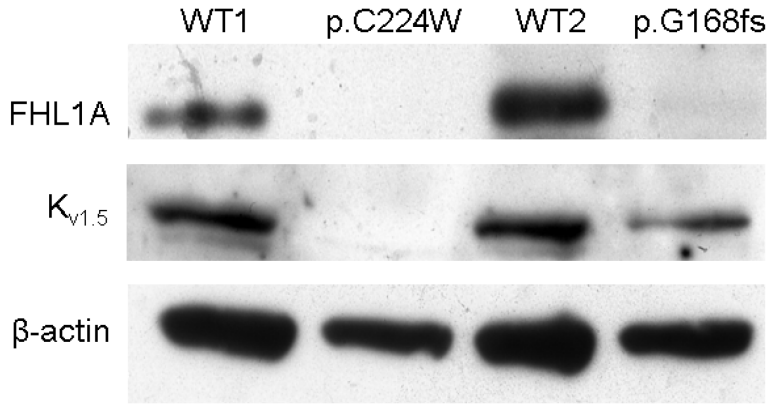


**Figure 4: Western blot for FHL1 and Kv1.5 in human myoblasts.** Protein lysates from controls (WT1, WT2) and XMPMA patient myoblasts (p.C224W, p.G168fs) were subjected to SDS-PAGE. Proteins were transferred to nitrocellulose membranes and immunoreactive bands were detected with anti-FHL1A or anti-Kv1.5 as primary antibodies. After stripping, the membranes were incubated with anti-β-actin antibody. (FHL1A=32 kDa; Kv1.5=68 kDa, β-actin=45 kDa). One representative experiment out of three is shown.

Densitometric evaluation of immunoreactive bands confirmed negligible amounts of FHL1A protein in patient myoblasts (Supplement, Figure 1A). Expression of $K_{v1.5}$ protein confirmed findings obtained on mRNA level (Figure 4). Densitometric evaluation of immunoreactive bands revealed only trace amounts of $K_{v1.5}$ in p.C224W myoblasts and an approx. 50% reduction in p.G168fs myoblasts when compared to controls (Supplement, Figure 1B).

As no cardiac biopsy material could be obtained from XMPMA patients' only material from non-XMPMA patients was available. Using RT-PCR technique, expression of all three FHL1 transcripts (FHL1A, FHL1B, and FHL1C) and $K_{v1.5,}$ respectively, was found in cardiac tissue (Figure 5A). Western blot experiments confirmed expression of FHL1A and $K_{v1.5}$ protein in cardiac tissue samples from non-XMPMA patients (Figure 5B).

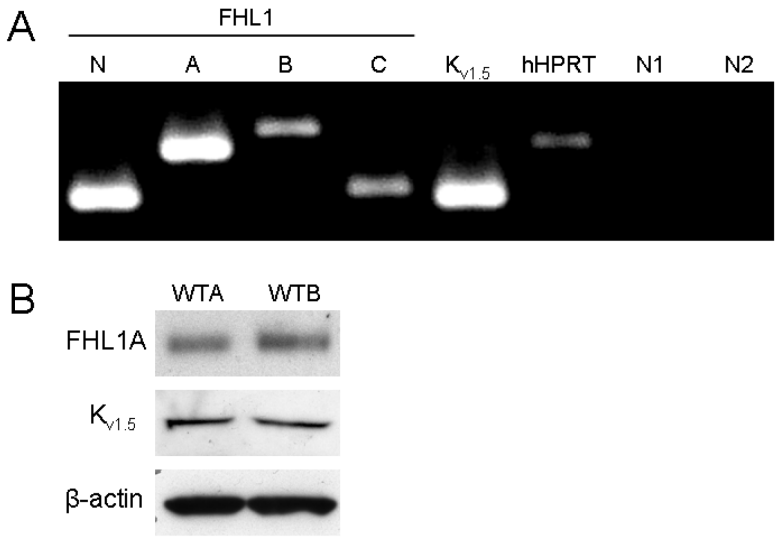


**Figure 5: FHL1 and Kv1.5 expression in human non-XMPMA patient cardiac tissue**
(A) Frozen sections of two human heart ears from human non-XMPMA patients (WTA, WTB) were thawed on ice and mRNA was isolated using TRIzol® reagent. Corresponding FHL1 and Kv1.5 constructs were amplified by RT-PCR using specific forward and reverse oligonucleotide primer pairs (Supplement, Table II) for (i) FHL1 N-terminus (FHL1 N) is identical for all three isoforms of FHL1, (ii) FHL1A, (iii) FHL1B, (iv) FHL1C and (v) Kv1.5 channel-specific sequences. N1 (negative control: RNA template), N2 (negative control: water template). To ensure equal gel loading, RT-PCR for human hypoxanthine phosphoribosyltransferase (HPRT1, Table II Supplement) was performed. Experiments were performed in triplicates. (B) Protein from the human heart ears (WTA, WTB) was isolated by homogenization of cardiac tissue with TissueRuptor in RIPA buffer. Western blot was performed with either anti-FHL1A (immunoreactive band at 32 kDa) or anti-Kv1.5 (immunoreactive band at 68 kDa) as primary antibodies. After stripping membranes anti-β-actin (immunoreactive band at 45 kDa) was used as a primary antibody. One representative experiment out of three is shown.

Densitometric evaluation of immunoreactive bands showed comparable levels of FHL1A and $K_{v1.5}$ in cardiac tissue from non-XMPMA patients (Supplement, Figure 2). β-actin expression levels were set to 1 and FHL1 and $K_{v1.5}$ were normalized accordingly.

### 3.4 Localization of FHL1 and Kv1.5 in the cardiac muscle

To further investigate FHL1 and $K_{v1.5}$ expression and localization in human cardiac muscle we have performed immunohistochemistry staining. As biopsies of XMPMA patients were not available, we have used heart sections from healthy individuals. Interestingly, staining pattern was changing through the different sections of the heart; in the atrium and

sinus valsalva region FHL1A immunoreactive signal was predominantly detected in at the membrane of the cells (Figure 6 A, B, and D in grey). This finding is similar to the previously reported staining in skeletal muscle (Windpassinger *et al.*, 2007; Schoser *et al.*, 2009). $K_{v1.5}$ signal was found in the cytoplasm (Figure 6, in red). On the other hand, partly blotchy, colocalized staining pattern was found in the ventricle for most of the fibers with some fibers predominantly expressing either FHL1A or $K_{v1.5}$ (Figure 6D).

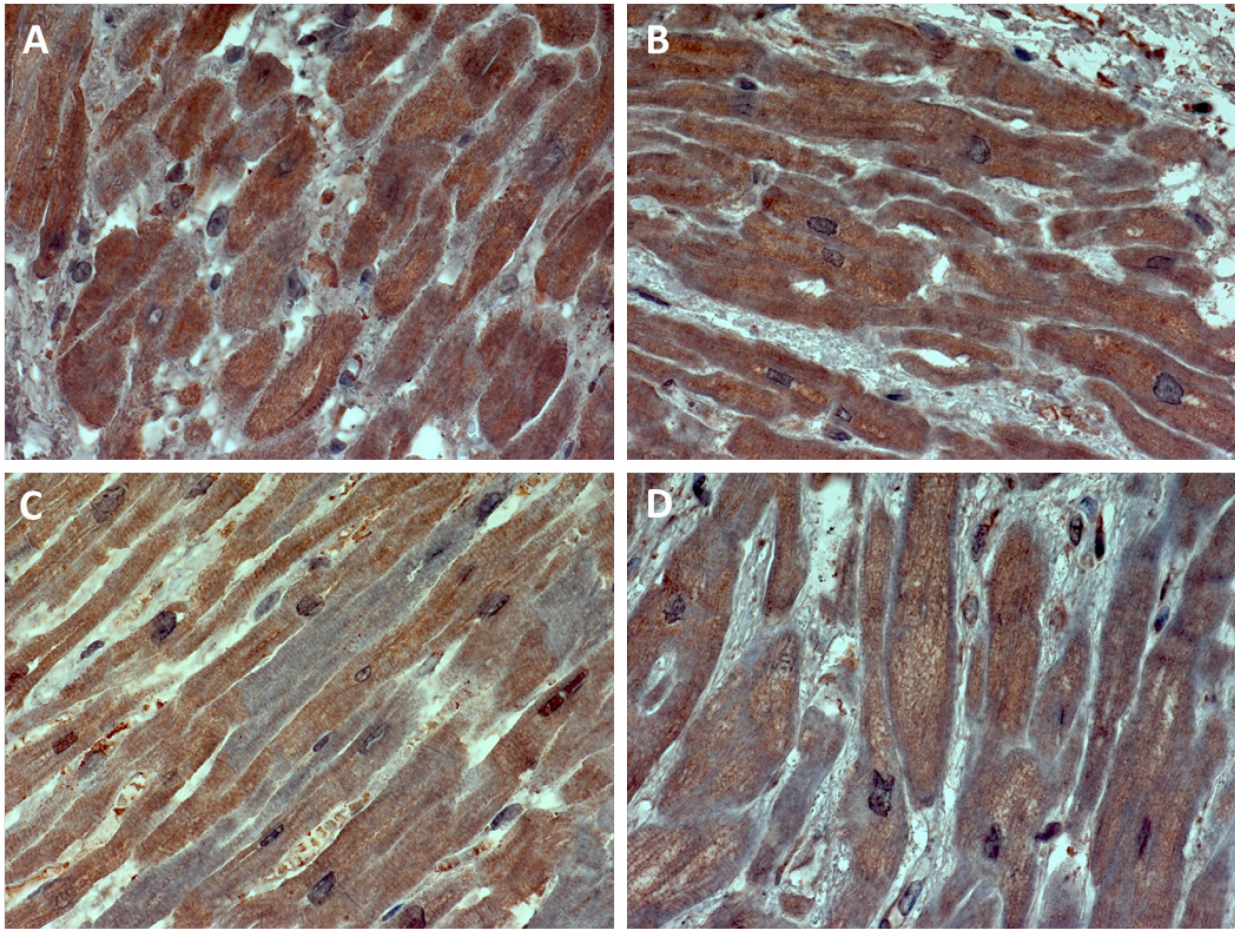


**Figure 6: Immunohystochemical characterization of human heart compartments.** Cardiac tissue samples were fixed on glass slides. Immunohistochemistry was performed using anti-FHL1 and anti-Kv1.5 as a primary antibody and biotinylated anti-mouse IgG or biotinylated Anti-sheep/goat Ig as secondary antibodies. FHL1A staining is shown in grey and Kv1.5 in red. (A) Right atrium: transversal section, FHL1A predominantly in membranes and presumably in the nucleus, Kv1.5 in the cytoplasm. (B) Left atrium shows identical staining to (A) but section is longitudinal. (C) Right ventricle representing very interesting staining pattern with one muscle fiber almost exclusively positive for FHL1A and several others for Kv1.5. However, most muscle fibers show positive staining for both antibodies. (D) Sinus of vasalvae staining very similar to atrium. Sonja Hochmeister at Neurology Department, Medical University of Graz, performed Immunohistochemistry.

### 3.5 Myoblast immunocytochemistry

The myoblast cell population of controls and patients consisted of a homogenous fraction and all were confirmed to be of satellite cell origin by staining with neural cell adhesion molecule (NCAM) antibody (Figure 7).

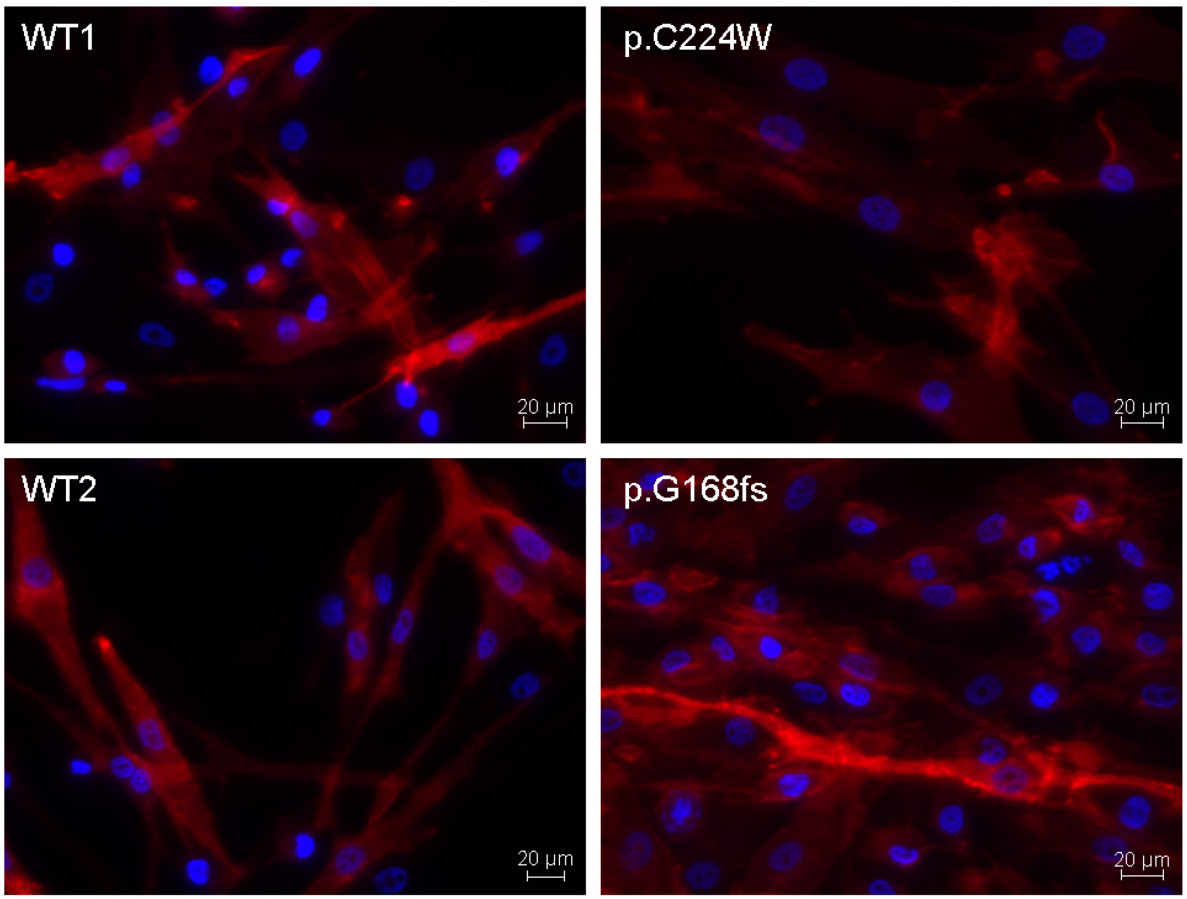


**Figure 7: Immunocytochemical characterization of human myoblasts** Cultured myoblasts from controls (WT1, WT2) and XMPMA patients (p.C224W, p.G168fs) were fixed with fixation buffer and washed with PBS. Immunocytochemistry was performed using mouse anti-human neural cell adhesion molecule antibody followed by Cy3-labeled goat anti-mouse IgG (red). Staining for nuclei was performed with 4', 6-diamidino-2-phenylindole (blue). One representative image out of three experiments is shown. Heidi Miedl (Division of Gynecology, Medical University of Graz) and Ivana Poparic performed Immunocytochemical characterization.

Interestingly, cultured C224W myoblasts were found to be significantly larger than other samples and their diameter of the cells did not change during the experiments.

Myogenin and myogenin D staining were also performed. Myogenin is used to detect myotube differentiation and MyoD as marker of satellite cell activation. Our goal was to

investigate whether there is difference in these two processes in XMPMA patient myoblasts compared to the controls. Both stainings were negative but rather unconvincing (Figure 8).

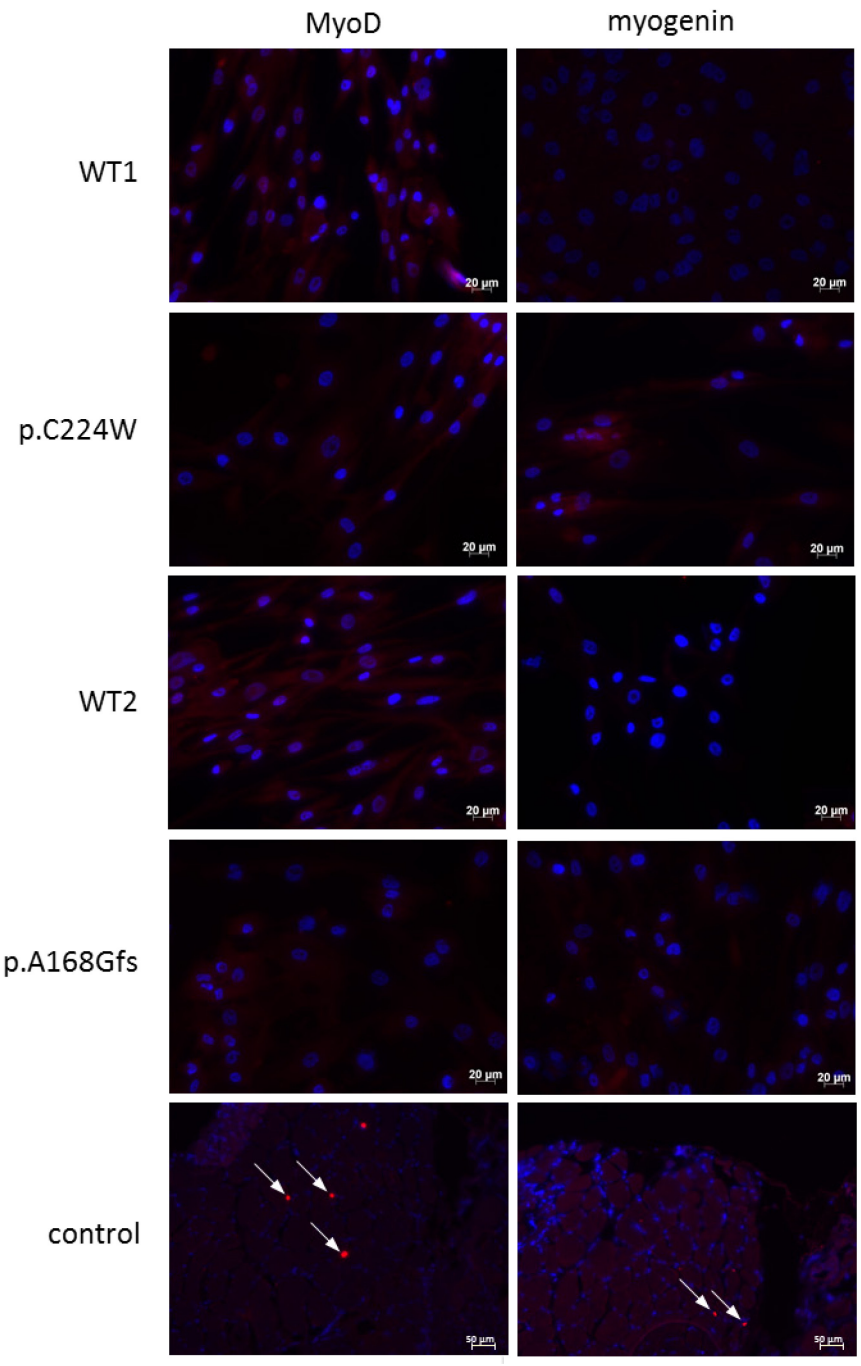


**Figure 8: Immunocytochemical characterization of human myoblasts with myogenin and myoD** Cultured myoblasts from controls (WT1, WT2) and XMPMA patients (p.C224W, p.G168fs) were prepared as in Figure 6. Immunocytochemistry was performed using mouse anti-myogenin and mouse anti-myoD antibodies followed by Cy3-labeled goat anti-mouse IgG (red). Staining for nuclei was performed with 4', 6-diamidino-2-phenylindole (blue). One representative image out of three experiments is shown. Heidi Miedl and Ivana Poparic at Division of Gynecology, Medical University of Graz, performed Immunocytochemical characterization.

In our experimental setup, we have used slides with myositis tissue as positive control. This problem could be result of low quality of preservation of the cells on the slides. However, human myoblasts myotube differentiation is not expected to occur in 48 h (after which cells were fixed). Therefore, we would expect myogenin staining to be negative.

### 3.6 Myoblast proliferation and cell cycle distribution

A recent report (Villalonga *et al.*, 2010) addressed the role of $K_{v1.5}$ as a possible regulator of myoblast proliferation. We observed a significant reduction in the number of viable FHL1-mutated myoblasts (24 h: $p<0.01$, 48 and 72 h: $p<0.001$) when compared to controls (Figure 9A). Total cell number count and measurements of the cell diameter excluded apoptosis and fibrosis to cause different number of viable cells in the samples. Thus, the difference in cell number is due to decreased proliferation rate in FHL1 mutant myoblasts (Figure 9A).

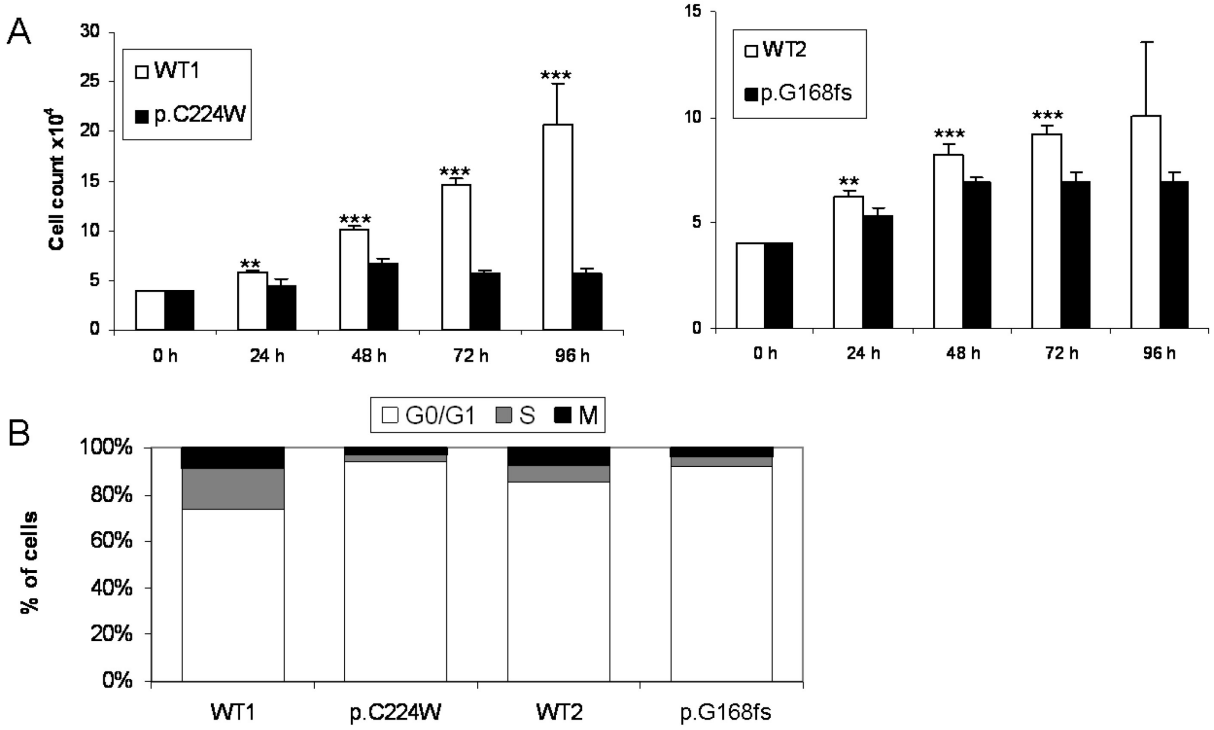


**Figure 9: Proliferation rate of human myoblasts** (A) Myoblasts (2x105 cells, 40% confluence) from controls (WT1, WT2) and XMPMA patients (p.C224W, p.G168fs) were seeded at identical densities in six-well plates and cultured for the indicated times. After trypsin treatment, cell proliferation was determined by measuring the number of viable cells

using Casy cell counter. Values represent mean ±SD of three experiments (six wells per one experiment). **p<0.01 and *** p<0.001. (B) Myoblasts (2x105 cells, 40% confluence) from controls (WT1, WT2) and XMPMA patients (C224W, c.688) were seeded in 6-well plates and cultured for 48 h, harvested and flow cytometry was used to estimate cell cycle, i.e. G0/G1 phase, S phase, and M phase, respectively. One representative experiment out of three is shown. Heidi Miedl at Division of Gynecology, Medical University of Graz, measured proliferation rate.

Villalonga and co-workers (Villalonga *et al.*, 2010) further suggested that $K_{v1.5}$ might regulate myoblast proliferation via blocking cell cycle progression in the $G_0$ phase. Due to the difference in proliferation rate (Fig. 4A) and expression levels of the $K_{v1.5}$ channel (Fig. 3) in XMPMA patients versus controls, FACS analysis was performed to follow cell cycle alterations. We found a significantly (p.C224W: 28% ($p<0.001$), p.G168fs: 8.1% ($p<0.001$)) higher number of myoblasts from XMPMA patients found in the $G_0/G_1$ phase when compared to control myoblasts (Figure 8B).

### 3.7 Functional effect of FHL1 coexpression on heterologously expressed $K_{v1.5}$ channels

In order to test whether FHL1 protein exerts functional effects on the $K_{v1.5}$ channel, both proteins were heterologously coexpressed in the *Xenopus* oocyte system and $K_{v1.5}$ currents were recorded with the two-electrode voltage clamp technique. We show that oocytes expressing $K_{v1.5}$ and FHL1A exerted markedly reduced currents when compared to oocytes expressing $K_{v1.5}$ only (Figure 10A and B). However, FHL1 proteins exerted profound effect on the maximal $K^+$ conductance ($G_{max}$; Figure 10C). $G_{max}$ of $K_{v1.5}$ was affected in a dose-dependent manner by coexpressing $K_{v1.5}$ and FHL1; FHL1C had the most pronounced effect on channel's conductivity followed by FHL1A and $FHL1A^{p.C224W}$. In order to investigate whether FHL1 generally interferes with the membrane insertion of ion channel complexes, the effect of coexpression of FHL1A on voltage-dependent sodium channels as well as on G-protein activated potassium channels was tested. Both GIRK1/4 and $Na_{v1.5}$ ion channels were functionally unaffected by FHL1A (Figure 10D).

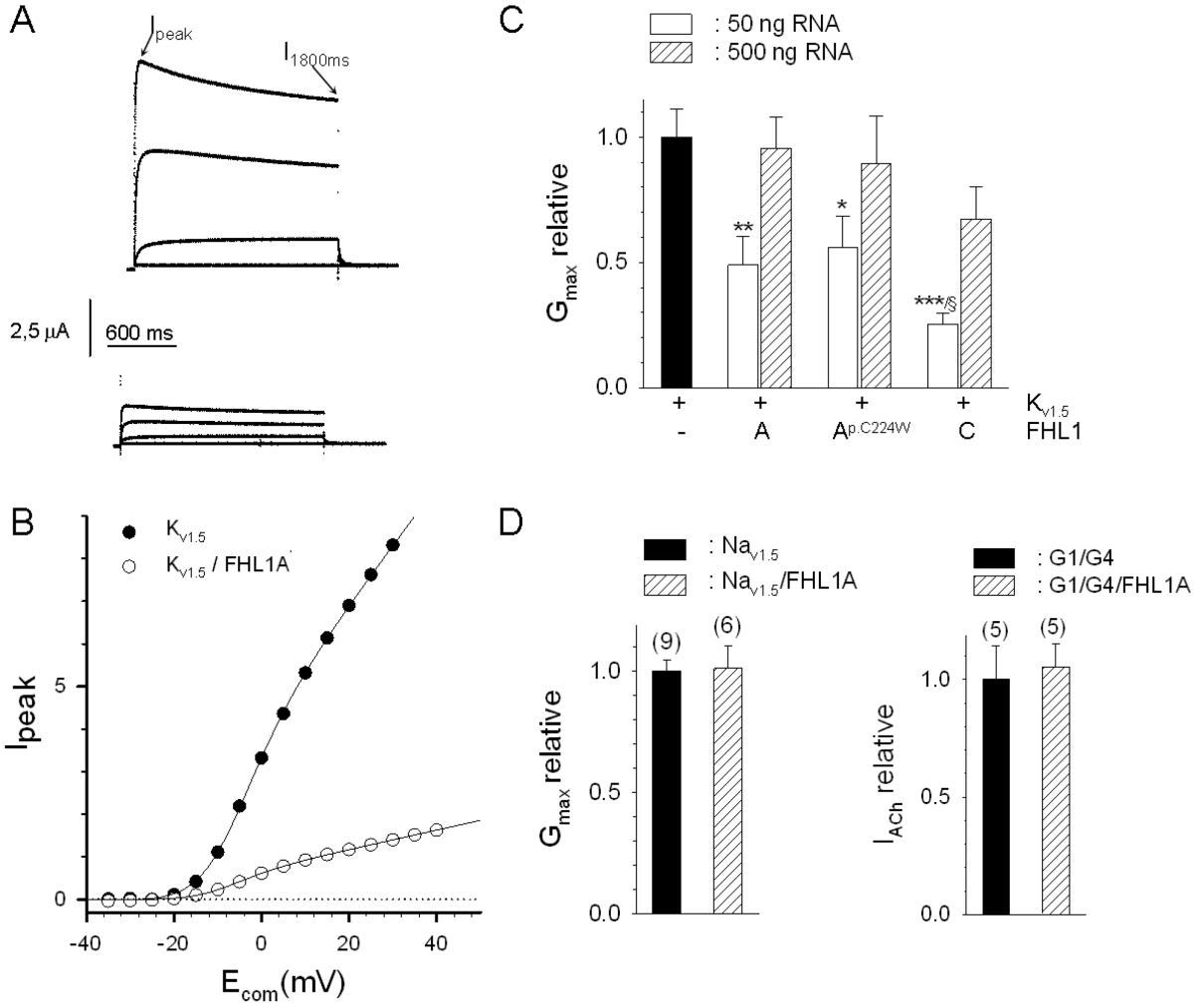


**Figure 10: Functional effects of FHL1 coexpression on Kv1.5 currents** (A) Original current recordings from oocytes expressing either Kv1.5 (upper panel) or Kv1.5 in combination with FHL1A (lower panel). The four traces shown on each panel were elicited by suprathreshold voltage pulses to -35, -10, +10 and +40 mV. (B) Ipeak/V relation from the oocytes shown in A. (C) Effect of coexpression of FHL1A, FHL1Ap.C224W and FHL1C on Gmax; Gmax values were normalized to Gmax for oocytes expressing Kv1.5 alone, for each batch of oocytes and experimental day. RNA for Kv1.5 (2 ng) or FHL1 (50 or 500 ng) was injected per oocyte. Values are mean ±SEM from six experiments (five oocytes per day per experimental group). *p<0.05, **p<0.01, *** p<0.001 significant difference versus oocytes expressing Kv1.5 alone. § = p<0.05 significant difference level versus oocytes coexpressing Kv1.5 and FHL1AWT. (D) Effect of FHL1A coexpression on ionic currents through sodium channel protein alpha subunit type 5 (Nav1.5, 1 ng RNA injected) and G protein-activated inward rectifier potassium channels 1 and 4 (GIRK1/GIRK4/m2R, 0.35 ng/0.7 ng/30 ng RNA injected) membrane channels. Values are given as mean ±SEM from the number of experiments given in parenthesis above each bar.

Voltage-dependent activation as well as channel inactivation were unaffected by coexpression of FHL1A, FHL1$^{p.C224W}$ or FHL1C (Figure 11). Hence, FHL1 proteins exert specific functional interaction with $K_{v1.5}$. The pronounced reduction of $G_{max}$ may be due to

interference of FHL1 with membrane trafficking of $K_{v1.5}$, i.e. reduced membrane insertion and/or increased removal from the plasma membrane. Alternatively, FHL1 may directly block $K_{v1.5}$ channels without interference with trafficking.

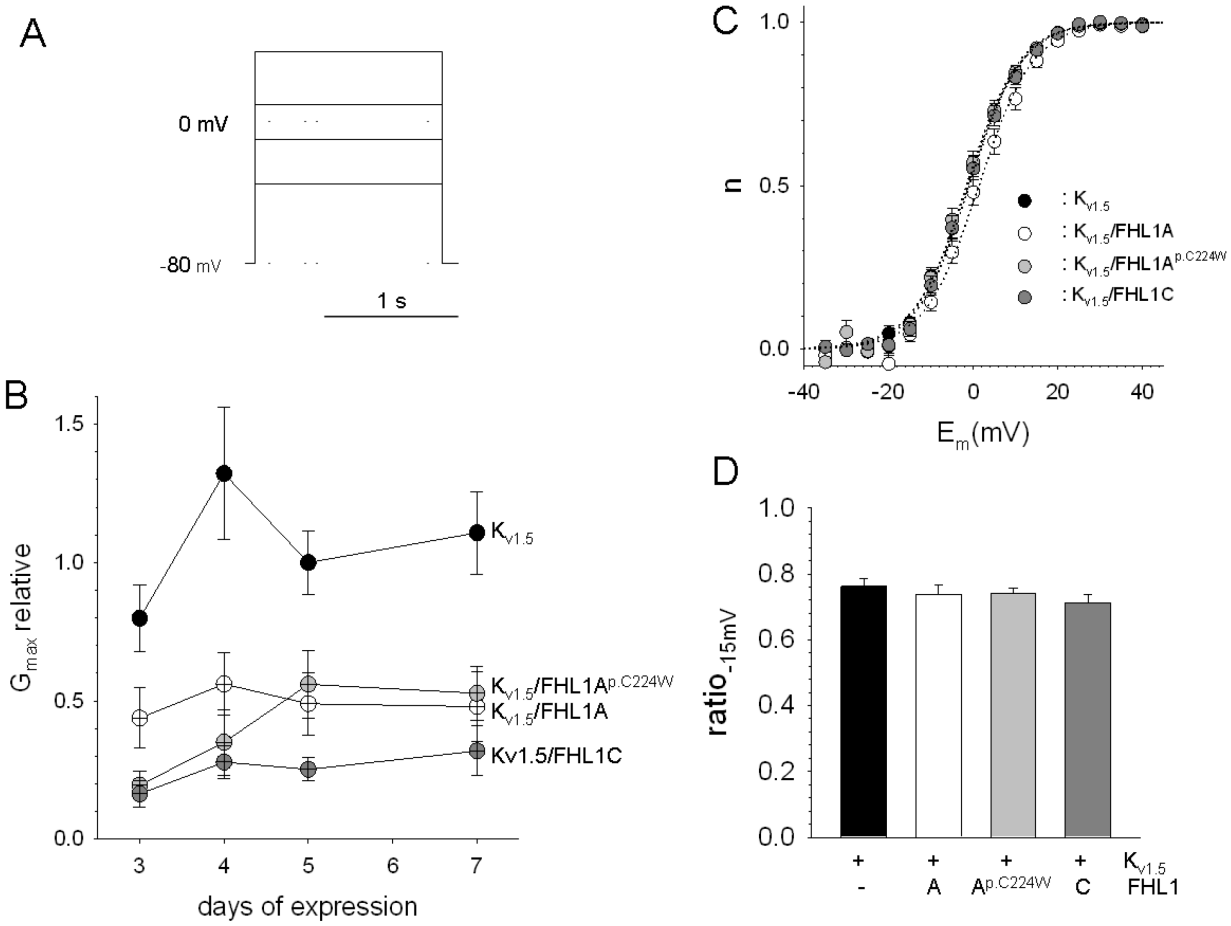


**Figure 11: Two-electrode voltage clamp protocol and results** (A) Voltage protocol for original current traces recorded from oocytes co-expressing Kv1.5 and FHL1A shown in Figure 3. Kv1.5 channels were characterized by the following voltage jump protocols: keeping the oocytes at a resting potential of -80 mV assessed voltage-dependent activation. K+ currents were elicited by consecutive voltage jumps repeated every seven sec (from -35 mV to +45 mV in 5 mV increments). The four traces shown on each panel were elicited by suprathreshold voltage pulses to -35, -10, +10 and +40 mV. (B) Time-dependence of Gmax relative in differential experimental groups. Three to seven days after mRNA injection of oocytes, whole cell oocyte currents were recorded. (C) Steady-state activation (five days of co-expression). (D) Channel inactivation (five days of co-expression). Inactivation of the Kv1.5 channel was quantified by the ratio of the magnitude of K+ current 1.8 sec after a suprathreshold pulse to +15 mV divided by the peak current at this potential.

Lin et al have recently described interaction between FHL2 and hERG channel (Lin *et al.*, 2008). FHL2 has a regulatory effect on channel function by upregulating the maximum current amplitude (Lin *et al.*, 2008). Since FHL1 is very similar in structure to FHL2, we have

decided to investigate whether it can have same effect on hERG functionality. Our preliminary results have showed that hERG channel conductivity is significantly downregulated on the oocyte coexpression with FHL1 constructs compared to when channel is expressed alone (Figure 12). However, due to the massiveness of the planned experiments we have not further investigated this interaction.

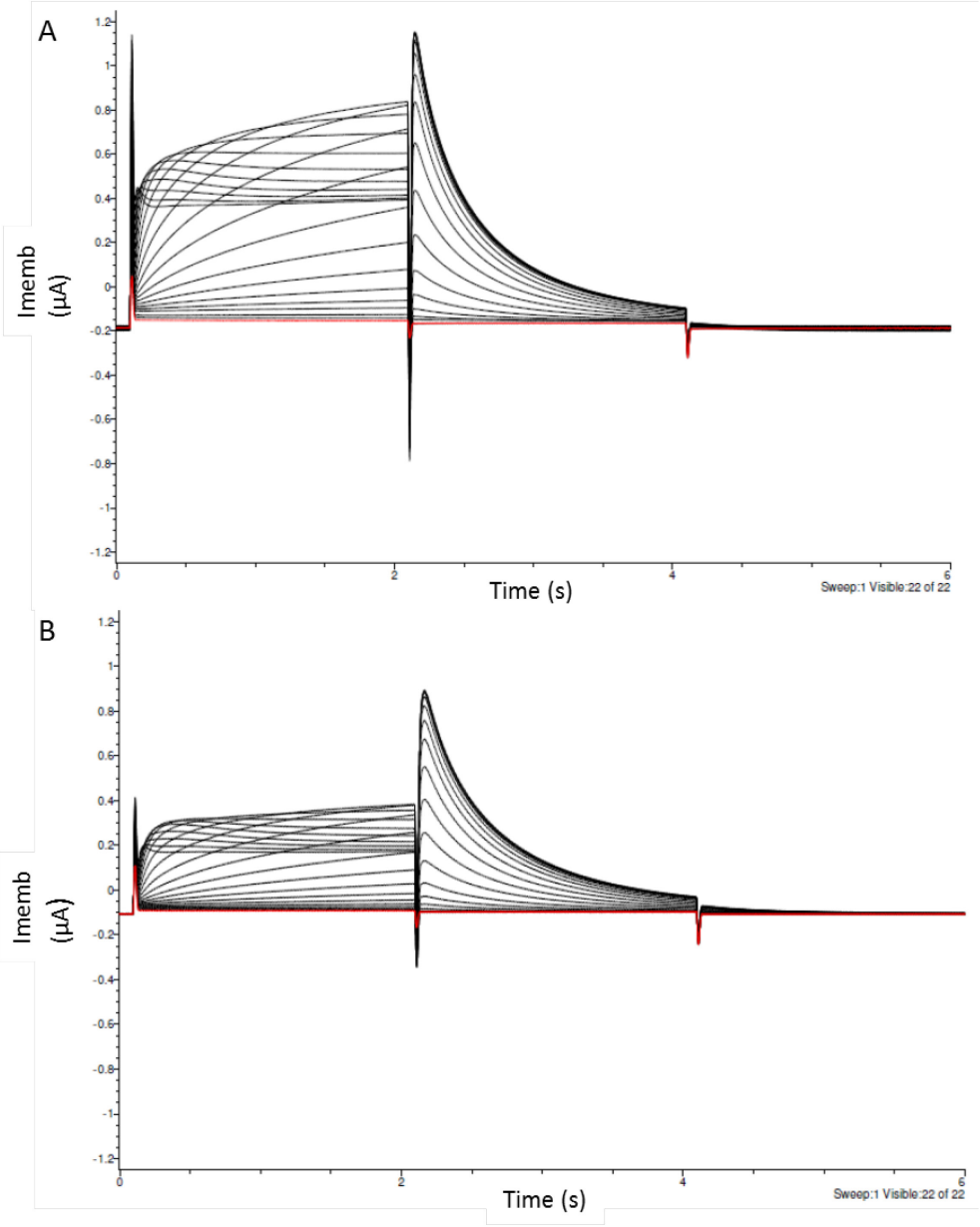


**Figure 12: Functional effects of FHL1 coexpression on hERG currents** Original current recordings, one series of measurements includes 22 sweeps. (A) Oocytes expressing hERG alone; (B) hERG expressed in combination with combination with FHL1A.

### 3.8 Interaction between FHL1C and $K_{v1.5}$

In order to investigate a direct interaction between FHL1C and $K_{v1.5}$, a standard pull-

down approach was performed. As FHL1A coimmunoprecipitates with $K_{v1.5}$ and thus may directly interact with the C-terminal portion of $K_{v1.5}$ (Yang *et al.*, 2008).

A GST-$K_{v1.5}$ fusion protein (containing amino acid residues 518 to 807 representing the C-terminus of $K_{v1.5}$) was designed, synthesized and used as bait for radioactively labeled FHL1C protein. Figure 12 shows that FHL1C interacts with the C-terminal portion of the $K_{v1.5}$ channel indicating that the functional effect described above (Figure 9, 10 and 11) is likely achieved by direct complex formation between both proteins.

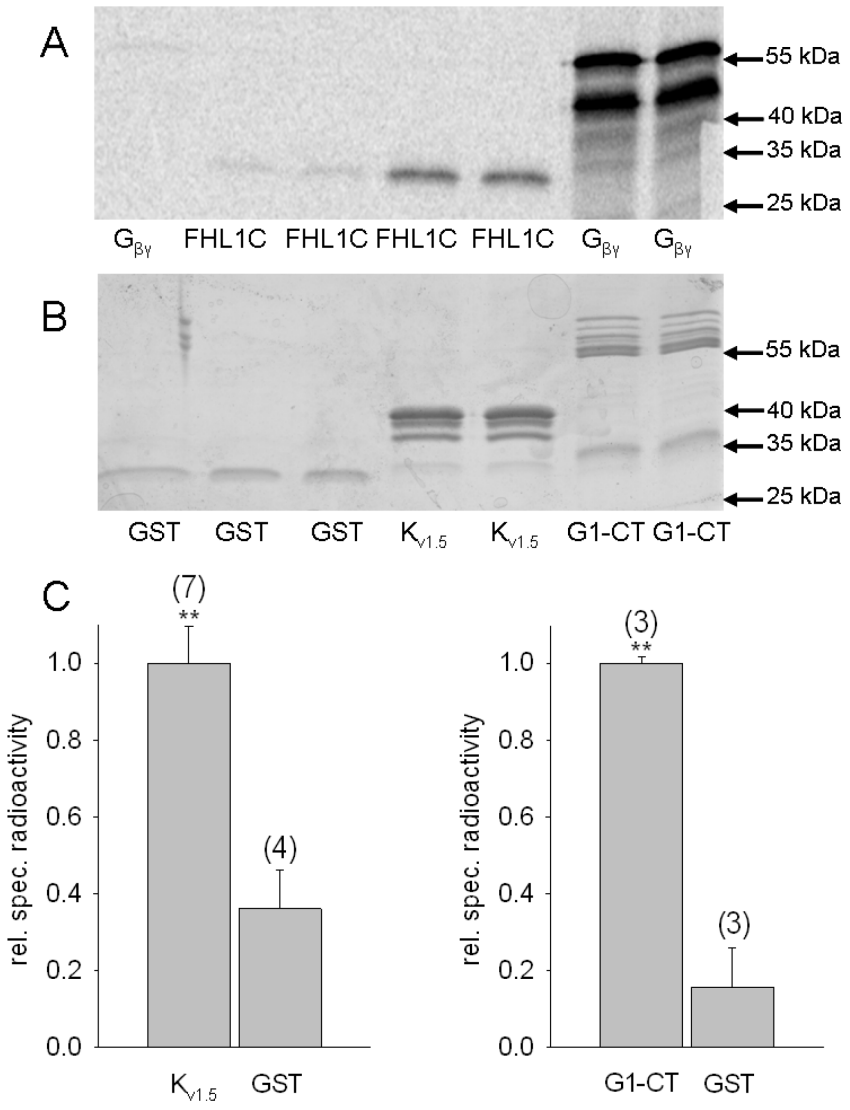


**Figure 13: Physical interaction of FHL1C with the $K_{v1.5}$ cytosolic C-terminus** (**A**) Autoradiography of the dried gel, showing the amount of radioactive protein associated with the bait. As radioactive protein, either FHL1C or the β/γ subunits of heterotrimeric G-protein ($G_{\beta\square\gamma}$; control) was used as indicated at the bottom of the lanes. (**B**) Commassie Brilliant Blue staining of the SDS gel shown in panel A. Bait proteins used are indicated at the bottom of the

lanes: GST protein alone (GST); GST-$K_{v1.5}$ C-terminus fusion protein ($K_{v1.5}$); C-terminus of GIRK1 fused with GST (G1-CT) as positive control. (**C**) Statistics of the bound radioactivity normalized to the amount of bait protein (relative specific radioactivity) for FHL1C using $K_{v1.5}$ and GST as a bait (left) and $G_{\beta\square\gamma}$ using G1-CT and GST as a bait (right). Values are given as means from the number of experiments given in parenthesis above each bar. Significant difference (**p<0.01) between GST and Kv1.5/G1-CT.

### 3.9 Subcellular localization of FHL1A, FHL1C and Kv1.5

As interaction of FHL1 with $K_{v1.5}$ could be confirmed physically (Figure 13) and on a functional level (Figure 9) we investigated whether both proteins colocalize within subcellular compartments. In order to answer this question fluorescently labeled $K_{v1.5}$ and FHL1 constructs were raised by PCR technique. As a cellular model the HL-1 mouse atrial cell line, that retains important atrial features like contractility and excitability (Claycomb *et al.*, 1998) was used. Figure 14 shows pronounced expression and predominant nuclear localization of FHL1A, FHL1A$^{p.C224W}$ and FHL1C. On the other hand, fluorescent staining for $K_{v1.5}$ was found exclusively in the cytoplasm but not in the nucleus.

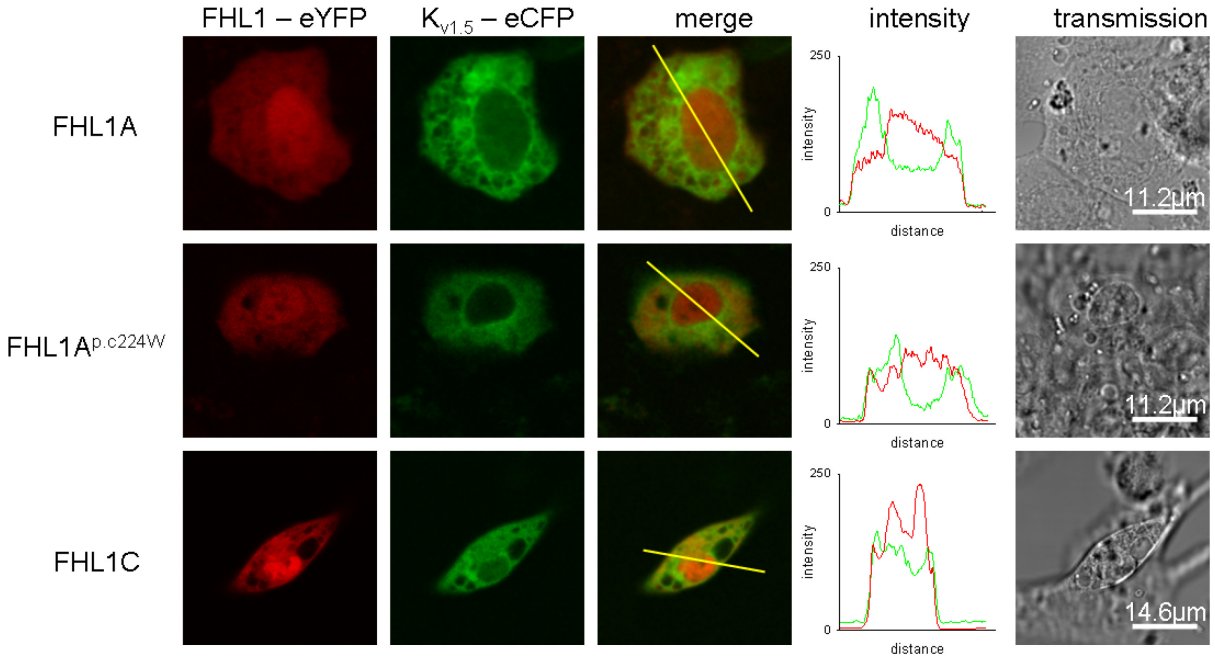


**Figure 14: Colocalization of heterologous expressed FHL1 variants and Kv1.5 in the atrial HL-1 cell line** HL-1 cells were transfected with pECFP-C1 and pEYFP-N1 clones and screened for signal after 24 to 48 h using confocal imaging. Each horizontal sequence of micrographs shows identical cells. The sequence of channels (from left to right) is: eYFP; eCFP; merge of eYFP and eCFP to visualize colocalization; intensity histograms of the section indicated with yellow line in merge; transmission. eYFP and eCFP are shown in green

and red, respectively, in order to make colocalization better visible (yellow in merge indicates colocalization). Intensity histogram shows the pixel-by-pixel analysis of the indicated section from left to right; green, Kv1.5; red, FHL1. Transmission shows phase image of stained HL-1 cell. The FHL1 variant used is indicated at the left side of each horizontal series of images. One representative image out of three series of experiments is shown.

In order to study subcellular distribution of $K_{v1.5}$ and FHL1, $K_{v1.5}$- or individual FHL1-tagged proteins were coexpressed with marker proteins for the sarcoplasmic reticulum or lipid raft domains of the plasma membrane (Figure 15).

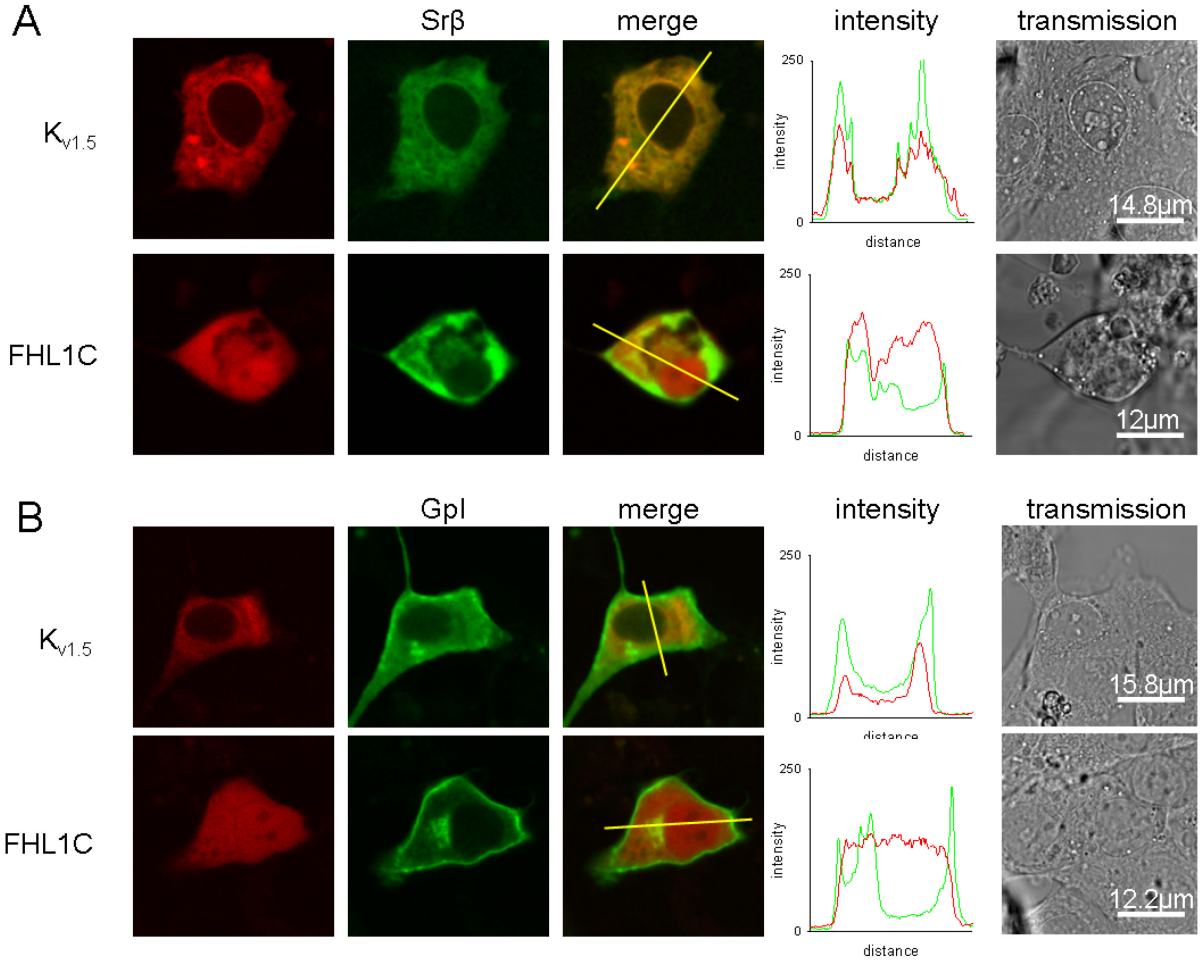


**Figure 15: Subcellular (co)localization of $K_{v1.5}$ and FHL1C with subcellular markers for sarcoplasmic reticulum and lipid raft domains** Transfection of HL1 cells was performed as described in Figure 7. Each horizontal sequence of micrographs shows identical cells. The sequence of channels (from left to right) is: eYFP; eCFP; merge of eYFP and eCFP to visualize colocalization; intensity histograms of the section indicated with yellow line in merge; transmission. eYFP and eCFP are shown in green and red, respectively, in order to make colocalization better visible (yellow in merge indicates colocalization). Intensity histogram shows the pixel-by-pixel analysis of the indicated section from left to right; $K_{v1.5}$ or FHL1C (red); subcellular marker (green). Transmission shows phase image of stained HL-1 cell. One representative image out of three is shown. (A) Upper horizontal sequence: $K_{v1.5}$ (red) coexpressed with Srß subcellular marker (green). Lower horizontal sequence: FHL1C

(red) coexpressed with Srß (green). (B) Upper horizontal sequence: $K_{v1.5}$ (red) coexpressed with GpI subcellular marker (green). Lower horizontal sequence: FHL1C (red) coexpressed with GpI (green).

Colocalization of $K_{v1.5}$ with the sarcoplasmic reticulum marker revealed predominant localization of the channel in the sarcoplasmic reticulum. Partial colocalization of $K_{v1.5}$ with the lipid raft domain marker is further indicative for its presence in plasma membrane rafts. Staining for FHL1C showed considerable overlap with both markers for the sarcoplasmic reticulum and the lipid raft domains of the plasma membrane, indicating substantial distribution of FHL1C throughout these cellular compartments.

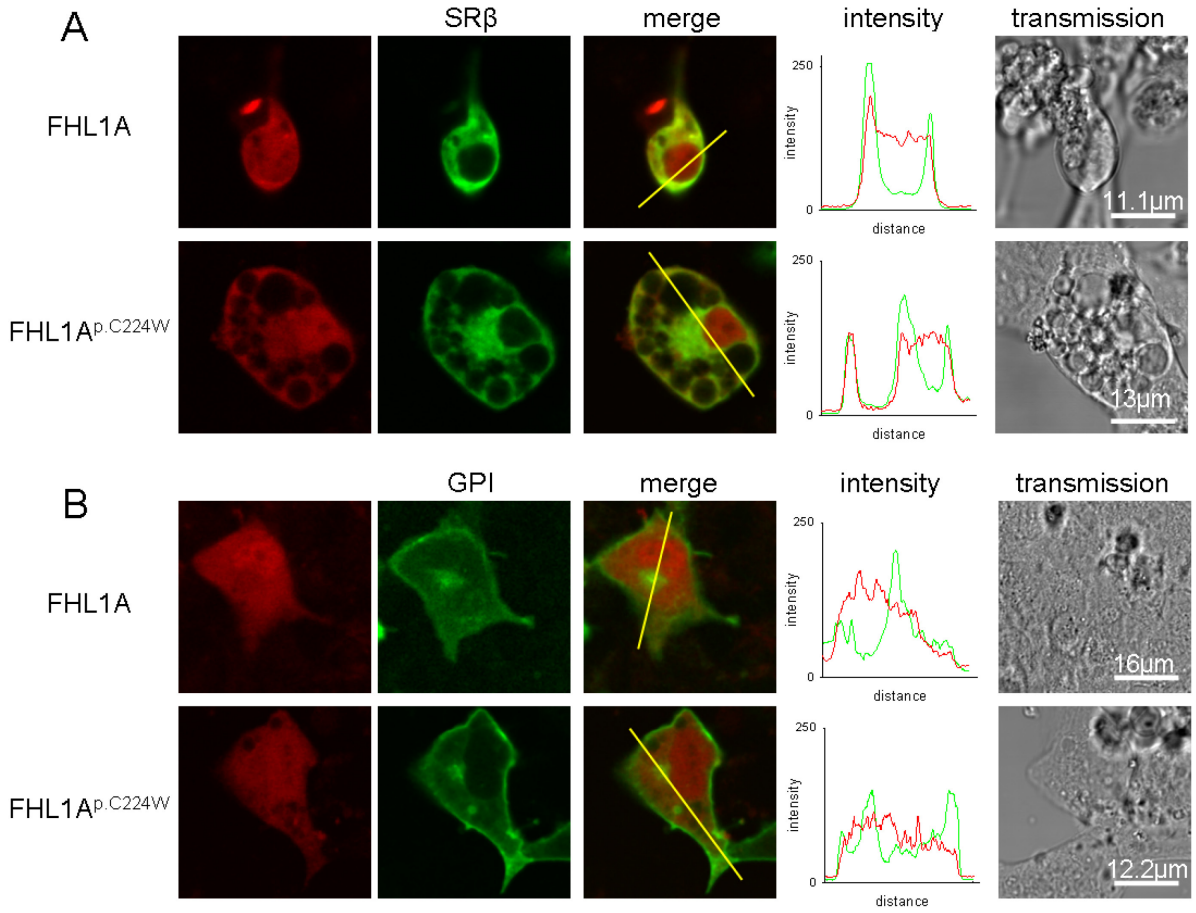


**Figure 16: Subcellular localization of $K_{v1.5}$ and FHL1A and FHL1A$^{p.C224W}$ with subcellular markers for sarcoplasmic reticulum and lipid raft domains** Transfection of HL-1 cells was performed as in Figure 7 and screened for signal after 24 to 48 h using confocal imaging. Each horizontal sequence of micrographs shows identical cells. The sequence of channels (from left to right) is: eYFP; eCFP; merge of eYFP and eCFP to visualize colocalization; intensity histograms of the section indicated with yellow line in merge; transmission. eYFP and eCFP are shown in green and red, respectively, in order to make colocalization better visible (yellow in merge indicates colocalization). Intensity

histogram shows the pixel-by-pixel analysis of the indicated section from left to right; FHL1A or FHL1A$^{p.C224W}$ (red); subcellular marker (green). Transmission shows phase image of stained HL-1 cell. The FHL1 variant used is indicated at the left side of each horizontal series of images. One representative image out of three experiments is shown. (A) Upper horizontal sequence: FHL1A coexpressed with subcellular marker Srß. Lower horizontal sequence: FHL1A$^{p.C224W}$ coexpressed with Srß. (B) Upper horizontal sequence: FHL1A coexpressed with subcellular marker GpI. Lower horizontal sequence: FHL1A$^{p.C224W}$ coexpressed with GpI.

A similar cellular distribution was observed for both FHL1A-tagged isoforms, i.e., FHL1A and FHL1A$^{p.C224W}$. Figure 16 further shows that expression of both FHL1A isoforms is less pronounced when compared to FHL1C, and consequently, less pronounced colocalization with the marker for lipid rafts of plasma membrane was observed.

# 4 DISCUSSION

Mutations in FHL1 (previously called skeletal muscle LIM protein 1) are associated with hereditary (cardio) myopathy and five distinct types of muscular dystrophies and myopathies: scapuloperoneal myopathy (SPM), reducing body myopathy (RBM), rigid spine syndrome (RSS), Emery-Dreifuss muscular dystrophy (EDMD) and X-linked myopathy characterized by postural muscle atrophy (XMPMA, see Windpassinger et al., 2008; Gueneau et al., 2009; Schessl et al., 2009; Schoser et al., 2009; Chen 2010; Knoblauch et al., 2010). Although indicated myopathies caused by mutations in FHL1 share some clinicopathological features they differ in other peculiarities such as age of onset, rate of progression, distribution and severity (Cowling et al., 2011).

Scapuloperoneal myopathy is a neuromuscular disorder involving muscle wasting and weakness, usually limited to the scapula and peroneal muscles, sometimes including facial muscles. It is marked by progressive muscular atrophy, which is often appearing asymmetrically. No sensory abnormalities, dysarthria, or contractures of the limbs are reported. One of the first reported mutations in FHL1 was found in a large Italian-American family presenting an X-linked dominant form of scapuloperoneal myopathy (Table 6, see also Quinzii *et al.*, 2008). A W122S substitution in a highly conserved residue was identified in second LIM domain and it is suggested to play important role in FHL1 protein formation and function. A second mutation at the same position, W122C, was recently described in another unrelated family with milder SPM (Chen *et al.*, 2010). Both mutations are predicted to intervene with stability of LIM domain as mutated tryptophan residue is highly conserved and present in all four LIM domains where it forms an intermolecular interaction with neighboring residues (F127, T120 and K107) (Quinzii *et al.*, 2008). Interestingly in the large Italian-American family, where 15 members are affected, loss of FHL1 is increasing parallel with severity of SPM as the male patients are hemizygous for the mutation and more severely affected than heterozygous female members (Quinzii *et al.*, 2008).

So far the greatest number of FHL1 mutations (ten missense mutations and one deletion in 22 patients from 16 unrelated families, see Table 5) was detected in patients with reducing body myopathy (Schessl *et al.*, 2008; Schessl *et al.*, 2009; Schessl *et al.*, 2010; Schalaby *et al.*, 2009). RBM is a rare neuromuscular disorder characterized by progressive muscle weakness and the presence of intracytoplasmatic aggregates in histological muscle fibers termed reducing bodies (Liewluck *et al.*, 2007). A large number of different proteins have been identified within inclusions and mutated FHL1 was found to be a major component (Schessl *et al.*, 2008; Liewluck *et al.*, 2007). FHL1 binding partners MyBPC and NFATc1 were also found in the reducing bodies (Schessl *et al.*, 2008). Similarly, to rigid spine syndrome (RSS) disease progression and severity in RBM is proportional in to number of reducing bodies found in the muscle fibers.

It is now known that mutant FHL1 expressed in C2C12 skeletal myotubes can form aggregates (Schessl *et al.*, 2008; Cowling *et al.*, 2008). Interestingly, wild type FHL1 does not have the same ability to form inclusion bodies, which might lead to conclusion that the mutant FHL1 is responsible for appearing inclusions in RBM patient muscles. Other features of the disease include weakness that is predominantly affecting proximal muscles, spinal rigidity and sometimes scoliosis and elevated creatine kinase levels. RBM has heterogeneous spectrum of features ranging from mild proximal muscle weakness starting in adult life to early onset cases with rapidly progressive muscle weakness leading to loss of ambulation, respiratory failure and death (Schessl *et al.*, 2009). Although clinical and histological features of RBM are well described, until mutations of FHL1 were identified in the patients etiology the disease remained unknown.

All FHL1 mutations found in RBM patients are localized in second LIM domain and affect zinc-coordinating cysteine and histidine residues leading to disrupted folding and destabilization of the zinc-fingers. As a result, FHL1 protein is missfolded and presumably forming reducing bodies in the muscle fibers of RBM patients. Interestingly, depending on the

localization of mutated cysteine and histidine residues within the LIM domain severity of the disease progression can be predicted: residues are on the inner surface between the two tandem zinc fingers severely disrupt the LIM structure and lead to more severe phenotype with an early onset (Schessl *et al.*, 2009; Schalaby *et al.*, 2009). On the other hand, mutations affecting more distal cysteine residues result in milder RBM (Schessl, 2009 *et al.*, Schalaby *et al.*, 2009).

Rigid spine syndrome is not a separate disorder itself but a clinical feature in heterogeneous group of early onset myopathies and muscular dystrophies. It is characterized by muscular atrophy with onset in early adolescence and accompanied by spinal contractures causing spinal rigidity as a prominent feature (Dubowitz *et al.*, 1973). Schalaby et al reported on an in-frame nine base pairs deletion in FHL1, termed p.151–153delVTC, identified in a male patient who initially presented with rigid spine syndrome and later developed prominent muscle wasting (Schalaby *et al.*, 2008). This mutation affects cysteine residue in the second LIM domain.

Spinal rigidity is, so far, reported in patients with FHL1 mutations that were initially diagnosed with RBM (Schessl *et al.*, 2008; Schessl *et al.*, 2009; Schessl *et al.*, 2010; Schalaby *et al.*, 2009), X-linked SPM (Quinzii *et al.*, 2008), XMPMA (Windpassinger *et al.*, 2007; Schoser *et al.*, 2009) and EDMD (Guenau *et al.*, 2009). However, in the only reported RSS patient small number of reducing bodies was found in the muscle fibers (Schalaby *et al.*, 2008). This finding suggests that this patient might be a misdiagnosed an actually have a milder form of RBM.

Emery-Dreifuss muscular dystrophy is a condition named after Alan Eglin H. Emery and Fritz E. Dreifuss. Early joint contractures, a rigid spine, muscle wasting and weakness in a scapuloperoneal/axial pattern characterize disease. Symptoms begin to appear from early childhood to teenage years and are predominantly starting with contractures, most often involving the elbows, ankles, and neck. In severe cases, contractures are accompanied by

slowly progressive muscle weakness and wasting. Cardiac features include cardiac conduction defects and arrhythmias that can lead to bradycardia, syncope, and an increased risk of cardiac arrest and sudden death. EDMD is reported to have both X-linked and autosomal patterns of inheritance and accordingly to the underlying cause condition is divided into six subtypes. EDMD type 1 is associated with mutations in the nuclear membrane proteins emerin, type 2 and 3 with lamin A/C and type 4 and 5 with mutations in nesprin (Ellis *et al.*, 2006; Zhang *et al.*, 2007). EDMD type 6 was described for the first time when Gueneau and collaborators have reported that mutations in FHL1 cause of X-linked EDMD in patients with disease onset in both childhood and during adult life (Gueneau *et al.*, 2009). So far, there have been seven FHL1 mutations identified in EDMD patients, all localized to C-terminal part of the protein. There are two mutations reported directly disrupting zinc-coordinating cysteines, one in third and second in fourth LIM domain. Other mutations include insertions and deletions and usually resulting in truncated FHL1 protein (Gueneau *et al.*, 2009).

Interestingly, more than 20 years ago a report by Voit and collaborators has described one EDMD patients (later found to also carry a FHL1 mutation) with strikingly similar features to XMPMA phenotype. Mutation found in this patient p.C276Y is localized to fourth LIM domain and, much like most mutations found in XMPMA patients, is affecting FHL1A isoform leaving isoform C intact (Gueneau *et al.*, 2009). First symptoms in this patient was stiffness of the neck at the age of 11, later on in the adult life progressing to mixed form of atrophy (type 1 and 2) and hypertrophy (also both type1 and 2) and cardiac pain (Voit *et al.*, 1988). Also similarly to XMPMA cases this patient was reported to be toe walking (consequence of shorter Achilles tendons, see Voit *et al.*, 1988). Mother of the patient was a carrier and not affected, and maternal uncle shared several symptoms such as elevated CK, stiff neck, elbow contractures and cardiac complains. Uncle died failure at the age of 65, probably from cardiac (Voit *et al.*, 1988). Evidently, this patient does not present typical EDMD features and resembles more to XMPMA phenotype and his diagnosis might be

reconsidered in future.

**Table 6: FHL1 mutations found in X-linked myopathies (excluding XMPMA).** Data adopted from Shathasivam *et al.*, 2001; Shalaby *et al.*, 2008; Schessl *et al.*, 2009; and Gueneau *et al.*, 2009.

| Mutation | LIM domain | Isoforms affected | Clinical features | Diagnosis |
|---|---|---|---|---|
| c.365G→C<br><br>p. W122S | 2 | A, B, C | Footdrop, proximal arm weakness, hand weakness, scapular winging, elevated CK levels, desmin-positive cytoplasmic bodies | Scapuloperoneal myopathy |
| c. 364G→C<br><br>p.W122C | 2 | A, B, C | Less severe than W122S, ubiquitin- and desmin-positive FHL1 inclusions | |
| c. 302G→T<br><br>p.C101F | 2 | A, B, C | Fatal infantile form, severity is correlated with the amount of the FHL1 protein | Reducing body myopathy |
| C.304-31del AAGGGGTGC<br><br>p.102-104del KFC | 2 | A, B, C | Adult-onset form, severity is correlated with the amount of the FHL1 protein | |
| c.310T→C<br><br>p.C104T | 2 | A, B, C | Familial, severity is correlated with the amount of the FHL1 protein | |
| c.367C→T<br><br>p.H123Y | 2 | A, B, C | Delayed motor development, poor head control, stands with hyperlordosis | |
| c.368A→T<br><br>p.H123L | 2 | A, B, C | Frequent falls, difficulties walking, running and getting up from the floor (Gowers' sign), scapular and pelvic girdle muscular weakness | |
| c.369C→G<br><br>p.H123Q | 2 | A, B, C | Frequent falls, abnormal gait | |
| c.369C→A<br><br>p. H123Q | 2 | A, B, C | Head drop, not able to climb stairs and roll over when lying flat, scapular muscle hypotrophy, abolished reflexes | |
| c.395G→T<br><br>p.C132F | 2 | A, B, C | Frequent falls and mild leg weakness | |
| c.449G→A<br><br>p.C150Y | 2 | A, B, C | Fatal infantile form, severity is correlated with the amount of the FHL1 protein | |
| Unknown<br><br>p.C150R | 2 | A, B, C | Not listed | |

| | | | | |
|---|---|---|---|---|
| c.457T→C<br><br>p.C153R | 2 | A, B, C | Rigid spine, rigidity and contractures at 10 years involving neck, elbows and wrists, muscle fatigability, difficulties with stairs, no weakness | |
| c.458G→A<br><br>p.C153Y | 2 | A, B, C | Difficulties with walking and stairs, frequent falls | |
| c.451-459del GTGACTTGC<br><br>p.151–153del VTC | 2 | A, B, C | Initially rigid spine syndrome and later developed prominent muscle wasting | Rigid spine syndrome |
| c.332_501del<br><br>p.D112FfsX51 | 2, 3 | A, B, C | Early onset, weakness, joint contractures, scoliosis, respiratory insufficiency | Emery-Dreifuss Muscular Dystrophy |
| c.332_688del<br><br>p.G111_T229delinsG | 2, 3 | A, B, C | Early onset, weakness, joint contractures, scoliosis, respiratory insufficiency | |
| c.371_372delAA<br><br>p.K124RfsX6 | 2, 3, 4 | A, B, C | Early onset, weakness, joint contractures, dysphonia, arrhythmias | |
| c.469_470delAA<br><br>p.K157VfsX36 | 3, 4, new LIM | A, B, C | Early onset, weakness, joint contractures, cardiac hypertrophy | |
| c.817dup<br><br>p.C273LfsX11 | 4 | A | Early onset, weakness, joint contractures, muscle hypertrophy, cardiac hypertrophy, sudden death | |
| c.827G→A<br><br>p.C276Y | 4 | A | Adult onset, weakness, joint contractures, muscle hypertrophy, arrhythmias, cardiac hypertrophy | |
| c.841T→G<br><br>p.X281E | After 4 | A | Early onset, weakness, joint contractures, scoliosis, dysphonia, cardiac hypertrophy | |
| c.625 T→C<br><br>p.C209R | 3 | A, B | Early onset, weakness, joint contractures, scoliosis, arrhythmias, LV dysfunction, cardiac hypertrophy, sudden death | Emery-Dreifuss-like syndrome |

When XMPMA was first described by our group two families, one from Austria and one from UK, were reported to share similar features (Windpassinger *et al.*, 2007). Some of the both families' members were previously diagnosed as to have other myopathies such as Becker muscular dystrophy, but their phenotype did not completely fit to any of the known disorders. For example, positive staining for desmin in core-like lesions excluded BMD as a

correct diagnosis (Schoser *et al.,* 2009). Immunohistochemical and western blot analysis for emerin, dysferlin, caveolin, and calpain excluded other known myopathies (DMD, EDMD and limb-girdle MDs, see also Windpassinger *et al.*, 2007). XMPMA is characterized by atrophy of postural muscles with rigid spine syndrome, pseudoathleticism or hypertrophy and hypertrophic cardiomyopathy (Windpassinger *et al.*, 2007). Pseudoathleticism or hypertrophy and hypertrophic cardiomyopathy are common features in other FHL1opathies. However, it is important to emphasize that the initial muscle hypertrophy is characteristic exclusively for XMPMA phenotype diagnosis (Schoser *et al.,* 2009). Besides with known FHL1opathies, XMPMA shares some similar features with myofibrillar myopathies; emblematic granulofilamentous material found in skeletal muscle biopsies of XMPMA patients resembles to secondary desmin protein accumulation characterizing myofibrillar myopathies diagnosis (Schoser *et al.,* 2009; Dubowitz *et al.*, 2007; Schroder *et al.*, 2007). Here again overlap with other diseases is not complete as reducing bodies found in XMPMA patients are not reported in myofibrillar myopathies. Disease development starts with a pseudoathletic appearance with neck rigidity and Achilles tendon shortening in as first symptoms. Later follow scapuloaxioperoneal syndrome, postural muscle atrophy and scapular winging, accompanied by progressive proximal weakness in a limb-girdle (Schoser *et al.,* 2009). Elevated creatine kinase (CK) levels are reported in most of the patients. In aged patients, moderate scoliosis and dull deep lower back pain are also found. Age of onset varies between 8 and 45 years with a marked disease progression in late 30s. XMPMA belongs to a group of mild myopathies with a wide range of life expectancy (42 to 75 years) and respiratory and cardiac failure as the leading cause of death (Schoser *et al.,* 2009). Respiratory failure is usually caused by progressive pulmonary insufficiency that is reported in some of the patients (Windpassinger *et al.*, 2007; Schoser *et al.,* 2009). Regarding the cardiac features, cardiac rhythm alterations, mild proximal myopathy and arrhythmias are reported in several carriers.

In addition, in two male patients a rare aneurysm of the sinus of Valsalva was found (Schoser *et al.,* 2009).

In 2008, our group has identified the *FHL1* gene on chromosome Xq26.3 as the causative gene for this new genetic disorder (Windpassinger *et al.*, 2007). First and most common mutation identified was amino acids substitution C224W found in several members of index family (Windpassinger *et al.*, 2007). Together with this initial discovery five mutations occurring in eight families from Austria, UK, Germany and Croatia were described (Table 7, Windpassinger *et al.*, 2007; Schoser *et al.,* 2009).

Since FHL3 has several roles skeletal and cardiac muscle and shares almost the same expression profile with FHL1 as a part of our project, we have performed the screening of undiagnosed myopathy patients to look for mutations in FHL3 gene. Despite promising results with one heterozygous missense mutation found in an undiagnosed myopathy patient due to the lack of family member data we were not able to continue research in that direction.

In our current work, we have focused on two mutations found in XMPMA patients. Naturally, our interest first turned to the p.C224W mutation, most commonly found in XMPMA. It is a missense mutation that replaces a highly conserved cysteine within the fourth LIM domain of FHL1 leaving the LIM domain disrupted (Scheme I). As a result, almost complete absence of FHL1A protein is recorded in skeletal muscle biopsies of affected individuals (Windpassinger *et al.*, 2007). The second mutation that we have addressed is the splice site mutation pA168GfsX195, (termed p.G168fs) located after the second LIM domain.

It is very important to notice that, exclusive of c.381_382insATC (p.F127_T128insI), FHL1 mutations found in XMPMA patients leave isoform C intact. In our opinion this results in considerably milder phenotype compared to other FHL1opathies. This hypothesis can be backed up by the fact that FHL1 mutations in more proximal part of protein reported in other myopathies such as RMB usually result in more severe phenotype.

**Table 7: FHL1 mutations found in XMPMA patients and clinical consequences.** Data collected from previous publications (Windpassinger *et al.*, 2007; Schoser *et al.,* 2009). *Numbers refer to FHL1B.

| Mutation | Localization | Affected isoform | Number of families | Clinical features |
|---|---|---|---|---|
| c.672C→G<br><br>p.C224W | exon 4<br><br>4th LIM(FHL1A)<br>or<br>1st NLS (FHL1B) | A, B | 4 | Childhood to adult onset, very heterogeneous phenotype: neck rigidity, elevated CK, progressive muscle weakness and atrophy, scapular winging, RSS, respiratory insufficiency leading to respiratory failure. Cardiac involvement: cardiomyopathy and cardiac ventricular arrhythmia. |
| c.381_382insATC<br><br>p.F127_T128insI | exon 3<br><br>2nd LIM | A, B, C | 1 | Late onset, progressive, starting with hip-flexor weakness, elevated serum CK levels. Later on athletic appearance, limited neck flexion, muscle hypertrophy (most prominent in shoulder girdle and arm muscles) and reduced lung function develop. Type I fiber atrophy, variation in fiber size found in skeletal muscle. No cardiac symptoms. |
| c.838 G3A*<br><br>p.V280M* | exon 5<br><br>3rd LIM | B | 1 | Childhood onset slowly progressing XMPMA, starting with exercise-induced fatigue, Achilles tendon shortening and proximal lower leg weakness in childhood. Later on: neck rigidity, posterior leg muscle atrophy and weakness. No cardiac involvement. |
| c.688+1:G→A<br><br>p.A168GfsX195 | exon 4<br><br>3rd and 4th LIM | A, B | 1 | Symptoms start with progressive Achilles tendon shortening in childhood. Some patients exhibit exercise-induced weakness and mild RSS. In two cases sinus of Valsalva aneurysm was found. |
| c.736 C3T<br><br>p.H246Y | exon 6<br><br>4th LIM(FHL1A)<br>or<br>1st NLS (FHL1B) | A, B | 1 | Teenage onset, mild myopathy starting with athletic appearance, mild rigid neck syndrome and contracture of the Achilles tendons. |

In addition, in XMPMA, in cases such as p.F127_T128insI mutation, although having a late onset, disease is very progressive compared to other mutations.

As these conditions are affecting both skeletal and cardiac muscle (Windpassinger *et al.*, 2007; Schoser *et al.,* 2009) we here focus on (patho)physiology of two FHL1A mutations in XMPMA patients leading to an altered LIM organization compared to FHL1A, the major occurring FHL1 isoform.

LIM domains play important roles in various cellular processes, such as cytoskeleton organization, signal transduction, gene expression and cell differentiation (Kadrmas *et al.*, 2004; Crowling *et al.,* 2011). Both addressed mutated FHL1A variants show alterations in the primary structure; (i) the missense mutation results in an amino acid exchange leads to disruption of the fourth LIM domain ($FHL1A^{p.C224W}$); (ii) the splice site mutation results in the deletion of the two C-terminal LIM domains and the resulting protein termed $FHL1A^{p.G168fs}$ resembles wild-type FHL1C protein.

Although both mutations are also affecting FHL1 isoform B, in our current work we have not addressed functional changes of this protein. FHL1B consists of three and a half N-terminal LIM domains (identical to isoform A) and a novel C-terminus containing three nuclear localization signals (NLS), a nuclear export sequence, and a C-terminal binding site for RBP-Jκ (Lee *et al.*, 1999). C224W mutation effects first nuclear localization signal (NLS1) and probably results in impaired FHL1B shuttling between nucleus and cytoplasm. Thus, functional consequences of C224W mutation on FHL1A and FHL1B variants are different. On the other hand, splice site mutation should have the same results in both FHL1A and B protein.

Although initially reported to be expressed only in the brain (Lee *et al*., 1999) FHL1B isoform is predominantly found in skeletal muscle (Brown *et al*., 1999). In skeletal muscle, FHL1B is predominantly expressed in the cell nucleus of the C2C12 myoblasts but in differentiated myotubes, protein shifts and becomes exclusively cytosolic suggesting a role in

cytoskeleton and nuclear-cytoplasmic communication (Brown *et al*., 1999). Other findings suggest FHL1B may protect skeletal muscle from apoptosis (Cottle *et al*., 2009).

To investigate FHL1 expression in skeletal muscle of affected patients we have performed RT-PCR. In XMPMA patient carrying the splice site mutation ($FHL1^{p.G168fs}$) FHL1A/B mRNA are only present in traces and as expected show a massive overexpression of FHL1C. No obvious differences in mRNA expression became apparent for cDNA of $FHL1A^{p.C224W}$ patient myoblasts. However, immunoblot experiments showed that both patient myoblast preparations do not express significant amounts of FHL1A wild-type protein. If FHL1B is expressed, the functionality of FHL1B in XMPMA patients might be impaired; the reason is that the p.C224W mutation will probably have an adverse effect on the functionality of the first nuclear localization sequence in the C-terminal portion of FHL1B (Scheme I) that could result in impaired shuttling of the mutated FHL1B protein between nucleus and cytoplasm in further consequence (Windpassinger *et al.*, 2007).

In contrast to control myoblasts $K_{v1.5}$ mRNA expression is decreased in myoblast preparations from both XMPMA patients. This finding was further confirmed on protein level. To our knowledge, this is a first report on altered expression of Kv1.5 in myopathy. In addition, functionality of this channel was never investigated before in connection to any pathological feature in skeletal muscle.

A recent paper (Weng *et al.*, 2011) reported that FHL1 knockdown significantly inhibits proliferation of rat aortic smooth muscle cells. Another publication (Kwapiszewska et al., 2008) demonstrated that silencing of FHL1 in primary human pulmonary artery smooth muscle cells also inhibits cell migration and proliferation, whereas overexpression had the opposite effect. We here show a reduced proliferation rate of XMPMA patient myoblasts; an increased number of cells in the $G_0/G_1$ phase was found (Fig. 9). Villalonga and co-workers have previously reported that $K_{v1.5}$ is involved in skeletal muscle proliferation by controlling $G_1$-phase progression through a mechanism that involves the CDKIs $p21^{cip\text{-}1}$ and $p27^{kip1}$, and

cyclins A and $D_1$ (Villalonga *et al*., 2008). Similarly recent report shows FHL1 inhibits lung cancer cell growth via both the G1 and the G2/M cell cycle arrest concomitant with a marked inhibition of cyclin A, cyclin B1 and cyclin D accompanied by upregulation of the cyclin dependent kinase inhibitors p21 and p27 (Niu *et al*., 2011). Since FHL1 is expressed in several tissues, we can speculate it may be involved in proliferation of other cell types as well, possibly through interaction with its binding partners.

What is particularly interesting for our work is that another group's in vitro experiments have shown that the reduced FHL1 expression found in EDMD patients with FHL1 mutations delays myogenin expression and myoblast fusion of primary cells (Guenau *et al.,* 2009). Same features were previously reported in Myotonic dystrophy type 1 (DM1) and hypertrophic cardiomyopathy (Amack *et al.,* 2001; de Luna *et al.,* 2006). In a recent study, Cowling and collaborators have demonstrated existence of correlation between FHL1 expression and myotube size (Cowling *et al.,* 2008). In our experiments, we have also attempted to investigate whether there is a difference in myotube differentiation and satellite cell activation between FHL1 mutated myoblasts and corresponding controls. As previously discussed, both stainings (for myogenin and myogenin D) were negative but also rather unconvincing. Weather the lack of conclusive finding was a result of inappropriate staining technique or the fact that cells were kept in culture for too short for myotube differentiation to occur we cannot draw any conclusions from obtained results.

Interestingly, among XMPMA patients one female carrier was reported to have pulmonary hypertension (PH). FHL1 is reported to be novel protein regulated in various forms of PH, including idiopathic pulmonary arterial hypertension (Kwapiszewska et al., 2008). Inhibited $K_{v1.5}$ channel expression and function have been reported in pulmonary artery smooth muscle cells (PASMC) from patients with idiopathic pulmonary arterial hypertension (IPAH). (Yuan *et al*., 1998a; Yuan *et al*., 1998b). Several other authors have also reported on

close link between $K_{v1.5}$ channel dysfunction and pulmonary vasoconstriction and PASMC proliferation (Archer *et al*., 2001: Platoshyn *et al*., 2001: Smirnov *et al*., 1994).

Another interesting clinical feature connecting $Kv_{1.5}$ and FHL1 is reported in two patients with splice site mutation: they both exhibit sinus of vasalvae aneurism. Downregulation of $K_{v1.5}$ was previously reported in microarray data from patients with abdominal aortic aneurism (Lenk *et al*., 2007). Although not in the same part of aorta (sinus valsalva aneurysm is located at the beginning of the aorta, where the coronary arteries arise from and abdominal aortic aneurysm is located in the abdomen) both are located in the aortic wall. In 2010, Weng and collaborators have reported FHL1 is downregulated in thoracic aortic dissection (TAD) patients compared to the controls (Weng *et al*., 2010). Since FHL1 knockdown inhibited proliferation of rat aortic SMC but had no effect on apoptosis, there is a possibility that FHL1 contributes to development of TAD by suppressing proliferation and affecting aortic wall remodeling (Weng *et al*., 2010).

We here show for the first time an interaction of FHL1C with $K_{v1.5}$. For these studies, the oocyte system, a well-known in vitro system to study membrane channel functionality, has been used. We show a different conductivity of $K_{v1.5}$ channel when coexpressed with FHL1 variants. The interaction between FHL1C and $K_{v1.5}$ had the strongest impact on channels conductivity when compared to FHL1A (wild type) and $FHL1A^{p.C224W}$. Since FHL1C is abundantly expressed on mRNA level in XMPMA patient carrying the p.G168fs mutation, coexpression of $K_{v1.5}$ with FHL1C is likely to mimic cardiac function in vivo.

In another study (Yang *et al*., 2008) it was recently reported that coexpression of $K_{v1.5}$ with FHL1 in CHO cells resulted in increased currents compared to expression of $K_{v1.5}$ alone. In our expression system, however, dose dependent expression of all FHL1 variants clearly resulted in dose-dependent reduction of $K_{v1.5}$ currents. Furthermore, the coexpression of FHL1 variants with two other ion channel complexes (GIRK1/GIRK4 and $Na_{v1.5}$) revealed the

effect specific for $K_{v1.5}$. Hence, this apparently contradictory result may be due to differential protein processing/trafficking in the CHO cell expression system.

Traffic and subcellular localization regulate ion channel activities that are essential to understand their role (Vincente *et al*., 2008). We here found that all three FHL1 variants (FHL1A, and FHL1A$^{p.C224W}$ and FHL1C) are localized in the cell nucleus and cytoplasm, in the latter they colocalized with $K_{v1.5}$. To our knowledge, this is the first report on $K_{v1.5}$ expression and functionality in muscular dystrophy patients, which is a direct result of mutations in FHL1. The presence of intact FHL1C, as occurring in our patients, is apparently resulting in the relative mild phenotype in XMPMA patients when compared to other FHL1 mutation associated myopathies (Cowling *et al*., 2011). Therefore, it is likely to assume that FHL1C could compensate either absence or reduced levels of other FHL1 isoforms.

Since FHL1 possibly regulates Kv1.5 functionality in both cardiac and skeletal muscle this channel could be considered as a possible new target for therapy of FHL1opathies. Blocking of Kv1.5 is already used in treatment of cardiac arrhythmias, particularly atrial fibrillation. Because Kv1.5 is highly expressed in atria and not in ventricles, inhibition of Kv1.5 can selectively prolong atrial action potential duration without interfering with ventricular action potential (Nattel *et al*., 1999, Wang *et al*., 1993). This is important because prolongation of ventricular action potentials could induce long QT syndrome. For that reason this channel became a promising and well-studied target in treatment of atrial fibrillation with many new blockers identified.

All of the so far identified Kv1.5 blockers are binding the S6 putative region of the channel. For that reason, it is speculated that this is the pore-lining region in the channel and it is crucial for determining drug affinity and specificity (Yeola *et al.,* 1996). Several residues in this region were confirmed to determine the binding of both neutral and acid drugs, which could suggest that there is a common receptor site in S6 that binds all of the blockers of Kv1.5 (Tamargo *et al.,* 2003). In 2004 another six residues within the same region were reported to

be responsible for binding of specific $I_{Kur}$ blocker S0100176. (Decher *et al.,* 2004). This finding has further confirmed importance of S6 region for activity of the Kv1.5. Besides blocking Kv1.5 these six residues were also found to overlap with binding sites for other blockers and Kv channels, suggesting a conservation of drug binding sites among different $K^+$ channel families (Tamargo *et al.,* 2003).

However, most of the well characterized Kv1.5 blockers, including S0100176, have turned out to be not selective but also block other ion channels including HERG and other sodium channels that can be expressed in heart as well as other tissues. In addition, Kv1.5 itself is expressed in other tissues besides in human atrium, such as vascular smooth muscle. Finally, a specific Kv1.5 blocker may require activity at a binding site other than the one located in the central cavity (Decher et al., 2004). All of this could lead to loss of previously mentioned atrial selectivity. In our work we have performed several two electrode voltage clamp experiments with HERG channel and found that FHL1 variants when coexpressed with HERG significantly reduce channel‘s currents. For that reason, in our opinion, FHL1 could not be considered as a potential target in treatment of cardiac arrhythmias.

In conclusion, we have described the interaction of FHL1 variants with $K_{v1.5}$. Since $K_{v1.5}$ expression and functionality are altered in XMPMA patients we propose FHL1 might regulate channel in both cardiac and skeletal muscle. Absence of FHL1 could result in lack of regulation of the channel and explain at least a part of the cardiac pathophysiology found in XMPMA patients.

## 5 FUNDING

This work received financial supported by the County of Styria (GZ: A3-16.R-10/2009-112). The PhD program Molecular Medicine of the Medical University of Graz, Austria funded Ivana Poparic.

# 6 CONTRIBUTION OF THE AUTHORS

Ivana Poparic performed the mRNA and protein isolations, synthesized RNA from DNA constructs, sequencing analysis, reverse transcription PCR, Real-time RT-PCR, Western blotting, HL1 cell culture, *Xenopus* oocytes expression and electrophysiology, confocal microscopy, statistics, planned the experiments and contributed in writing the manuscript.

Astrid Gorischek has operated on *Xenopus leavis*, prepared Xenopus oocytes, synthetized proteins for pull-down assay, and produced RNA for TEVC control experiments.

Astrid Gorischek and Ivana Poparic have produced DNA constructs and adopted protocol for the pull-down assay.

Heidi Miedl has established myoblast cell culture, performed proliferation assay and cell cycle analysis by flow cytometry.

Heidi Miedl and Ivana Poparic have performed the immunocytochemistry and analyzed results from proliferation assay and flow cytometry.

Sonja Hochmeister performed the immunohistochemistry.

Josepha Binder provided the human heart samples and performed section of the cardiac compartments.

Benedikt Schoser provided the myoblast samples and protocols for myoblast cell culture and contributed to planning of experiments related to myoblast samples.

Julia Wantschitz provided immunocytochemistry antibodies and protocol and advised on immunocytochemistry experiments.

Gernot Desoye planned the experiments and contributed to writing the manuscript.

Stefan Quasthoff planned the experiments and contributed to writing the manuscript.

Heinrich Maechler provided the heart ear samples.

Klaus Wagner planned the experiments and contributed to writing the manuscript.

Wolfgang Schreibmayer planned the experiments and contributed to writing the manuscript.

Christian Windpassinger planned the experiments and contributed to writing the manuscript.

Ernst Malle planned the experiments and contributed to writing the manuscript.

# 7 LITERATURE

Aldred MA, Huang Y, Liyanarachchi S, Pellegata NS, Gimm O, Jhiang S, et al. Papillary and follicular thyroid carcinomas show distinctly different microarray expression profiles and can be distinguished by a minimum of five genes. J Clin Oncol. 2004;22:3531-3539.

Amack JD, Mahadevan MS. The myotonic dystrophy expanded CUG repeat tract is necessary but not sufficient to disrupt C2C12 myoblast differentiation. Hum. Mol.Genet. 2001;10:1879–1887.

Archer SL, London B, Hampl V, Wu X, Nsair A, Puttagunta L, et al. Impairment of hypoxic pulmonary vasoconstriction in mice lacking the voltage-gated potassium channel Kv1.5. FASEB J. 2001;15:1801–1803.

Bach I. The LIM domain: regulation by association. Mech Dev. 2000;91:5-17.

Beggs AH, Hoffman EP, Snyder JR, Arahata K, Specht L, Shapiro F et al. Exploring the molecular basis for variability among patients with Becker muscular dystrophy: dystrophin gene and protein studies. Am J Hum Genet. 1991;49:54–67.

Bhattacharjee A, Richards WG, Staunton J, Li C, Monti S, Vasa P et al. Classification of human lung carcinomas by mRNA expression profiling reveals distinct adenocarcinoma subclasses. Proc Natl Acad Sci U S A. 2001;98:13790-13795.

Bonne G, Carrier L, Bercovici J, Cruaud C, Richard P, Hainque B, et al. Cardiac myosin binding protein-C gene splice acceptor site mutation is associated with familial hypertrophic cardiomyopathy. Nat Genet. 1995;11:438-440.

Brendel J, Peukert S. Blockers of the Kv1.5 channel for the treatment of atrial arrhythmias. Curr Med Chem Cardiovasc Hematol Agents. 2003;1:273-287.

Brown S, McGrath MJ, Ooms LM, Gurung R, Maimone MM, Mitchell CA. Characterization of two isoforms of the skeletal muscle LIM protein 1, SLIM1. Localization of SLIM1 at focal adhesions and the isoform slimmer in the nucleus of myoblasts and cytoplasm of myotubes

suggests distinct roles in the cytoskeleton and in nuclear-cytoplasmic communication. J Biol Chem. 1999; 274: 27083-27091.

Chen DH, Raskind WH, Parson WW, Sonnen JA, Vu T, Zheng Y et al. A novel mutation in FHL1 in a family with X-linked scapuloperoneal myopathy: phenotypic spectrum and structural study of FHL1 mutations. J Neurol Sci. 2010; 296:22–29.

R. Chittajallu, Y. Chen, H. Wang, X. Yuan, C.A. Ghiani, T. Heckman, et al. Regulation of Kv1 subunit expression in oligodendrocyte progenitor cells and their role in G1/S phase progression of the cell cycle, Proc. Natl. Acad. Sci. USA. 2002;99:2350–2355.

Chung HJ, Qian X, Ehlers M, Jan YN, Jan LY. Neuronal activity regulates phosphorylation-dependent surface delivery of G protein-activated inwardly rectifying potassium channels. Proc Natl Acad Sci USA. 2009;106:629-634.

Claycomb WC, Lanson NA Jr, Stallworth BS, Egeland DB, Delcarpio JB, Bahinski A et al. HL-1 cells: a cardiac muscle cell line that contracts and retains phenotypic characteristics of the adult cardiomyocyte. Proc Natl Acad Sci USA. 1998;95:2979-2984.

Coghill ID, Brown S, Cottle DL, McGrath MJ, Robinson PA, Nandurkar HH, et al. FHL3 is an actin-binding protein that regulates alpha-actinin-mediated actin bundling: FHL3 localizes to actin stress fibers and enhances cell spreading and stress fiber disassembly. J Biol Chem. 2003;278:24139-24152.

Cottle DL, McGrath MJ, Cowling BS, Coghill ID, Brown S, Mitchell CA. FHL3 binds MyoD and negatively regulates myotube formation. J Cell Sci. 2007;120:1423-1435.

Cottle DL, McGrath MJ, Wilding BR, Cowling BS, Kane JM, D'Arcy CE, et al. SLIMMER (FHL1B/KyoT3) interacts with the proapoptotic protein Siva-1 (CD27BP) and delays skeletal myoblast apoptosis. J Biol Chem. 2009;284:26964-26977.

Cowling BS, Cottle DL, Wilding BR, D'Arcy CE, Mitchell CA, McGrath MJ. Four and a half LIM protein 1 gene mutations cause four distinct human myopathies: A comprehensive

review of the clinical, histological and pathological features. Neuromuscul Disord. 2011; 21:237-251.

Cowling BS, McGrath MJ, Nguyen MA, Cottle DL, Kee AJ, Brown S, et al. Identification of FHL1 as a regulator of skeletal muscle mass: implications for human myopathy. J Cell Biol 2008;183:1033-1048.

Curran ME, Splawski I, Timothy KW, Vincent GM, Green ED, Keating MT. A molecular basis for cardiac arrhythmia: HERG mutations cause long QT syndrome. Cell. 1995;80:795–803.

Decher N, Pirard B, Bundis F, Peukert S, Baringhaus KH, Busch AE, Steinmeyer K, Sanguinetti MC. Molecular basis for Kv1.5 channel block: conservation of drug binding sites among voltage-gated K+ channels. J Biol Chem. 2004;279:394-400.

de Luna N, Gallardo E, Soriano M, Dominguez-Perles R, de la Torre C, Rojas-Garcia R, Garcia-Verdugo JM, Illa I. Absence of dysferlin alters myogenin expression and delays human muscle differentiation “in vitro”. J. Biol. Chem. 2006;281:17092–17098.

Dhanasekaran SM, Barrette TR, Ghosh D, Shah R, Varambally S, Kurachi K, et al. Delineation of prognostic biomarkers in prostate cancer. Nature. 2001;412:822-826.

Ding L, Wang Z, Yan J, Yang X, Liu A, Qiu W, et al. Human four-and-a-half LIM family members suppress tumor cell growth through a TGF-beta-like signaling pathway. J Clin Invest. 2009;119:349-361.

Dubowitz V. Rigid spine syndrome: a muscle syndrome in search of a name. Proc R Soc Med. 1973;66:219–220.

Dubowitz V, Sewry CA. Muscle Biopsy: A Practical Approach. 3rd ed. Edinburgh: Saunders/Elsevier; 2007.

Ehrlich JR, Biliczki P, Hohnloser SH, Nattel S. Atrial-selective approaches for the treatment of atrial fibrillation. J Am Coll Cardiol. 2008;51:787–792.

Ellis JA. Emery–Dreifuss muscular dystrophy at the nuclear envelope: 10 years on. Cell Mol

Life Sci. 2006;63:2702–2709.

Ericson J, Thor S, Edlund T, Jessell T, Yamanda T. Early stages of motor neuron differentiation revealed by expression of homeobox gene Islet-1. Science. 1992;256:1555–1560.

Feng J, Wible B, Li GR, Wang Z, Nattel S. Antisense oligodeoxynucleotides directed against Kv1.5 mRNA specifically inhibit ultra rapid delayed rectifier K+ current in cultured adult human atrial myocytes. Circ Res. 1997;80:572-579.

Ferguson E, Horvitz HR. Identification and characterization of 22 genes that affect the vulval cell lineages of Caenorhabditis elegans. Genetics 1985;110:17-72.Ferguson EL, Sternberg PW, Horvitz HR. A genetic pathway for the specification of the vulval cell lineages of Caenorhabditis elegans. Nature. 1982;326:259-267.

Fimia GM, De Cesare D, Sassone-Corsi P. A family of LIM-only transcriptional coactivators: tissue-specific expression and selective activation of CREB and CREM. Mol Cell Biol. 2000;20:8613-8622.

Finley DJ, Zhu B, Barden CB, Fahey TJ 3rd. Discrimination of benign and malignant thyroid nodules by molecular profiling. Ann Surg. 2004;240:425-436.

Flashman E, Redwood C, Moolman-Smook J, Watkins H. Cardiac myosin-binding protein C. Circ Res. 2004;94:1279–1289.

Foster LJ, Rudich A, Talior I, Patel N, Huang X, Furtado LM, et al. Insulin-dependent interactions of proteins with GLUT4 revealed through stable isotope labeling by amino acids in cell culture (SILAC). J Proteome Res. 2006;5:64-75.

Freyd G, Kim SK, Horvitz HR. Novel cysteine-rich motif and homeodomain in the product of the Caenorhabditis elegans cell lineage gene lin-11. Nature. 1990;344:876–879.

Fryknäs M, Wickenberg-Bolin U, Göransson H, Gustafsson MG, Foukakis T, Lee JJ, et al. Molecular markers for discrimination of benign and malignant follicular thyroid tumors. Tumour Biol. 2006;27:211-220.

Glebov OO, Nichols BJ. Lipid raft proteins have a random distribution during localized activation of the T-cell receptor. Nat Cell Biol 2004;6:238–243.

Geier C, Gehmlich K, Ehler E, Hassfeld S, Perrot A, Hayess K, et al. Beyond the sarcomere: CSRP3 mutations cause hypertrophic cardiomyopathy. Hum Mol Genet. 2008;17:2753-2765.

Geier C, Perrot A, Ozcelik C, Binner P, Counsell D, Hoffmann K, et al. Mutations in the Human Muscle LIM Protein Gene in Families With Hypertrophic Cardiomyopathy Circulation. 2003;107:1390-1395.

Gueneau L, Bertrand AT, Jais JP, Salih MA, Stojkovic T, Wehnert M, et al. Mutations of the FHL1 gene cause Emery-Dreifuss muscular dystrophy. Am J Hum Genet. 2009;85:338-353.

Gupta BP, Wang M, Sternberg PW. The C. elegans LIM homeobox gene lin-11 specifies multiple cell fates during vulval development. Development. 2003;130:2589-2601.

High FA, Epstein JA. The multifaceted role of Notch in cardiac development and disease. Nat Rev Genet. 2008;9:49-61.

Hofer D, Lohberger B, Steinecker B, Schmidt K, Quasthoff S, Schreibmayer W. A comparative study of the action of tolperisone on seven different voltage dependent sodium channel isoforms. Eur J Pharmacol. 2006;538:5-14.

Ivanina T, Rishal I, Varon D Mullner C, Frohnwieser-Steinecke B, Schreibmayer W, et al. Mapping the Gbetagamma-binding sites in GIRK1 and GIRK2 subunits of the G protein-activated K+ channel. J Biol Chem. 2003;278:29174-29183.

Jiang F, Yin Z, Caraway NP, Li R, Katz RL. Genomic profiles in stage I primary non small cell lung cancer using comparative genomic hybridization analysis of cDNA microarrays. Neoplasia. 2004;6:623-635.

Johannessen M, Møller S, Hansen T, Moens U, Van Ghelue M. The multifunctional roles of the four-and-a-half-LIM only protein FHL2. Cell Mol Life Sci. 2006;63:268-284.

Kadrmas JL, Beckerle MC. The LIM domain: from the cytoskeleton to the nucleus. Nature Reviews Molecular Cell Biology. 2004;5:920-931.

Karlsson O, Thor S, Norberg T, Ohlsson H, Edlund T. Insulin gene enhancer binding protein Isl-1 is a member of a novel class of proteins containing both a homeo- and a Cys-His domain. Nature. 1990;344:879–882.

Kennett EC, Rees MD, Malle E, Hammer A, Whitelock JM, Davies MJ. Peroxynitrite modifies the structure and function of the extracellular matrix proteoglycan perlecan by reaction with both the protein core and the heparan sulfate chains. Free Radic Biol Med. 2010;49:282-293.

Kleiber K, Strebhardt K, Martin BT. The biological relevance of FHL2 in tumor cells and its role as a putative cancer target. Anticancer Res. 2007;27:55-61.

Knoblauch H, Geier C, Adams S et al. Contractures and hypertrophic cardiomyopathy in a novel FHL1 mutation. Ann Neurol 2010; 67: 136-140.

Kosa JL, Michelsen JW, Louis HA, Olsen JI, Davis DR, Beckerle MC, et al. Common metal ion coordination in LIM domain proteins. Biochemistry. 1994;33:468–477.

Kovacevic A, Hammer A, Sundl M Pfister B, Hrzenjak A, Ray A, et al. Expression of serum amyloid A transcripts in human trophoblast and fetal-derived trophoblast-like choriocarcinoma cells. FEBS Lett. 2006;580:161-167.

Kupershmidt S, Yang IC, Sutherland M, Wells KS, Yang T, Yang P, et al. Cardiac-enriched LIM domain protein fhl2 is required to generate I(Ks) in a heterologous system. Cardiovasc Res. 2002;56:93–103.

Kwapiszewska G, Wygrecka M, Marsh LM, Schmitt S, Trösser R, Wilhelm J, et al. Fhl-1, a new key protein in pulmonary hypertension. Circulation. 2008;118:1183-1194.

LaTulippe E, Satagopan J, Smith A, Scher H, Scardino P, Reuter V, et al. Comprehensive gene expression analysis of prostate cancer reveals distinct transcriptional programs associated with metastatic disease. Cancer Res. 2002;62:4499-4506.

Lee SM, Li HY, Ng EK Or SM, Chan KK, Kotaka M, et al. Characterization of a brain-specific nuclear LIM domain protein (FHL1B) which is an alternatively spliced variant of

FHL1. Gene. 1999;237:253-263.

Lee SM, Tsui SK, Chan KK, Garcia-Barcelo M, Waye MM, Fung KP, et al. Chromosomal mapping, tissue distribution and cDNA sequence of four-and-a-half LIM domain protein 1 (FHL1). Gene. 1998;216:163-170.

Lenk GM, Tromp G, Weinsheimer S, Gatalica Z, Berguer R, Kuivaniemi H. Whole genome expression profiling reveals a significant role for immune function in human abdominal aortic aneurysms. BMC Genomics. 2007;8:237.

Lesage F, Attali B, Lazdunski M, Barhanin J. Developmental expression of voltage-sensitive K+ channels in mouse skeletal muscle and C2C12 cells. FEBS Lett. 1992;310:162–166.

Li X, Jia Z, Shen Y, Ichikawa H, Jarvik J, Nagele RG, et al. Coordinate suppression of Sdpr and Fhl1 expression in tumors of the breast, kidney, and prostate. Cancer Sci. 2008;99:1326-1333.

Liang L, Zhang HW, Liang J, Niu XL, Zhang SZ, Feng L, et al. KyoT3, an isoform of murine FHL1, associates with the transcription factor RBP-J and represses the RBP-J-mediated transactivation. Biochim Biophys Acta. 2008;1779:805-810.

Liewluck T, Hayashi YK, Ohsawa M, Kurokawa R, Fujita M, Noguchi S, et al. Unfolded protein response and aggresome formation in hereditary reducing-body myopathy. Muscle Nerve. 2007;35:322–326.

Lin J, Lin S, Yu X, Choy PC, Shen X, Deng C, et al. The four and a half LIM domain protein 2 interacts with and regulates the HERG channel. FEBS J. 2008;275:4531-4539.

Martens JR, Kwak Y-G, Tamkun MM. Modulation of Kv channel α/β subunit interactions. Trends Cardiovasc. Med. 1999;9:253–258.

McGrath MJ, Cottle DL, Nguyen MA, Dyson JM, Coghill ID, Robinson PA et al. Four and a half LIM protein 1 binds myosin-binding protein C and regulates myosin filament formation and sarcomere assembly. J Biol Chem. 2006;281:7666–7683.

Meeson AP, Shi X, Alexander MS, Williams RS, Allen RE, Jiang N et al. Sox15 and Fhl3

transcriptionally coactivate Foxk1 and regulate myogenic progenitor cells. EMBO J. 2007:26:1902-1912.

Michelsen JW, Schmeichel KL, Beckerle MC, Winge DR. The LIM motif defines a specific zinc-binding protein domain. Proc Natl Acad Sci USA. 1993;90:4404–4408.

Morgan MJ, Madgwick AJA. The Fourth Member of the FHL Family of LIM Proteins Is Expressed Exclusively in the Testis. Biochem Biophys Res Commun. 1999;255:251-255.

Morgan MJ, Whawell SA. The structure of the human LIM protein ACT gene and its expression in tumor cell lines. Biochem Biophys Res Commun. 2000;273:776-783.

Müller JM, Metzger E, Greschik H, Bosserhoff AK, Mercep L, Buettner R, et al. The transcriptional coactivator FHL2 transmits Rho signals from the cell membrane into the nucleus. EMBO J. 2002;21:736–748.

Nattel S, Yue L., Wang Z. Cardiac ultrarapid delayed rectifiers. A novel potassium current family of functional similarity and molecular diversity. Cell Physiol. Biochem. 1999;9:217–226.

Newman AP, Acton GZ, Hartwieg E, Horvitz HR, Sternberg PW. The lin-11 LIM domain transcription factor is necessary for morphogenesis of C. elegans uterine cells. Development. 1999;126:5319-5326.

Ng EK, Lee SM, Li HY, Ngai SM, Tsui SK, Waye MM, et al. Characterization of tissue-specific LIM domain protein (FHL1C) which is an alternatively spliced isoform of a human LIM-only protein (FHL1). J Cell Biochem. 2001;82:1-10.

Niu C, Liang C, Guo J, Cheng L, Zhang H, Qin X, et al. Downregulation and growth inhibitory role of FHL1 in lung cancer. Int J Cancer. 2011 [Epub ahead of print]

Olson TM, Alekseev AE, Liu XK Park S, Zingman LV, Bienengraeber M, et al. Kv1.5 channelopathy due to KCNA5 loss-of-function mutation causes human atrial fibrillation. Hum Mol Genet. 2006;15:2185-2191.

Perou CM, Sørlie T, Eisen MB, van de Rijn M, Jeffrey SS, Rees CA, et al. Molecular portraits

of human breast tumors. Nature. 2000;406:747-752.

Pfaff S-L, Mendelsohn M, Stewart CL, Edlund T, Jessell TM. Requirement for LIM homeobox gene Isl1 in motor neuron generation reveals a motor neuron-dependent step in interneuron differentiation. Cell. 1996;84:309–320.

Platoshyn O, Yu Y, Golovina VA, McDaniel SS, Krick S, Li L, et al. Chronic hypoxia decreases KV channel expression and function in pulmonary artery myocytes. Am J Physiol Lung Cell Mol Physiol 2001;280:801–812.

Poparic I, Schreibmayer W, Schoser B, Desoye G, Gorischek A, Miedl H, et al. Four and a half LIM protein 1C (FHL1C): a binding partner for voltage-gated potassium channel Kv1.5. PLoS ONE 2011 [Epub ahead of print]

Prasad KV, Ao Z, Yoon Y, Wu MX, Rizk M, Jacquot S, et al. CD27, a member of the tumor necrosis factor receptor family, induces apoptosis and binds to Siva, a proapoptotic protein. Proc Natl Acad Sci U S A. 1997;94:6346-6351.

Qin H, Du D, Zhu Y, Li J, Feng L, Liang Y, et al. The PcG protein HPC2 inhibits RBP-J-mediated transcription by interacting with LIM protein KyoT2. FEBS Lett. 2005;579:1220-1226.

Qin H, Wang J, Liang Y, Taniguchi Y, Tanigaki K, Han H. RING1 inhibits transactivation of RBP-J by Notch through interaction with LIM protein KyoT2. Nucleic Acids Res. 2004;32:1492-1501.

Quinzii CM, Vu TH, Min KC, Tanji K, Barral S, Grewal RP, et al. X-linked dominant scapuloperoneal myopathy is due to a mutation in the gene encoding four and- a-half-LIM protein 1. Am J Hum Genet. 2008;82:208–213.

Rauh A, Windischhofer W, Kovacevic A, DeVaney T, Huber E, Semlitsch M et al. Endothelin (ET)-1 and ET-3 promote expression of c-fos and c-jun in human choriocarcinoma via ET(B) receptor-mediated G(i)- and G(q)-pathways and MAP kinase activation. Br J Pharmacol. 2008;154:13-24.

Sakashita K, Mimori K, Tanaka F, Kamohara Y, Inoue H, Sawada T, et al. Clinical significance of loss of Fhl1 expression in human gastric cancer. Ann Surg Oncol. 2008;15:2293-2300.

Samson T, Smyth N, Janetzky S, Wendler O, Müller JM, Schüle R et al. The LIM-only proteins FHL2 and FHL3 interact with alpha- and beta-subunits of the muscle alpha7beta1 integrin receptor. J Biol Chem. 2004:279:28641-28652.

Sanguinetti MC, Jiang C, Curran ME, Keating MT. A mechanistic link between an inherited and an acquired cardiac arrhythmia: HERG encodes the IKr potassium channel. Cell. 1995;81:299–307.

Sanguinetti MC, Tristani-Firouzi M. hERG potassium channels and cardiac arrhythmia. Nature 2006;440:463–469.

Schessl J, Columbus A, Hu Y, Zou Y, Voit T, Goebel HH et al. Familial reducing body myopathy with cytoplasmic bodies and rigid spine revisited: identification of a second LIM domain mutation in FHL1. Neuropediatrics. 2010;41:43–46.

Schessl J, Taratuto AL, Sewry C, Battini R, Chin SS, Maiti B, et al. Clinical, histological and genetic characterization of reducing body myopathy caused by mutations in FHL1. Brain. 2009;132:452–464.

Schessl J, Zou Y, McGrath MJ, Cowling BS, Maiti B, Chin SS, et al. Proteomic identification of FHL1 as the protein mutated in human reducing body myopathy. J Clin Invest. 2008;118:904–912.

Schoser B, Goebel HH, Janisch I, Quasthoff S, Rother J, Bergmann M, et al. Consequences of mutations within the C terminus of the FHL1 gene. Neurology. 2009;73:543-551.

Schroder R, Vrabie A, Goebel HH. Primary desminopathies. J Cell Mol Med. 2007;3:416–426.

Schreibmayer W, Lester HA, Dascal N. Voltage clamping of Xenopus laevis oocytes utilizing agarose-cushion electrodes. Pflugers Arch. 1994;426:453-458.

Shalaby S, Hayashi YK, Goto K, Ogawa M, Nonaka I, Noguchi S, et al. Rigid spine syndrome caused by a novel mutation in four-and-a-half LIM domain 1 gene (FHL1). Neuromuscul Disord. 2008;18:959–961.

Shalaby S, Hayashi YK, Nonaka I, Noguchi S, Nishino I. Novel FHL1 mutations in fatal and benign reducing body myopathy. Neurology. 2009;72:375–376.

Shathasivam T, Kislinger T, Gramolini AO. Genes, proteins and complexes: The multifaceted nature of FHL family proteins in diverse tissues. J Cell Mol Med. 2010;14:2702-2720.

Sheikh F, Raskin A, Chu PH, Lange S, Domenighetti AA, et al. An FHL1-containing complex within the cardiomyocyte sarcomere mediates hypertrophic biomechanical stress responses in mice. J Clin Invest. 2008;118:3870–3880.

Shen Y, Jia Z, Nagele RG, Ichikawa H, Goldberg GS. SRC uses Cas to suppress Fhl1 in order to promote nonanchored growth and migration of tumor cells. Cancer Res. 2006;66:1543-1552.

Smirnov SV, Robertson TP, Ward JPT, Aaronson PI. Chronic hypoxia is associated with reduced delayed rectifier K+ current in rat pulmonary artery muscle cells. Am J Physiol Heart Circ Physiol. 1994;266:365–370.

Tamargo J, Caballero R, Gómez R, Valenzuela C, Delpón E. Pharmacology of cardiac potassium channels. Cardiovasc Res. 2004;62:9-33.

Taniguchi Y, Furukawa T, Tun T, Han H, Honjo T. LIM protein KyoT2 negatively regulates transcription by association with the RBP-J DNA-binding protein. Mol Cell Biol. 1998;18:644-654.

Trudeau MC, Warmke JW, Ganetzky B, Robertson GA. HERG, a human inward rectifier in the voltage-gated potassium channel family. Science 1995;269:92–95.

Tsuchida T, Ensini M, Morton SB, Baldassare M, Edlund T, Jessell TM et al. Topographic organization of embryonic motor neurons defined by expression of LIM homeobox genes Cell. 1994;79:957–970.

Van Wagoner DR, Pond AL, McCarthy PM, Trimmer JS, Nerbonne JM. Outward K+ current densities and Kv1.5 expression are reduced in chronic human atrial fibrillation. Circ Res. 1997;80:772–781.

Villalonga N, Martínez-Mármol R, Roura-Ferrer M, David M, Valenzuela C, Soler C et al. Cell cycle-dependent expression of Kv1.5 is involved in myoblast proliferation. Biochim Biophys Acta. 2008;1783:728-736.

Vicente R, Villalonga N, Calvo M, Escalada A, Solsona C, Soler C et al. Kv1.5 association modifies Kv1.3 traffic and membrane localization. J Biol Chem. 2008;283:8756-8764.

Voit T, Krogmann O, Lenard HG, Neuen-Jacob E, Wechsler W, Goebel HH, et al. Emery-Dreifuss muscular dystrophy: disease spectrum and differential diagnosis. Neuropediatrics. 1988;19:62-71.

Wagner V, Stadelmeyer E, Riederer M Regitnig P, Gorischek A, Devaney T et al. Cloning and characterization of GIRK1 variants resulting from alternative RNA editing of the KCNJ3 gene transcript in a human breast cancer cell line. J Cell Biochem. 2010;110:598-608.

Wang J, Juhaszova M, Conte JV Jr, Gaine SP, Rubin LJ, Yuan JX-J. Action of fenfluramine on voltage-gated K+ channels in human pulmonary artery smooth-muscle cells. Lancet. 1998;359:290.

Wang Z, Fermini B, Nattel S. Sustained depolarization-induced outward current in human atrial myocytes. Evidence for a novel delayed rectifier K+ current similar to Kv1.5 cloned channel currents. Circ Res. 1993;73:1061-1076.

Ward TH, Brandizzi F. Dynamics of proteins in Golgi membranes: Comparisons between mammalian and plant cells highlighted by photobleaching techniques. Cell Mol Life Sci. 2004;61:172–185.

Watkins H, Conner D, Thierfelder L, Jarcho JA, MacRae C, McKenna WJ, et al. Mutations in the cardiac myosin binding protein-C gene on chromosome 11 cause familial hypertrophic cardiomyopathy. Nat Genet. 1995;11:434-437.

Way JC, Chalfie M. mec-3, a homeobox-containing gene that specifies differentiation of the touch receptor neurons in C. elegans. Cell. 1988;54:5-16.

Weiss U, Cervar M, Puerstner P, Schmut O, Haas J, Mauschitz R, et al. Hyperglycemia in vitro alters the proliferation and mitochondrial activity of the choriocarcinoma cell lines BeWo, JAR and JEG-3 as models for human first-trimester trophoblast. Diabetologia. 2001;44:209-219.

Weng J, Liao M, Zou S, Bao J, Zhou J, Qu L, et al. Downregulation of FHL1 Expression in Thoracic Aortic Dissection: Implications in Aortic Wall Remodeling and Pathogenesis of Thoracic Aortic Dissection. Ann Vasc Surg. 2010; 25:240-247.

Windpassinger C, Schoser B, Straub V, Hochmeister S, Noor A, Lohberger B et al. An X-linked myopathy with postural muscle atrophy and generalized hypertrophy, termed XMPMA, is caused by mutations in FHL1. Am J Hum Genet. 2008;82:88-99.

Wong CH, Fung YW, Ng EK, Lee SM, Waye MM, Tsui SK. LIM domain protein FHL1B interacts with PP2A catalytic β subunit--a novel cell cycle regulatory pathway. FEBS Lett. 2010;584:4511-4516.

Yang Z, Browning CF, Hallaq H, Yermalitskaya L, Esker J, Hall MR, et al. Four and a half LIM protein 1: a partner for KCNA5 in human atrium. Cardiovasc Res. 2008;78:449-457.

Yang T, Yang P, Roden DM, Darbar D. Novel KCNA5 mutation implicates tyrosine kinase signaling in human atrial fibrillation. Heart Rhythm. 2010; 7:1246-1252.

Yeola SW, Rich TC, Uebele VN, Tamkun MM, Snyders DJ. Molecular analysis of a binding site for quinidine in a human cardiac delayed rectifier K+ channel. Role of S6 in antiarrhythmic drug binding. Circ Res. 1996;78:1105-1114.

Yuan JX-J, Aldinger AM, Juhaszova M, Wang J, Conte JV Jr, Gaine SP, et al. Dysfunctional voltage-gated K+ channels in pulmonary artery smooth muscle cells of patients with primary pulmonary hypertension. Circulation. 1998;98:1400–1406.

Yuan JX-J, Wang J, Juhaszova M, Gaine SP, Rubin LJ. Attenuated K+ channel gene

transcription in primary pulmonary hypertension. Lancet. 1998;351:726–727.

Zhang Q, Bethmann C, Worth NF, Davies JD, Wasner C, Feuer A, et al. Nesprin-1 and -2 are involved in the pathogenesis of Emery–Dreifuss muscular dystrophy and are critical for nuclear envelope integrity. Hum Mol Genet. 2007;16:2816–2833.

# 8 SUPPLEMENTARY INFORMATION

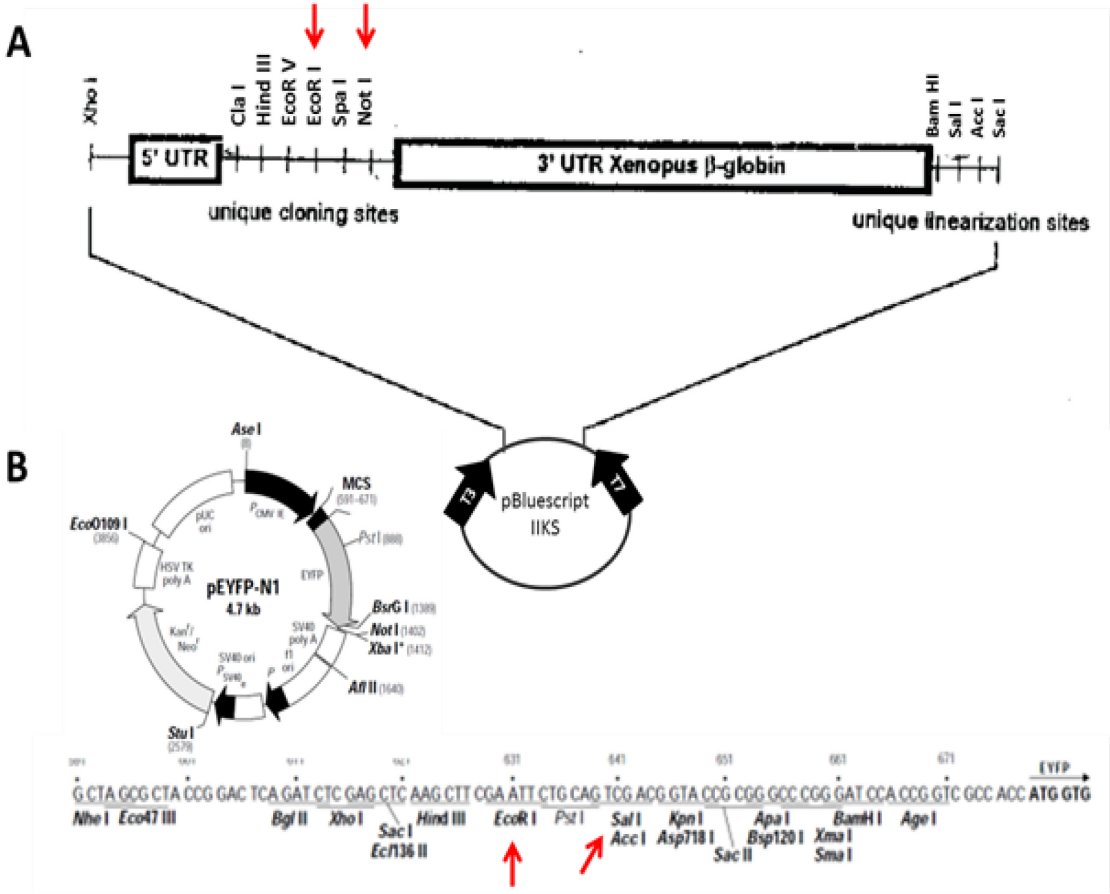


**Supplemetary Scheme I: Vector restriction Map and Multiple Cloning Site (MCS)** Restriction sites (red arrows) were used and primers were designed accordingly. (A) pBS-MXT vector, EcoR I and Not I restriction sites were used for primer design; scheme adopted from Prof. Schreibmayer notes. (B) pEYFP-N1 vector from Clontech, unique restriction sites are in bold. EcoR I and Sal I restriction sites were used. Image adopted from clontech.com

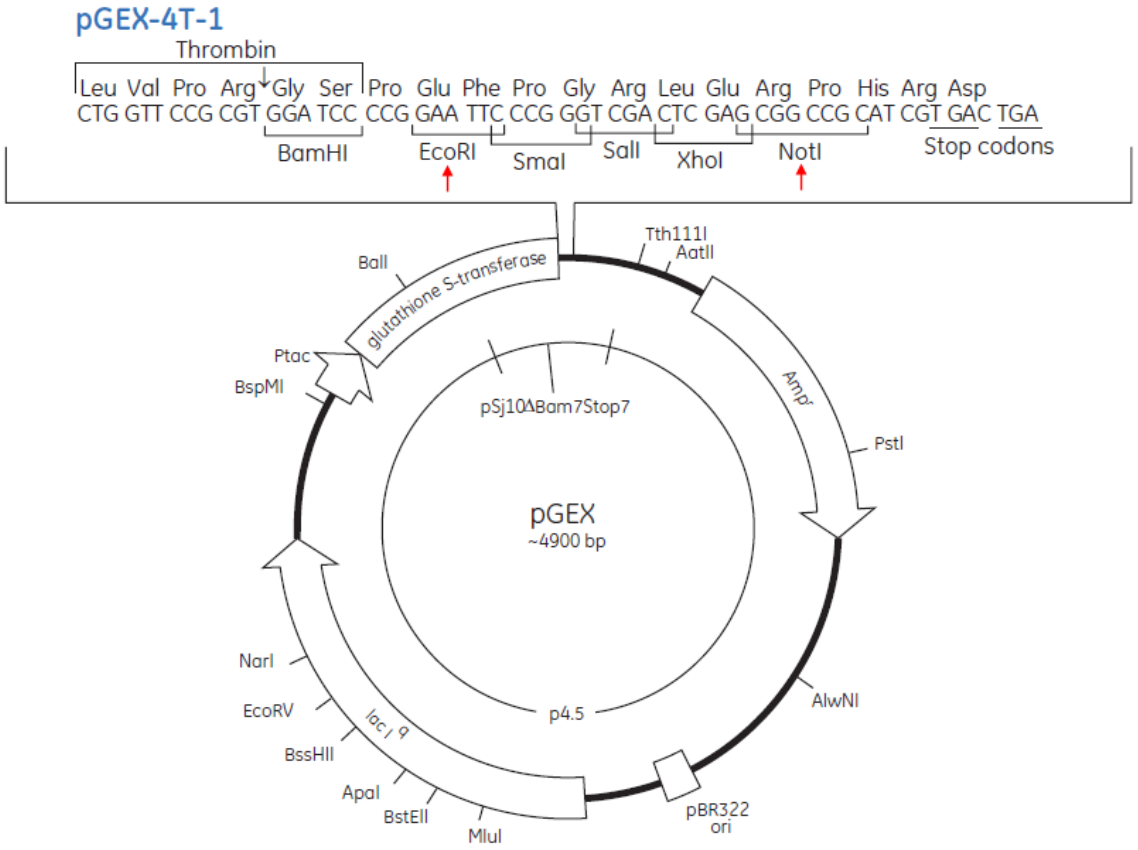


**Supplementary Scheme II: Modified pGEX-4T-1 vector map from Amersham GE Healthcare** As affinity label we use glutathione-S-transferase already encoded in the commercially available vector pGEX-4T-1. Via PCR, we have cycled out the appropriate coding sequence of C-terminal Kv1.5 from a plasmid containing the entire, native Kv1.5 sequence. For our experimental setup, EcoR1 and Not1 restriction sites were used and primers were designed accordingly. Scheme was adopted from Prof. Schreibmayer notes.

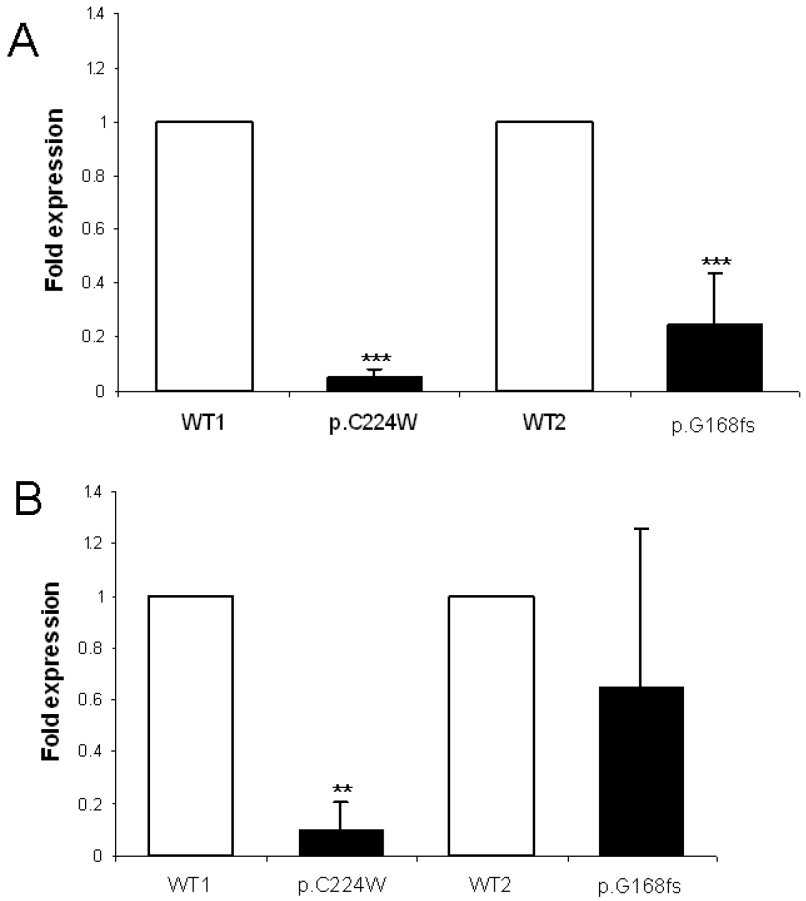


**Supplementary Figure 1: Densitometric evaluation of FHL1A and $K_{v1.5}$ expression in human myoblasts** (A) FHL1A expression in control (WT1, WT2) and XMPMA patient (p.C224W, p.G168fs) myoblasts. Values for control samples are set to 1 and for XMPMA patients normalized to corresponding controls. Experiments were performed in triplicates. (B) $K_{v1.5}$ expression in myoblasts using the same samples as listed in (A). Experiments were performed in triplicates.

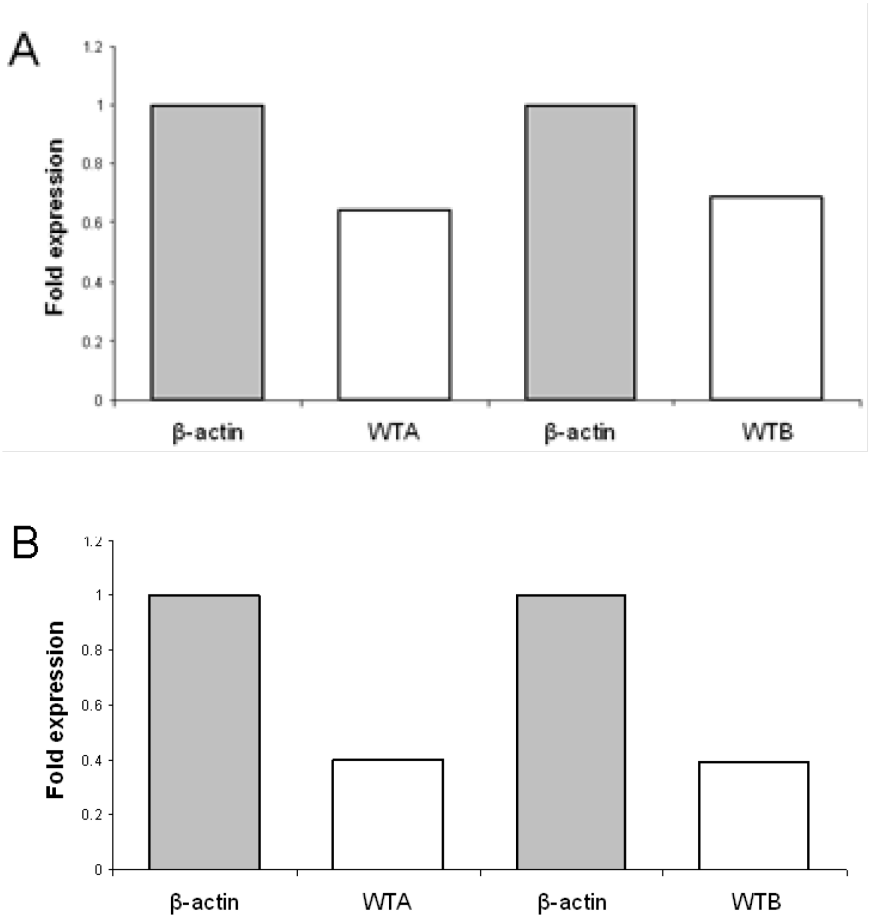


**Supplementary Figure 2: Densitometric evaluations of FHL1A and Kv1.5 expression in non-XMPMA patient cardiac tissue** (A) FHL1A expression in human heart ears (WTA, WTB), values are normalized to β-actin that was set to 1. Experiments were performed in triplicates. (B) $K_{v1.5}$ expression was performed using the same samples as in (A). Experiments were performed in triplicates.

**CURRICULUM VITAE**

# Ivana Poparić, MSc


**CONTACT** Ilica 82, 10000 Zagreb, Croatia

Mobile: +385 98 556476
Mobile 2: +43 650 3906474

E-mail: ipoparic@gmail.com


**PERSONAL INFORMATION** Born in Zagreb, Croatia, on August, 23rd 1981

**WORK EXPERIENCE**

| | |
|---|---|
| 10/2007 – 2011 | **Medical University Graz**, Austria<br>PhD student |
| | PI Prof Klaus Wagner |
| | Project: Mutations in FHL1 impair expression and functionality of potassium voltage-gated channel $K_{v1.5}K_{v1.5}$ in myopathy patients |
| | Laboratory work, , scientific writing (papers, progress reports), presenting at scientific meetings and conferences (posters, short talks), training undergraduate students, genetic counseling: interpreter for foreign patients |
| 5/2007-6/2007 | **Johnson & Johnson S.E. d.o.o.**, Consumer & OTC Division, Zagreb, Croatia |
| | Student internship |
| | Preparing promotion materials, preparing and executing surveys, analysis of results |
| 7/2006 – 8/2006 | **Imperial College, Faculty of Medicine**, Division of Surgery, Oncology, Reproductive Biology and Anaesthetics, London |
| | Student internship, laboratory work |
| 2/2005 – 12/2006 | **Ruđer Bošković Institute**, Division of Molecular Medicine, Zagreb<br>PI Dr Sanja Kapitanovic |
| | Master thesis student |
| | Project: Polymorphism of *NOD2 (CARD15)* gene in Croatian population |
| 7/2005 – 8/2005 | **Institute of Molecular Genetics**, Prague |
| | Student internship, laboratory work |

**EDUCATION**

| | |
|---|---|
| 2007 – present | Molecular Medicine PhD program, Medical University of Graz, Austria |
| | PhD thesis |
| | Awaiting for the PhD defence |

| | | |
|---|---|---|
| | 2000 – 2006 | Masters program, Faculty of Science, University of Zagreb, Croatia |
| | | Major: Molecular biology |
| | | Graduated with excellent mark |
| | 1996 – 2000 | Science and mathematics program secondary school (XV gimnazija, MIOC), Zagreb, Croatia |
| | | Graduated with excellent mark |
| **ADDITIONAL EDUCATION** | 2010 | **Biobusiness summer school** (AMC center, Amsterdam): product development, patents & licenses, from start-up to IPO, biopharma business models, new market opportunities, pharmacopolicy, pharmacoeconomics, business ethics, entrepreneurship |
| | 2010 | **Scientific writing in English** (Medical University of Graz): papers, presentations, project proposals and reports. |
| **AWARDS AND SPONSORSHIPS** | 2006 | Končar d.d., Zagreb |
| | | Sponsorship for international student internship |
| | 2005 | Open Society Institute Croatia: |
| | | Grant for international student internship |
| | 2005 | Gradske ljekarne Zagreb (City of Zagreb pharmacies) |
| | | Sponsorship for international student internship |
| **OTHER SKILLS** | Languages | English, fluent<br>German, fluent<br>French, intermediate<br>Croatian, native |
| | Driving licence | |
| | MS office package | |
| **PUBLICATIONS** | Available upon request | |